



A NEW, EXTRAORDINARILY DIVERSE, EARLIEST LATE MIOCENE (EARLY TUROLIAN, MN 11) SMALL VERTEBRATE “REFERENCE” ASSEMBLAGE FROM THE CSODABOGYÓS CAVE (KESZTHELY HILLS, WESTERN HUNGARY)

PIROSKA PAZONYI^{1,2,*}, LUKÁCS MÉSZÁROS³, MÁRIA TREMBECZKI¹, ZOLTÁN SZENTESI⁴, MARTIN SEGESDI^{3,4,5}, IVAN HORÁČEK⁶, LUTZ CHRISTIAN MAUL⁷, JÁNOS HÍR⁸

¹ HUN-REN-MTM-ELTE Research Group for Paleontology, Hungarian Research Network, Ludovika tér 2, 1083 Budapest, Hungary; e-mail: pinety@gmail.com, mk.trembeczki@gmail.com.

² Institute of Geography and Earth Sciences, ELTE Eötvös Loránd University, Pázmány Péter sétány 1/c, 1117 Budapest, Hungary.

³ Department of Paleontology, Institute of Geography and Earth Sciences, ELTE Eötvös Loránd University, Pázmány Péter sétány 1/c, 1117 Budapest, Hungary; e-mail: lgy.meszáros@gmail.com.

⁴ Department of Paleontology and Geology, Hungarian Natural History Museum, Hungarian National Museum Public Collection Centre, Ludovika tér 2, 1083 Budapest, Hungary; e-mail: crocutaster@gmail.com.

⁵ Department of Zoology, Hungarian Natural History Museum, Hungarian National Museum Public Collection Centre, Ludovika tér 2, 1083 Budapest, Hungary; e-mail: martinsegedi@gmail.com.

⁶ Department of Zoology, Charles University in Prague, Faculty of Science, Viničná 7, 128 43 Praha 2, Czech Republic; e-mail: ivan.horacek@natur.cuni.cz.

⁷ Quaternary Palaeontology, Senckenberg Research Institute and Natural History Museum Frankfurt, Am Jakobskirchhof 4, 99423 Weimar, Germany, e-mail: lutz.maul@senckenberg.de.

⁸ Municipal Museum of Pásztó, Múzeum tér 5, 3060 Pásztó, Hungary; e-mail: hirjanos@gmail.com.

* corresponding author

Pazonyi, P., Mészáros, L., Trembeczki, M., Szentesi, Z., Segesdi, M., Horáček, I., Maul, L. Ch., Hír, J. (2025): A new, extraordinarily diverse, earliest Late Miocene (early Turolian, MN 11) small vertebrate “reference” assemblage from the Csodabogyós Cave (Keszthely Hills, Western Hungary). – Fossil Imprint, 81(1-2): 114–153, Praha. ISSN 2533-4050 (print), ISSN 2533-4069 (online).

Abstract: The Csodabogyós Cave in western Hungary yielded a rich terrestrial vertebrate fauna during two excavations in 2023. The material comprises 1,053 amphibian and reptile remains, 51 bird bones, 5,640 identifiable mammal teeth and bones, and thousands of bone fragments. The fauna of the Csodabogyós Cave is most similar to that of the nearby Kohfidisch site (Burgenland, Austria). In the description of the shrew material, we raise the need to establish a new genus for “*Petenyia*” *dubia* BACHMAYER et WILSON, 1970, we extend the stratigraphic range of *Asoriculus gibberodon* (PETÉNYI, 1864) to the beginning of the MN 11 Zone, and we present a morphological transition between *Crusafontina kormosi* (BACHMAYER et WILSON, 1970) and its descendant, *Amblycoptus oligodon* KORMOS, 1924. Within the bat fauna, *Myotis* is the richest genus, with six forms. All three size ranges of *Rhinolophus* are represented, and *Miniopterus* and *Plecotus* also occur at the site. In addition, to the typical Late Miocene species of the rodent fauna, a new species of glirid (*Vasseuromys* n. sp.) and the westernmost and one of the oldest finds of the genus *Microscoptes* are described from the site. Based on the paleoecological analysis, the site’s environment was highly diverse. On the shores of Lake Pannon, a gallery forest and shrub vegetation were found, while further away from the lake was a wooded savannah, with semi-open karstic areas on the higher parts. It may have been warm, but drier than the Middle Miocene, with a seasonal climate, probably characterised by hot, dry summers and cool, wet winters. The age of the fauna is estimated to be approximately 8.7–8.5 million years (early Turolian, MN 11).

Key words: Late Miocene, Turolian, MN 11, mammal, herpetofauna, Aves, Insectivora, Chiroptera, Rodentia

Received: December 20, 2024 | Accepted: July 1, 2025 | Issued: December 18, 2025

Zoobank: <http://zoobank.org/pub:02523DF6-0742-408F-84D6-12BB5BFF179F>

Introduction

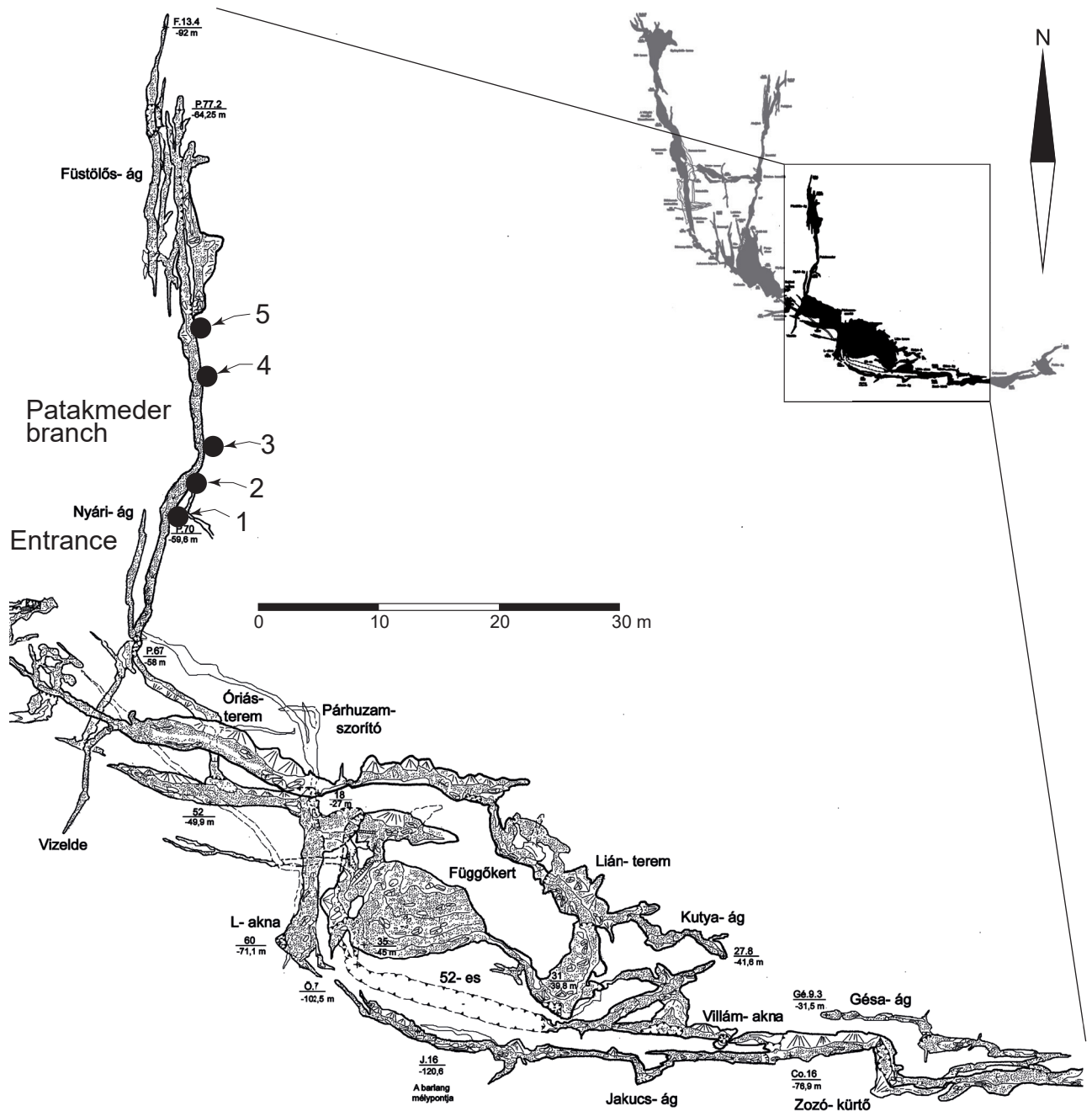
The Csodabogyós Cave is located north of Lake Balaton, on the eastern edge of the Keszthely Hills, near the village of Balatonederics at an altitude of 393 m above sea level, 46.79706° N, 17.36458° E (Text-fig. 1). The cave is named

after a plant called “szúrós csodabogyó” (*Ruscus aculeatus*, butcher’s broom), which is very common around the cave entrance.

The fossil-rich sediment in the cave’s north, known as the “Patakmeder” branch, was discovered by speleologists during excavation of a tunnel in autumn of 2022. The



Text-fig. 1. Location of Csodabogyós Cave. a: map of Hungary, rectangle indicates location of enlarged map, b: location of Csodabogyós Cave (yellow star) in Keszthely Hills.



Text-fig. 2. Map of Csodabogyós Cave showing entrance and five sampling points in the "Patakmeder" branch (modified after Polacsek and Szittner 2006).

fossils were recovered from a sandy, clayey aleurite, which according to our studies was wind-blown to the plateau (and the cave) after a short transport. They may have originated from the delta system that filled Lake Pannon. The speleologists handed the sediment over to Krisztina Sebe (University of Pécs), who after screen washing, sent the remains (turtle shell and bone fragments) to the Department of Paleontology and Geology of the Hungarian Natural History Museum, for analysis by Pirooska Pazonyi and Zoltán Szentesi. Although most of the bone fragments could not be identified, Zoltán Szentesi suggested that the turtle remains belonged to the Miocene terrestrial species *Testudo kalksburgensis*.

In April 2023, Krisztina Sebe and Pirooska Pazonyi, assisted by cavers, collected 10 kg of material for screen washing from all four points on the “Patakmeder” branch (sampling points 1–4; Text-fig. 2). The extremely rich, excellently-preserved terrestrial vertebrate fauna from these samples, mainly of small mammals, confirmed the Miocene age indicated by *Testudo kalksburgensis*, and indicated that a more extensive excavation in the cave would quite likely be worthwhile. That new excavation was conducted in August of 2023 by János Hír, Krisztina Sebe and Pirooska Pazonyi, with the assistance of cavers and volunteers. During the excavation, large amounts of material (approximately 150 kg) were collected from two locations (sampling points 4 and 5; Text-fig. 2).

This paper aims to taxonomically classify the terrestrial vertebrate fauna from the Csodabogyós Cave, to interpret it paleoecologically, and to determine its biostratigraphic age. We would like to note that detailed descriptions of two species, the newly described *Vasseuromys* n. sp. and *Neocricetodon* cf. *skofleki* are published in two separate papers in this issue (Hír 2025, Hír et al. 2025).

Material and methods

During the sample collection and excavation, sediments of various amounts were collected for screen washing from 5 sampling points (Text-fig. 2) in the Csodabogyós Cave. We collected the least material at sampling points 1, 2, and 3, from each of which 10 kg of sediment was harvested. Significantly more sediment was analysed from sampling points 4 (120 kg) and 5 (43 kg). The material collected from the different sampling points was treated separately, to ensure that sediments of potentially different ages were not mixed. Later, taxonomic analyses revealed that the material from all sampling points was of the same age, and that the differences between them, e.g., the species richness of sampling point 4, were not due to different ages but to different sample sizes (Tab. 1). For this reason, the material from all the sampling points will be discussed together.

All material was screen-washed on a sieve with a 0.5 mm mesh size, and then the vertebrate remains were picked out from the sediment. A total of 1,053 amphibian and reptile remains, 51 bird bones, 5,640 identifiable mammal teeth and bones, and thousands of bone fragments were recovered from the cave.

The remains of insectivores, bats and rodents’ molars were measured under a stereomicroscope. In the cases of some

Table 1. Fauna of different sampling points in Csodabogyós Cave. Remains that can only be identified at a lower taxonomic level and small mammal groups not discussed in detail in this article (*Erinaceomorpha*, *Desmaninae*, *Talpidae*) are not listed here. These were found at all sampling points. The complete faunal list can be found in Table 3.

Taxa	Sampling points				
	1	2	3	4	5
<i>Mioproteus caucasicus</i>				+	+
<i>Lissotriton vulgaris</i>				+	
cf. <i>Palaeobatrachidae</i> indet.				+	
<i>Latonia</i> cf. <i>gigantea</i>		+		+	+
<i>Pelobates fuscus</i>			+	+	+
<i>Bufo bufo</i>				+	
<i>Bufo viridis</i>	+		+	+	
<i>Hyla arborea</i>				+	
<i>Rana temporaria</i>				+	+
<i>Pelophylax</i> kl. <i>esculentus</i>		+		+	
<i>Emys orbicularis</i>	+	+	+	+	+
<i>Testudo</i> cf. <i>kalksburgensis</i>	+	+		+	
Lacertidae indet.			+	+	+
<i>Pseudopus</i> cf. <i>pannonicus</i>				+	+
<i>Anguis fragilis</i>				+	
<i>Hierophis viridiflavus</i>		+		+	+
<i>Elaphe</i> cf. <i>paralongissima</i>				+	
<i>Zamenis longissimus</i>				+	
<i>Natrix tessellata</i>				+	
<i>Vipera</i> sp.				+	
Passeriformes indet.	+	+	+	+	+
Corvidae indet.				+	
Phasianidae indet.				+	+
<i>Crusafontina kormosi</i>	+	+	+	+	+
“ <i>Petenya</i> ” <i>dubia</i>	+	+	+	+	+
<i>Asoriculus gibberodon</i>	+	+	+	+	+
Soricinae sp. indet. 1				+	
Soricinae sp. indet. 2				+	
<i>Paenelimoecus repenningi</i>	+	+	+	+	+
<i>Rhinolophus grivensis</i>		+		+	+
<i>Rhinolophus lissiensis</i>	+	+		+	
<i>Rhinolophus delphinensis</i>	+	+		+	
<i>Myotis</i> cf. <i>bavaricus</i>	+	+	+	+	
<i>Myotis</i> aff. <i>gundersheimensis</i>	+			+	+
<i>Myotis</i> sp. indet. 1				+	
<i>Myotis</i> sp. indet. 2	+			+	
<i>Myotis</i> sp. indet. 3				+	
<i>Myotis</i> sp. indet. 4				+	
<i>Plecotus</i> cf. <i>atavus</i>		+		+	
<i>Miniopterus</i> cf. <i>fossilis</i>		+		+	
<i>Csakvaromys sciurinus</i>				+	
<i>Muscardinus pliocaenicus</i>				+	
<i>Myomimus dehmi</i>			+	+	+
<i>Vasseuromys</i> n. sp.	+	+	+	+	+
<i>Eomyops</i> sp.				+	
<i>Keramidomys</i> sp.				+	
<i>Eozapus intermedius</i>				+	
<i>Neocricetodon</i> cf. <i>skofleki</i>	+	+	+	+	+
<i>Microscoptes</i> sp.			+		
<i>Epimeriones austriacus</i>		+	+	+	+
<i>Progonomys hispanicus</i>	+	+	+	+	+
<i>Apodemus lugdunensis</i>	+	+	+	+	+
<i>Prosopalax petteri</i>	+	+	+	+	+
Sum	18	22	18	51	23

Table 2. Sites mentioned in paper, along with their ages (MN Zone).

Locality	MN Zone	Country	References
Çapak	MN 4	Türkiye	Bilgin et al. 2021
Goldberg	MN 6	Germany	Rachl 1983
Neudorf a. March	MN 6	Slovakia	Rachl 1983
Sansan	MN 6	France	Ginsburg and Mein 2012
La Grive	MN 7	France	Van de Weerd 1976, Topál 1979
Petersbuch 6	MN 7	Germany	Ziegler 2003
Petersbuch 7	MN 7	Germany	Ziegler 2003
Petersbuch 18	MN 7	Germany	Ziegler 2003
Felsőtárkány 3/2	MN 7/8	Hungary	Hír 2003
Petersbuch	MN 7/8	Germany	Ziegler 2003
Tauț	MN 7/8	Romania	Hír et al. 2011
Bujor	MN 9	Moldova	Lungu 1981
Götzendorf	MN 9	Austria	Daxner-Höck et al. 2016
Gritsev/Grytsiv	MN 9	Ukraine	Rosina et al. 2019, Nesin and Kovalchuk 2021
Nebelbergweg	MN 9	Switzerland	Kälin and Engesser 2001
Pedregueras	MN 9	Spain	De Bruijn 1966
Richardhof-Golfplatz	MN 9	Austria	Daxner-Höck et al. 2016, Daxner-Höck and Höck 2009
Rudabánya	MN 9	Hungary	Bernor et al. 2004
Saray 1	MN 9	Russia	Daxner-Höck et al. 2013
Suchomasty	MN 9	Czech Republic	Fejfar 1989
Montredon	MN 10	France	Aguilar 1982, Bolliger 1999
Peralejos C	MN 10	Spain	van Dam 1997
Pezinok	MN 10	Slovakia	Joniak 2016
Richardhof-Wald	MN 10	Austria	Daxner-Höck and Höck 2015
Schernham	MN 10	Austria	Daxner-Höck and Höck 2015
Sümeg	MN 10	Hungary	Mészáros 1996
Csákvár	MN 11	Hungary	Kretzoi 1951
Eichkogel	MN 11	Austria	Daxner-Höck 1972, Daxner-Höck and Höck 2009
Gavardovsky	MN 11	Russia	Tesakov et al. 2017
Kohfidisch	MN 11	Austria	Daxner-Höck and Höck 2009, Daxner-Höck 2009, Wöger 2011
Peralejos D	MN 11	Spain	van Dam 1997
Volchaya Balka	MN 11	Russia	Tesakov et al. 2017
Tardosbánya	MN 12	Hungary	Mészáros 1998
Can Vilella	MN 13	Spain	Agusti and Casanovas-Vilar 2003
Ertemte 2	MN 13	China	Wu 1985, Fahlbusch 1987, Fejfar et al. 2011
Harr Obo 2	MN 13	China	Wu 1985
Lissieu	MN 13	France	Agusti and Casanovas-Vilar 2003
Polgárdi	MN 13	Hungary	Mészáros 1999
Maramena	MN 13/14	Greece	De Bruijn 1995
Kroczyce	MN 14	Poland	Kowalski 1974
Osztramos 1	MN 14	Hungary	Trávníčková 2016
Gundersheim	MN 16	Germany	Horáček and Trávníčková 2019

rodents (*Progonomys*, *Apodemus*), the data obtained were sorted into separate databases for each tooth, and statistical analyses were performed within the R software environment (v. 4.3.1; R Core Team 2023). The size distributions of the

length and width, as well as the L/W or W/L ratio of each upper and lower molar were examined separately for each of the different upper and lower tooth positions. The assumed normality of the distributions was checked by a Shapiro-

Wilks test (Shapiro and Wilk 1965), using the shapiro test () function of the R. Normality was rejected if the resulting p-value was less than an a-priori selected significance level, $\alpha = 0.05$; thus, the consequent decision has a 95 % confidence. Next, the size of the populations from the Csodabogyós Cave was compared with that of similar-age sites, such as Kohfidisch and Eichkogel (both Austria) (Wöger 2011, Daxner-Höck and Höck 2015). We used János Hír's earlier unpublished measurements for Kohfidisch and Eichkogel *Apodemus* material.

The mean L, W, L/W and W/L values were compared with each other using their 95 % confidence bounds. For the same reason, Welch's t-tests (Welch 1947) were also used and performed by the T test function of R with the same 0.05 significance level as above.

Pictures of Soricidae and Chiroptera specimens were made with a Delta Optical 5MP Pro digital microscope. The micrographs of the rodent teeth were taken with a CMEX-5 digital microscope. JH made retouches.

Abbreviations used in the morphological descriptions and tables: teeth: A – antemolar, C – canine, D – deciduous tooth, I – incisor, M – molar, P – praemolar, uppercase = upper teeth, lowercase = lower teeth; measurements: AW – anterior width, BL – buccal length, H – height, L – length, LL – lingual length, PW – posterior width, TAW – talonid width, TRW – trigonid width, W – width.

The sites mentioned in the paper, along with their ages (MN Zone), are listed in Table 2.

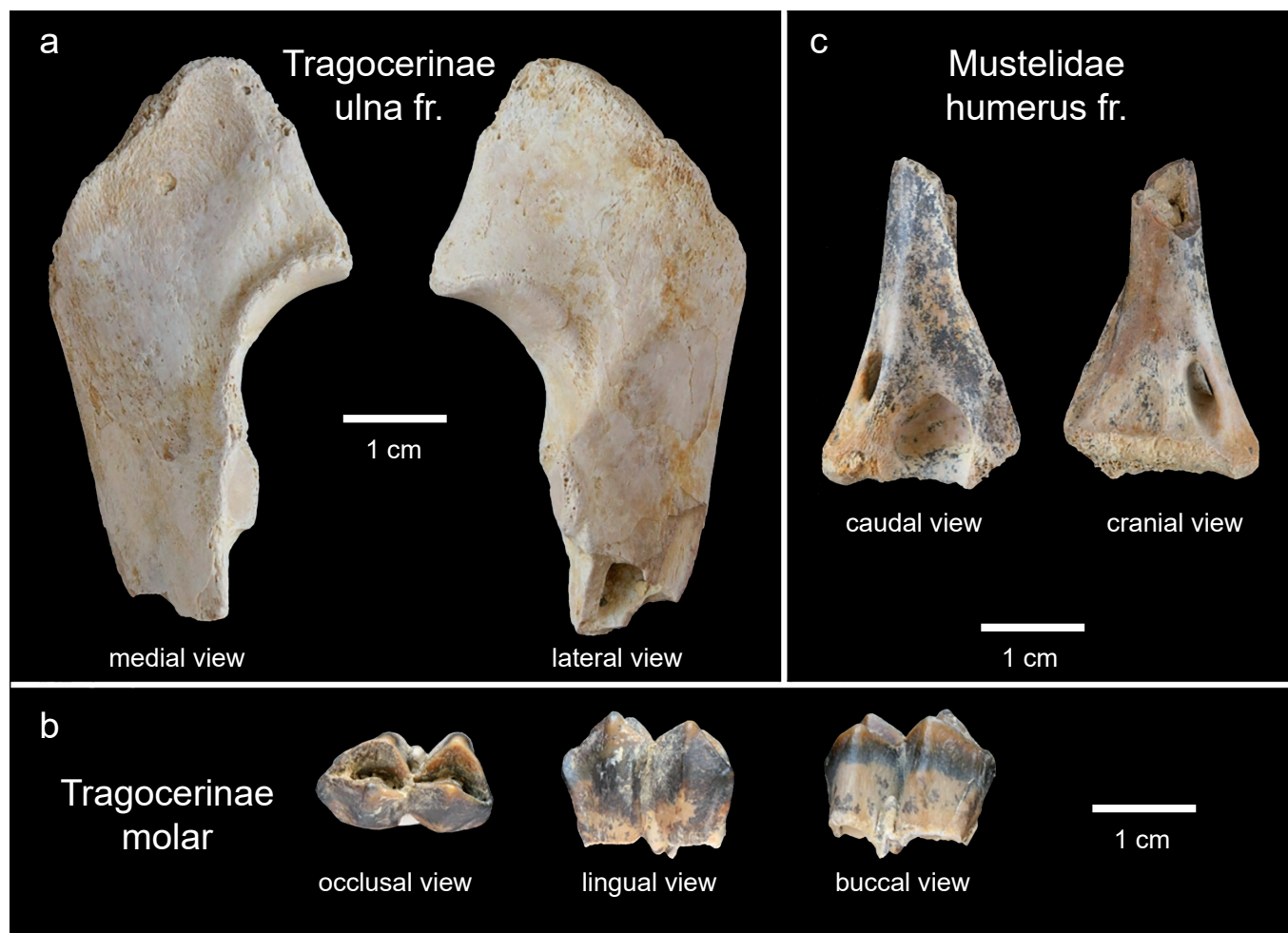
Systematic paleontology

While the taxonomic classification of small mammal remains is detailed, herpetofauna and avian taxa are only documented in a list.

Within the herpetofauna, most of the species-level identifiable remains are from sampling site 4. This comprises 264 bones, compared to 622 examples classified at the higher taxonomic level. At the genus level, 20 fossil bones could be identified from this sampling site (Tab. 3).

Of the material from the Csodabogyós Cave, 51 specimens can be classified as birds. Phasianidae specimens are from sampling points 4 and 5, while the Corvidae specimen is from sampling point 4. Passeriformes bones were found in all sampling sites (Tab. 3).

Three large mammal remains were found in the cave (Text-fig. 3). Two of these, a tooth and a proximal fragment of an ulna (Text-fig. 3a–b), probably belong to a small antelope. We compared the specimens with the Bovidae material of Csákvár. From Csákvár, Kretzoi (1951) described several Bovidae based on horn cores (*Tragoreas* cf. *oryxoides* SCHLOSSER, 1904, *Miotragocerus*(?) *csakvarensis* KRETZOI,



Text-fig. 3. Large mammal remains from Csodabogyós Cave. a: proximal fragment of Tragocerinae ulna (VER 2024.511), b: Tragocerinae molar (VER 2024.512), c: distal fragment of Mustelidae humerus (VER 2024.513).

Table 3. Vertebrate fauna of the Csodabogyós Cave.

Taxa	Number of specimens
Amphibians	
<i>Mioproteus caucasicus</i> ESTES et DAREVSKY, 1978	27
<i>Lissotriton vulgaris</i> (LINNEAUS, 1758)	3
Salamandridae indet.	58
cf. Palaeobatrachidae indet.	1
<i>Latonia</i> cf. <i>gigantea</i> (LARTET, 1851)	14
<i>Pelobates fuscus</i> LAURENTI, 1768	21
<i>Bufo bufo</i> (LINNEAUS, 1758)	3
<i>Bufo viridis</i> (LAURENTI, 1768)	3
<i>Hyla arborea</i> (LINNEAUS, 1758)	7
<i>Rana temporaria</i> LINNEAUS, 1758	5
<i>Pelophylax</i> kl. <i>esculentus</i>	3
Ranidae indet.	8
Anura indet.	228
Turtles	
<i>Emys orbicularis</i> LINNEAUS, 1758	27
<i>Testudo</i> cf. <i>kalksburgensis</i> TOULA, 1896	31
<i>Testudo</i> sp.	4
Testudines indet.	4
Lizards	
Lacertidae indet.	33
<i>Pseudopus</i> cf. <i>pannonicus</i> (KORMOS, 1911)	150
<i>Anguis fragilis</i> LINNEAUS, 1758	17
Anguidae indet.	124
Sauria indet.	36
Snakes	
<i>Hierophis viridiflavus</i> LACÉPÈDE, 1789	5
<i>Elaphe</i> cf. <i>paralongissima</i> SZYNDLAR, 1984	3
<i>Zamenis longissimus</i> (LAURENTI, 1768)	4
<i>Natrix tessellata</i> (LAURENTI, 1768)	4
<i>Natrix</i> sp.	18
Colubridae indet.	208
<i>Vipera</i> sp.	4
Aves	
Aves indet.	29
Passeriformes indet.	14
Corvidae indet.	1
Non-Passeriformes indet.	1
Phasianidae indet.	6
Mammals	
Erinaceomorpha	
<i>Schizogalerix</i> sp.	numerous
Erinaceidae gen. et sp. (various species)	numerous
Eulipotyphla	
Desmaninae gen. et sp.	numerous
Talpidae gen. et sp. (various species)	numerous
<i>Crusafontina kormosi</i> (BACHMAYER et WILSON, 1970)	1,107
“ <i>Petenya</i> ” <i>dubia</i> BACHMAYER et WILSON, 1970	1,328
<i>Asoriculus gibberodon</i> (PETÉNYI, 1864)	145
Soricinae gen. et sp. indet. 1.	4
Soricinae gen. et sp. indet. 2.	1

<i>Paenelimoecus repenningi</i> (BACHMAYER et WILSON, 1970)	50
Chiroptera	
<i>Rhinolophus grivensis</i> (DÉPÉRET, 1895)	19
<i>Rhinolophus lissiensis</i> MEIN, 1964	23
<i>Rhinolophus delphinensis</i> GAILLARD, 1899	5
<i>Myotis</i> cf. <i>bavaricus</i> ZIEGLER, 2003	34
<i>Myotis</i> aff. <i>gundersheimensis</i> HELLER, 1936	45
<i>Myotis</i> sp. indet. 1	10
<i>Myotis</i> sp. indet. 2	2
<i>Myotis</i> sp. indet. 3	5
<i>Myotis</i> sp. indet. 4	2
<i>Plecotus</i> cf. <i>atavus</i> TOPÁL, 1989	2
<i>Miniopterus</i> cf. <i>fossilis</i> ZAPFE, 1950	2
Rodentia	
<i>Csakvaromys sciurinus</i> KRETZOI, 1951	2
<i>Muscardinus pliocaenicus austriacus</i> (BACHMAYER et WILSON, 1970)	5
<i>Myomimus dehmi</i> (DE BRUJN, 1966)	227
<i>Vasseuromys</i> n. sp.	282
<i>Eomyops</i> sp.	1
<i>Keramidomys</i> sp.	2
<i>Eozapus intermedius</i> (BACHMAYER et WILSON, 1970)	52
<i>Neocricetodon</i> cf. <i>skofleki</i> (KORDOS, 1987)	783
<i>Microtoscopes</i> sp.	1
<i>Epimeriones austriacus</i> DAXNER-HÖCK, 1972	73
<i>Progonomys hispanicus</i> MICHAUX, 1971	68
<i>Apodemus lugdunensis</i> (SCHAUB, 1938)	989
<i>Prospalax petteri</i> BACHMAYER et WILSON, 1970	440
Carnivora	
Mustelidae indet.	1
Artiodactyla	
Tragocerinae indet.	2

1930, *Pikermicrus(?) platyceros* KRETZOI, 1930, *Graecoryx esterhazyi* KRETZOI, 1942, *Gazella capricornis* (WAGNER, 1848), *Gazella* sp.). However, the teeth could only be identified at the subfamily level (Tragocerinae div. sp.). Based on the material of Csákvár, we identified the antelope tooth from the Csodabogyós Cave as Tragocerinae indet. Based on the anterior-posterior diameter of the ulna (DAPmin = 28 mm; Text-fig. 3a), the specimen was slightly larger than *Miotragocerus monacensis* STROMER, 1928 (DAPmin = 26.2 mm; 12–11.6 Ma; Fuss et al. 2015). Its size may have been similar to that of the extant sitatunga (*Tragelaphus speki* SPEKE, 1863; DAPmin = 27 mm; body weight: 76 kg, body length: 1.5 m; Martínez-Navarro et al. 2004).

The third remain, a distal fragment of a radius (Text-fig. 3c), is most similar in morphology to that of a badger (Salesa et al. 2020), but is significantly smaller than the extant forms. In comparison, the humerus epicondylar width (HEW) of the specimen from the Csodabogyós Cave is 1.9 cm, and the HEW of the recent *Meles meles* (LINNAEUS, 1758) = 3.2 cm (Rose et al. 2014). Unfortunately, the literature and the comparative material did not allow a closer identification.

The following is a detailed discussion of small mammals in taxonomic order.

Phylum Vertebrata LINNAEUS, 1758
Class Mammalia LINNAEUS, 1758
Order Eulipotyphla WADDELL, OKADA et
HASEGAWA, 1999

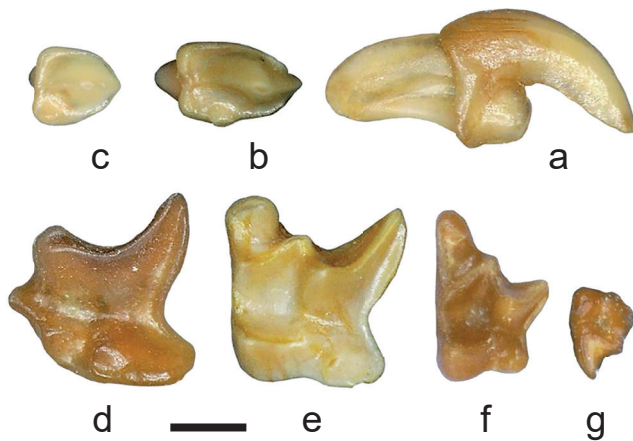
Comments. Many remains of various insectivorous mammals were found at the site. Of these, only the species of the Soricidae family are presented in this article. Other families belonging to the order Eulipotyphla and related groups (e.g., Erinaceidae, Talpidae, Dimylidae) are represented by approximately 1,500 remains, which will be reported in a later article. The morphological terms were used and measurements were taken after Reumer (1984), from his taxonomical description of Soricidae.

Family Soricidae FISCHER, 1817
Subfamily Soricinae FISCHER, 1817
Tribe Anourosoricini ANDERSON, 1879

Genus *Crusafontina* GIBERT, 1974

***Crusafontina kormosi* (BACHMAYER et WILSON, 1970)**
 Text-figs 4a–g, 5a–f

Material. 17 maxillary and 136 mandible fragments; in situ and separated teeth: 109 I1, 66 A1, 52 A2, 106 P4, 96 M1, 70 M2, 2 M3, 169 i1, 12 a1, 70 a2, 138 m1, 106 m2, 14 m3.

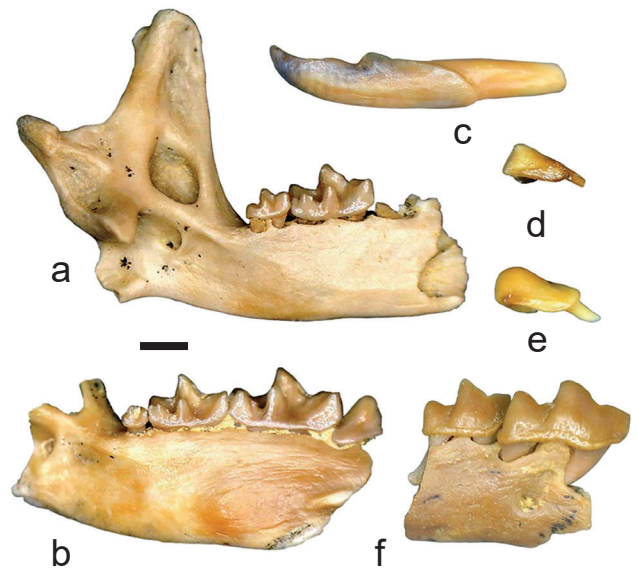


Text-fig 4. *Crusafontina kormosi*. a: right I1, buccal view (VER 2024.411.11), b: right A1, occlusal view (VER 2024.514.1), c: right A2, occlusal view (VER 2024.413.11), d: left P4, occlusal view (VER 2024.414.10), e: left M1, occlusal view (VER 2024.415.5), f: left M2, occlusal view (VER 2024.416.7), g: right M3, occlusal view (VER 2024.417.1). Scale bar = 1 mm.

Measurements. Raw measurement data are provided in the supplementary material, and summary data are presented in Table 4.

Description. No pigmentation is visible on the teeth.

Mandible. The ascending and horizontal rami form a slightly obtuse angle. As in all species of the tribe Anourosoricini, the coronoid process is widened, but the extent of this is different in the specimens. The internal



Text-fig 5. *Crusafontina kormosi*. a: left mandible fragment with m1, m2 and unreduced, two-rooted m3, lingual view (VER 2024.514.2), b: left mandible fragment with m2 and reduced, one-rooted m3, lingual view (VER 2024.514.3), c: left i1, buccal view (VER 2024.514.4), d: left a1, buccal view (VER 2024.419.1), e: left a2, buccal view (VER 2024.420.3), f: right mandible fragment with m1–m2, buccal view (VER 2024.514.5). Scale bar = 1 mm.

temporal fossa is deep and tight, its shape is subtriangular to round, and its size is from the most common *Crusafontina kormosi* to the typical size of *Amblycoptus oligodon* KORMOS, 1926. The external temporal fossa is shallow; the coronoid spicule usually starts from the antero-dorsal corner of the coronoid process and forms an angle of 45 degrees with the process. Both articular facets of the condyloid process are well-visible in the medial view. In the posterior view, the interarticular area is extremely narrow, the upper articular facet forms a perfect triangle, and the lower one is oblong. The medio-dorsal corner of the lower facet is slightly rounded. The mental foramen is tiny, situated in the middle of the mandibular tooth (m1) or a bit further back. In front of it, the broad and shallow muscular depression often extends almost until the teeth.

I1. The apex is sharp and strongly downturned. Its edge is slightly S-shaped. There is a conule and a cingulum at the basal margin of the buccal side. The conule is well-visible also in ventral view. The basal margin may be convex, straight or a little concave. The tooth is not fissident.

A1. It is an elongated tooth. Its main cone (the paracone) and the long edges before and behind it are situated on the buccal side, rather than in the sagittal plane. At the lingual margin, usually at about the 2/3 point of the tooth, there is a small protocone. A slightly smaller hypocone is situated in the postero-lingual corner. The buccal and the lingual cingula thin out forward.

A2. This single-rooted, triangular tooth is far smaller than A1. Its length and width are nearly the same. The large paracone is situated in the anterior corner. The cone and the short edge, reaching backwards from it, are in the sagittal plane. The tiny hypocone is in the postero-lingual corner. The buccal and lingual cingula thin out forward.

Table 4. Measurements of *Crusafontina kormosi* material from the Csodabogyós Cave. M2 values were only measured on the specimens that were unreduced and had talons. Unreduced, two-rooted and reduced, one-rooted m3 values are included in the table. The high values of standard deviations indicate an extremely diverse population morphology (see the text for more details). Abbreviations: SD – standard deviation, CV – coefficient of variation.

Tooth	Data	n	min–max	mean	SD	CV
I1	L	17	2.51–3.03	2.69	0.143	5.31
	H	17	1.68–2.15	1.89	0.132	6.96
A1	L	20	1.61–1.95	1.80	0.085	4.72
	W	20	0.98–1.37	1.20	0.100	8.33
A2	L	20	1.05–1.32	1.14	0.064	5.57
	W	20	0.88–1.12	1.01	0.062	6.19
P4	BL	20	2.22–2.71	2.50	0.136	5.43
	LL	20	1.42–1.71	1.57	0.093	5.88
	W	20	2.15–2.44	2.31	0.091	3.93
M1	LL	20	1.63–2.00	1.86	0.095	5.09
	BL	20	1.98–2.37	2.14	0.108	5.04
	AW	20	2.00–2.44	2.19	0.121	5.52
	PW	20	1.90–2.37	2.07	0.116	5.60
M2	LL	20	1.05–1.22	1.12	0.052	4.63
	BL	20	1.22–1.42	1.30	0.052	4.00
	AW	20	1.78–2.12	1.97	0.098	4.96
	PW	20	1.07–1.29	1.16	0.056	4.81
M3	L	2	0.98–1.00	0.99	0.017	1.75
	W	2	1.34–1.37	1.35	0.017	1.27
i1	L	20	4.66–5.61	5.01	0.257	5.12
	H	20	1.02–1.37	1.17	0.074	6.29
a1	L	5	1.07–1.39	1.27	0.126	9.90
	H	5	0.63–0.81	0.70	0.068	9.64
a2	L	5	1.66–1.88	1.77	0.087	4.92
	H	5	0.78–0.88	0.82	0.040	4.86
m1	L	20	2.27–2.64	2.44	0.098	4.03
	TRW	20	1.17–1.37	1.25	0.063	5.05
	TAW	20	1.17–1.32	1.25	0.047	3.77
m2	L	20	1.61–1.85	1.73	0.064	3.67
	TRW	20	0.95–1.12	1.01	0.040	3.92
	TAW	20	0.85–1.02	0.93	0.040	4.26
m3	L	8	0.71–1.20	1.01	0.151	14.99
	W	8	0.51–0.73	0.59	0.074	12.42

A3. It is a significantly reduced tooth between the postero-lingual corner of A2 and the antero-lingual one of P4. Its tiny cone (paracone) barely protrudes from the flat ventral surface.

P4. It is a trapezoid (or, more correctly, a pentagonal tooth, considering the position of the parastyle). There is a strong edge between the large paracone and the metastyle.

The protruding parastyle is situated nearer to the protocone than to the paracone. A deep valley separates the paracone and the well-developed hypocone. The posterior margin of the flat talon is strongly notched.

M1. The paracone and parastyle are slightly smaller than the metacone and metastyle, but they are all well-developed, whereas the mesostyle is quite short. As the metacone is situated somewhat more lingually than the paracone, the PW of this subquadrate tooth is slightly less than the AW. The trigone basin is deep, and is posteriorly closed by a metaloph. The posterior margin of the talon is concave.

M2. In most cases, this tooth is far less reduced than that in the dimylid shrew forms, but much shorter than M1. Nevertheless, the trigone of this specimen is very short and narrow, and all cones and styles are identifiable. The protocone, the paracone, the metacone and the parastyle are still large, but the hypocone and the metastyle are reduced. The metastyle is about as short as the mesostyle. There is a little notch on the posterior margin of the talon. At the same time, a shortened talon of M2 can be observed in some specimens. The hypocone of some of these teeth is reduced to a very small conule, while in others it disappears completely and the tooth thus becomes triangular.

M3. This is a very reduced triangular tooth. The relics of the protocone, metacone, and paracone are visible as tiny protuberances. The buccal angle may be identified as the parastyle, and a small mesostyle is also recognisable.

i1. In most cases, a bicuspluate tooth has a sharp lateral margin and upturned edge. In lateral view, the basal margin of its crown extends backwards almost until the back margin of a2. In several specimens, the cuspules are low and are only barely recognisable as small waves on the dorsal edge. This reduction may increase to such an extent that some teeth appear quite acuspulate.

a1. The single-rooted, unicuspid tooth, except for the slightly turned enormous paracone, is covered by a2 in occlusal view.

a2. It is very much like the a1 but is somewhat larger. The back part of the crown barely extends under m1 in lingual view, but to the middle of the molar in buccal view.

m1. The entostylid and the entoconid are separated. There may be a pre-, post-, and ectocingulid on the lower molars, but this is absent in most of the specimens. The entoconid crest joins the base of the metaconid.

m2. Its structure is like the m1, but it is smaller.

m3. Most of these tiny teeth are double-rooted. The hypoconid and entoconid are never separated on m3; talonids are reduced to one conid or a slight edge. On several teeth, the talonid is missing, and the teeth are single-rooted.

Comments. Most of the Anourosoricini specimens determined from this locality show the typical features of *Crusafontina kormosi*. However, some jaws and teeth are more similar to those of *Amblycoptus oligodon*, or exhibit a transitional morphology between the two species. Such a characteristic in the mandible, e.g., the narrowing of the internal temporal fossa. In the dentition, e.g., the reduction of the M2 trigone, the i1 becoming acuspulate, the shortening and becoming single-rooted of the m3 (Fig. 5a, b). But since we have found the upper and lower third molars (or at least their alveolus) on every maxilla or mandible preserved well

enough to examine this feature, we believe that *Amblycoptus* KORMOS, 1926 is not present in the fauna.

Several evolutionary events of the tribe Anourosoricini can be located in the Pannonian basin during the Late Miocene. Their first Vallesian representative, *Crusafontina endemica* GIBERT, 1974, is present in the Hungarian localities in MN 9–10 (Tab. 2). Its descendant, *C. kormosi*, became one of the dominant shrew species throughout the MN 11–13 (Mészáros 2000), while some of its isolated populations became the starting points for the development of new Anourosoricini forms. We infer that *Amblycoptus oligodon* appeared at the end of the MN 10 on this evolutionary branch, and then *Kordosia topali* (JÁNOSSY, 1972) developed from the latter species in the MN 13 (Mészáros 2000). The fauna living on the coastline and its coastal islands of the Pannonian Lake provided excellent opportunities for these evolutionary events.

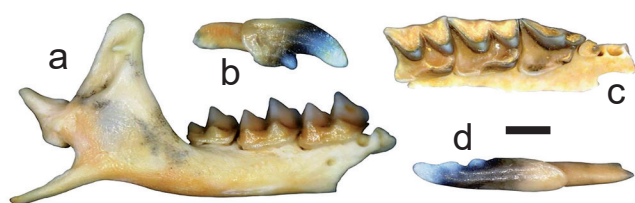
Tribe Blarinellini REUMER, 1998

Genus Blarinellini incertae sedis

“*Petenya*” *dubia* BACHMAYER et WILSON, 1970

Text-fig. 6a–d

Material. 88 maxillary and 307 mandible fragments; in situ and separated teeth: 107 I1, 103 A1, 1 A5, 128 P4, 212 M1, 167 M2, 13 M3, 47 i1, 2 a1, 13 a2, 279 m1, 274 m2, 89 m3.



Text-fig 6. “*Petenya*” *dubia*. a: right mandible fragment with m1, m2 and m3, buccal view (VER 2024.430.12), b: right I1, buccal view (VER 2024.515.1), c: right maxillary fragment with A4, P4, M1 and M2, occlusal view (VER 2024.515.2), d: left i1, buccal view (VER 2024.515.3). Scale bar = 1 mm.

Measurements. Raw measurement data are provided in the supplementary material, and summary data are presented in Table 5.

Description. A significant area of the teeth cones is whitely pigmented.

Mandible. The external temporal fossa usually extends ventrally to the level of the centre, but sometimes only to the top of the condyle. The coronoid spicule is short and is situated in the upper third of the coronoid process. The upper articular facet of the condyle is cylinder-shaped and makes an angle of about 45° with the lower facet. The interarticular area is broad. The internal temporal fossa is triangular, high, and is subdivided by a horizontal bar. The mandibular foramen is situated at the middle of the fossa. The mental foramen is placed under the re-entrant valley of M1.

Table 5. Measurements of “*Petenya*” *dubia* material from the Csodabogyós Cave. Abbreviations: SD – standard deviation, CV – coefficient of variation.

Tooth	Data	n	min–max	mean	SD	CV
I1	L	20	2.07–2.29	2.17	0.064	2.95
	H	20	1.20–1.34	1.27	0.040	3.17
P4	BL	20	1.42–1.59	1.52	0.051	3.38
	LL	20	0.98–1.17	1.07	0.044	4.09
	W	20	1.32–1.54	1.42	0.064	4.54
M1	LL	20	1.32–1.49	1.41	0.042	2.94
	BL	20	1.42–1.52	1.46	0.036	2.43
	AW	20	1.42–1.61	1.51	0.045	3.01
	PW	20	1.54–1.71	1.62	0.045	2.77
M2	LL	20	1.24–1.42	1.32	0.049	3.66
	BL	20	1.27–1.37	1.31	0.028	2.10
	AW	20	1.49–1.74	1.56	0.062	3.95
	PW	20	1.39–1.59	1.46	0.048	3.26
M3	L	7	0.56–0.63	0.59	0.022	3.73
	W	7	1.17–1.32	1.25	0.074	5.91
i1	L	20	3.51–3.86	3.69	0.096	2.61
	H	20	0.83–0.93	0.87	0.031	3.51
m1	L	20	1.44–1.71	1.58	0.060	3.77
	TRW	20	0.76–0.93	0.83	0.039	4.68
	TAW	20	0.76–0.98	0.90	0.053	5.89
m2	L	20	1.34–1.61	1.47	0.065	4.38
	TRW	20	0.78–0.93	0.86	0.035	4.03
	TAW	20	0.79–0.93	0.87	0.028	3.27
m3	L	20	1.12–1.24	1.18	0.038	3.23
	W	20	0.66–0.78	0.71	0.039	5.48

I1. The upper incisor is not fissident. Its superior and posterior margins form a acute angle. There is a broad buccal cingulum along the convex basal margin. The tip of the talon is sharp and pigmented, the apex is long, down-curved and similarly coloured.

AA sup. The first antemolar has a little second cusp beside the main cone, on the lingual cingulum. Only a few in situ A5 are present in the material, but the alveolus of the last antemolar is well identifiable in front of P4 in all maxillary fragments.

P4. The linguallly-placed parastyle is in contact with the paracone by a parastylar crest. The protocone forms an antero-lingual corner. The hypocone is only slightly raised from the ridge of the extended hypoconal flange. The posterior emargination is very slightly concave.

M1–M2. Their trigones are posteriorly closed by a low metaloph. AW < PW on M1 but AW > PW on M2. The hypocone is not developed; only the ridge is present on the deeply excavated hypoconal flange. The posterior margin is very slightly concave.

M3. The third upper molar is reduced, only its trigone is present. Paracone and parastyle are well-developed, the

protocone is small, and a tiny third conule is present on the postero-lingual margin of the relatively deep trigone basin.

i1. The mandibular incisor is bicuspluate, the cusps are whitely pigmented. In most of the specimens, the cingulum does not appear on the buccal side, but some i1 have a barely visible buccal cingulid, only on the upper part of the basal margin. On the symphyseal side, the cingulum is always present.

aa inf. a1 has only one conid, but a2 seems to be two-cusped in buccal view. A broad cingulum is present on both sides of the mandibular antemolars.

m1–m2. The entoconid is placed very close to the metaconid, and a high entoconid crest connects them together. Cingula are weak, but the buccal one is somewhat more developed than the lingual one. The oblique crest is present, has a strongly lingual direction, and is near the metaconid.

m3. The talonid of the third lower molar is not basined; it is reduced to one conid. The cingulum is weak on both sides.

Comments. “*Petenyia*” *dubia* was originally described by Bachmayer and Wilson (1970) from Kohfidisch as *Petenyia dubia* nov. spec. The species name expressed doubt, because the authors were not sure whether this form belonged to the genus *Petenyia*.

Reumer presented a comparative list of the distinction between *Blarinella* THOMAS, 1911 and *Petenyia* KORMOS, 1934 (Reumer 1984: 66), and classified *dubia* as *Blarinella*, based on these characters. Several authors, including Rabeder (1985), Rzebik-Kowalska (1989), Kordos (1991), and Mészáros (1996, 1998, 1999), have adopted this classification. Storch (1995), who has conducted a detailed investigation of recent and fossil *Blarinella* species in Asia, disagrees with Reumer’s argument for generic reclassification and lists significant differences between *Blarinella dubia* and fossil *Blarinella* species. Ziegler (2006) and Furió et al. (2014) agree with Storch’s conclusion, and mention the species name in its original combination.

Bachmayer and Wilson (1970) mention that a sufficiently intact maxilla was not available in the type material to determine *dubia*’s dental formula, and this was the main reason for their uncertainty regarding the taxonomic position of the findings. However, based on the exceptionally rich *dubia* material described by Mészáros (1999) from Polgárdi, it is certain that the dental formula is 163/123, which differs from the dentition of *Petenyia* in the presence of the fifth upper antemolar. The dental formula and many differences of the mandible from that of *Petenyia hungarica* KORMOS, 1934 (e.g., the division of the internal temporal fossa, the shape of the external one, the position and shape of the spiculum coronoideum) are confirmed by the Csodabogyós material described above.

Based on the above, we are of the opinion that *dubia* does not belong to the *Petenyia* genus. At the same time, we accept the result of Storch (1995), that *Blarinella* is not a suitable classification either. Therefore, we consider it necessary to establish a new genus for the *dubia* species. Until this is confirmed, the species will be referred to by the original genus name, but in quotation marks: “*Petenyia*” *dubia*.

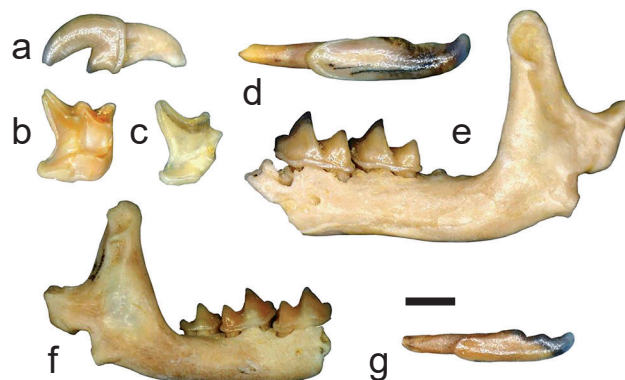
Tribe Neomyini MATSCHIE, 1909

Genus *Asoriculus* KRETZOI, 1959

Asoriculus gibberodon (PETÉNYI, 1864)

Text-fig. 7a–e

Material. 1 maxillary and 36 mandible fragments; in situ and separated teeth: 16 I1, 1 A1, 2 A2, 10 P4, 7 M1, 11 M2, 32 i1, 3 a2, 22 m1, 17 m2, 9 m3.



Text-fig. 7. *Asoriculus gibberodon*. a: left I1, buccal view (VER 2024.433.6), b: right M1, occlusal view (VER 2024.435.5), c: right P4, occlusal view (VER 2024.434.2), d: right i1, buccal view (VER 2024.437.4), e: left mandible fragment with m1 and m2, buccal view (VER 2024.438.1), f: right mandible fragment with m1, m2 and m3, buccal view (VER 2024.445.4), g: right i1, buccal view (VER 2024.446.6). Scale bar = 1 mm.

Measurements. Raw measurement data are provided in the supplementary material, and summary data are presented in Table 6.

Description. The very tips of the teeth are pigmented, but the original colour of the pigmentation is not identifiable.

Mandible. The coronoid process of the mandible is high, with a concave anterior margin. The interarticular area of the condyle is narrow, the upper articular facet is cylindrical, and the lower one is strongly elongated in a lingual direction. The mandibular foramen is situated under the posterior part of the internal temporal fossa. The mental foramen is below the re-entrant valley of the protocone. The internal temporal fossa is relatively high and narrow, and continues upwards as a shallow groove into the upper part of the process. The external temporal fossa is shallow, and reaches halfway down the condyle. The coronoid spicule is short, and situated at the fossa’s upper third. The lower margin of the horizontal ramus is concave.

I1. The upper incisor is slightly fissident. A weak cingulum surrounds the convex posterior margin. The tip of the talon is pointed.

A1–A2. The first upper antemolar is subquadrate, the second one is rather quadrate. Besides the main cone, both of them have a small cusplet on the lingual margin.

P4. The parastyle is protruding, and connected to the high paracone by a narrow parastylar crest. The protocone is separated from the well-developed hypocone by a wide valley. The hypoconal flange is bordered by a high ridge, and the posterior margin is strongly concave.

Table 6. Measurements of *Asoriculus gibberodon* material from the Csodabogyós Cave. Abbreviations: SD – standard deviation, CV – coefficient of variation.

Tooth	Data	n	min–max	mean	SD	CV
I1	L	6	1.52–1.73	1.61	0.078	4.83
	H	6	1.09–1.22	1.16	0.049	4.19
P4	BL	2	1.46–1.51	1.48	0.035	2.32
	LL	2	0.85–0.85	0.85	–	–
	W	2	1.41–1.46	1.43	0.035	2.40
M1	LL	6	1.39–1.48	1.43	0.036	2.50
	BL	6	1.40–1.46	1.42	0.024	1.71
	AW	6	1.46–1.56	1.52	0.037	2.43
	PW	6	1.63–1.78	1.70	0.052	3.06
M2	LL	5	1.22–1.31	1.24	0.040	3.23
	BL	5	1.22–1.31	1.29	0.040	3.09
	AW	5	1.56–1.73	1.64	0.080	4.86
	PW	5	1.43–1.51	1.47	0.037	2.51
i1	L	5	2.82–2.87	2.85	0.026	0.90
	H	5	0.78–0.82	0.80	0.018	2.30
m1	L	6	1.31–1.53	1.44	0.075	5.19
	TRW	6	0.65–0.85	0.77	0.078	7.79
	TAW	6	0.74–0.92	0.82	0.064	7.79
m2	L	5	1.26–1.43	1.34	0.072	5.33
	TRW	5	0.68–0.87	0.77	0.079	10.26
	TAW	5	0.72–0.87	0.77	0.068	8.73
m3	L	5	0.88–1.02	0.97	0.052	5.34
	W	5	0.54–0.68	0.59	0.053	8.91

M1–M2. All the cones of the trigone are well-developed, and the trigone basin is very deep. A weak and low metaloph is present. The protocone and the hypocone are separated by a narrow valley, which has a small cingulum at the lingual margin. The metastyle of M1 protrudes, but it protrudes less in M2. Therefore, PW relative to AW is significantly less at M2, while AW < PW at M1. The anterior margin bends obliquely next to the protocone. The hypocone is slightly more lingually placed than the protocone, but this is more pronounced in M1 than in M2. The talon is short, because the posterior margin is deeply notched.

i1. Short and bicuspluate tooth, of which the anterior cuspule is long and low. The apex is strongly upturned. A buccal cingulum is present along the posterior part of the tooth, not only dorsally, but also reaching the ventral margin.

a1–a2. The lower antemolars have cingula on both sides. There is only one cusp in a1, but a2 has two cusps.

m1–m2. The entoconid crest is present in m1–m2. The lingual end of the postcrisid and the entoconid are separated by a deep valley. The cingula are present on either the buccal or lingual sides.

m3. The buccal cingulum is weak and slightly undulated, and the lingual one is less developed. The talonid is basined, and possesses both entoconid and hypoconid. The talonid is narrower than the trigonid.

Comments. The specimens described here are somewhat larger than those from Tardosbánya (Mészáros 1998: tab. 5) and Polgárdi (Mészáros 1999: tab. 10). The difference is more pronounced in the case of the remains from Tardosbánya. However, the size range of the Csodabogyós Cave shrews overlaps with the remains of shrews from both Turolian sites.

Soricinae gen. et sp. indet. 1

Material and measurements. 1 M1 (LL: 1.38, BL: 1.34, AW: 1.34, PW: 1.61); 2 M2 (LL: 1.07–1.15, BL: 1.13–1.34, AW: 1.34–1.51, PW: 1.32–1.34); 1 i1 (L: 2.44, H: 0.81).

Description. The molars and the lower incisors are very similar in their morphology to *Asoriculus gibberodon* teeth.

Comments. The teeth are significantly smaller in size than the abovementioned *Asoriculus* specimens. Based on this, it cannot be ruled out that another species of the genus is also present at the site. However, the few teeth found are not enough to make a detailed taxonomic determination.

Soricinae gen. et sp. indet. 2

Material and measurements. 1 M1 (LL: 0.98, BL: 0.98, AW: 0.91, PW: 0.98).

Description. In the occlusal view, M1 is square-shaped, and only AW is slightly smaller than PW. The posterior margin is much less concave.

Comments. A small shrew species, about the size of *Paenelimnoecus repenningi* described next, but its M1 morphology is completely different. The pigmentation and dental features are very similar to “*Petenyia*” *dubia*.

Subfamily Allosoricinae FEJFAR, 1966

Genus *Paenelimnoecus* BAUDELOT, 1972

Paenelimnoecus repenningi (BACHMAYER et WILSON, 1970)

Text-fig. 7f, g

Material. 5 maxillary and 19 mandible fragments; in situ and separated teeth: 5 I1, 6 P4, 1 M1, 4 M2, 10 i1, 12 m1, 7 m2, 2 m3.

Measurements. Raw measurement data are provided in the supplementary material, and summary data are presented in Table 7.

Description. **Mandible.** The upper facet of the condyloid process is oval, the lower one is lingually barely elongated, and the interarticular area is short and narrow. The coronoid process is high and narrow; its top is rounded. The internal temporal fossa is subtriangular and higher than wide. It continues upwards as a shallow basin into the upper part of the process. The inferior margin of the fossa is backwardly ascending. The mandibular foramen is placed

Table 7. Measurements of *Paenelimnoecus repenningi* material from the Csodabogyós Cave. Abbreviations: SD – standard deviation, CV – coefficient of variation.

Tooth	Data	n	min–max	mean	SD	CV
I1	L	2	1.12–1.14	1.13	0.017	1.52
	H	2	0.80–0.83	0.82	0.024	2.94
P4	BL	3	1.04–1.07	1.06	0.014	1.32
	LL	3	0.75–0.80	0.78	0.024	3.13
	W	3	0.97–1.00	0.98	0.014	1.43
M1	LL	1	–	0.98	–	–
	BL	1	–	1.00	–	–
	AW	1	–	1.22	–	–
	PW	1	–	1.22	–	–
M2	LL	1	–	0.88	–	–
	BL	1	–	0.98	–	–
	AW	1	–	1.22	–	–
	PW	1	–	1.22	–	–
i1	L	4	2.24–2.44	2.34	0.081	3.80
	H	4	0.63–0.65	0.64	0.012	1.90
m1	L	9	1.12–1.34	1.21	0.077	6.29
	TRW	9	0.61–0.68	0.64	0.027	4.22
	TAW	9	0.61–0.73	0.65	0.039	5.90
m2	L	4	1.12–1.20	1.16	0.031	2.64
	TRW	4	0.63–0.68	0.66	0.026	3.88
	TAW	4	0.64–0.68	0.66	0.016	2.45
m3	L	2	0.83–0.93	0.88	0.066	7.40
	W	2	0.51–0.57	0.54	0.045	8.24

under the middle of the fossa. The external temporal fossa is narrow; its lower part bends backwards. The long coronoid spicule is situated at the upper quarter of the fossa temporalis externa, and reaches the width of the fossa transversally. The lower margin of the mandibular corpus is straight or only slightly concave.

I1. A slight buccal cingulum is apparent, but a lingual cingulum is absent. The posterior margin is straight or slightly convex.

P4. The tooth is much wider than long. The weak parastyle turns towards the buccal side and is situated close to the large paracone. A separate hypocone is absent on the ridge of the hypoconal flange, but the protocone is present.

M1–M2. The metastyle is longer than the parastyle. The mesostyle is well-developed. The metacone is a little higher than the paracone. The trigone basin is deep and open on M1, but a small metaloph is visible on M2. The protocone is the lowest cone. Hypocone is absent on the ridge of the hypoconal flange. The posterior emargination is deeply notched.

i1. There is no cingulum on the buccal side of the short and bicuspidate mandibular incisor.

m1–m2. An entoconid crest is absent. The lingual end of the postcrisid is separated from the entoconid. The buccal and lingual cingulids are weak.

m3. The talonid is reduced to a single cusp. Weak cingulids are present both on the buccal and lingual sides.

Comments. *Paenelimnoecus repenningi* is a typical shrew species of the Pannonian Basin, having been recorded from several sites in Hungary, including Rudabánya, Sümeg, Csákvár, Tardosbánya and Polgárdi. The morphology and dimensions of the specimens described here correspond to those of other *Paenelimnoecus* finds from the Pannonian Basin, as listed by Mészáros (2000).

Order Chiroptera BLUMENBACH, 1779

Comments. The bat material was less numerous and more poorly preserved than that of insectivores and rodents. Most of the Chiroptera assemblage consisted of isolated teeth and fragments; intact maxillae or mandibles did not occur in the sample. Only a small portion of the nearly 300 remains could be taxonomically determined. The morphological terms used and measurements taken (in mm) are based on Van Valen (1966), Menu (1985), and Horáček and Špoutil (2012).

Family Rhinolophidae GRAY, 1825

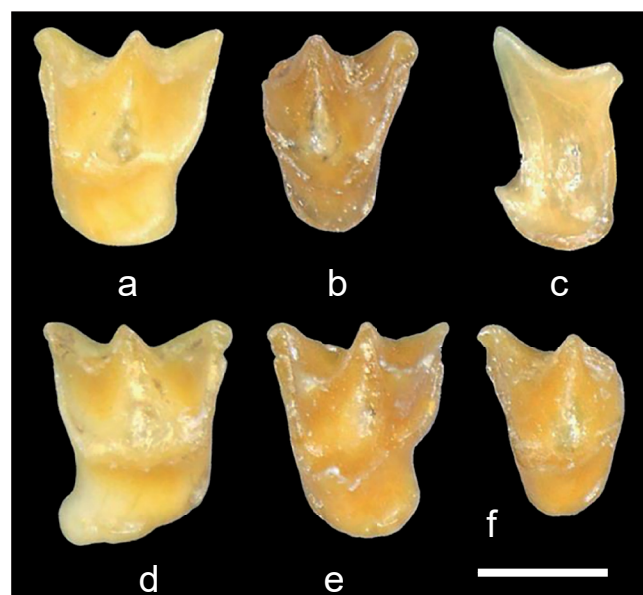
Genus *Rhinolophus* LACÉPÈDE, 1799

Rhinolophus grivensis (DEPÉRET, 1892)

Text-figs 8c–f, 10a

Material. 1 mandible fragment with m2, 1 mandible fragment with m3; isolated teeth: 3 c1, 2 p4, 2 m2, 2 m3, 1 P4, 1 M1, 4 M2, 1 M3.

Measurements. Raw measurement data are provided in the supplementary material, and summary data are presented in Table 8.



Text-fig. 8. *Rhinolophus lissiensis*. a: left M2 (VER 2024.402.19), b: right M3 (VER 2024.402.21). *Rhinolophus grivensis*. c: right P4 (VER 2024.400.12), d: right M1 (VER 2024.400.14), e: left M2 (VER 2024.400.15), f: left M3 (VER 2024.400.18). All in occlusal view. Scale bar = 1 mm.

Table 8. Measurements of *Rhinolophus grivensis* material from the Csodabogyós Cave. Abbreviations: SD – standard deviation, CV – coefficient of variation.

Tooth	Data	n	min–max	mean	SD	CV
P4	L	1	–	1.07	–	–
	W	1	–	1.22	–	–
	H	1	–	0.98	–	–
M1	L	1	–	1.46	–	–
	W1	1	–	1.46	–	–
	W2	1	–	1.80	–	–
M2	L	4	1.42–1.49	1.45	0.037	2.56
	W1	4	1.46–1.61	1.53	0.075	4.88
	W2	3	1.76–1.80	1.79	0.028	1.58
M3	L	1	–	1.17	–	–
	W1	1	–	1.32	–	–
	W2	1	–	1.22	–	–
c1	L	3	0.97–0.97	0.97	0.000	0.00
	W	3	0.88–0.97	0.93	0.049	5.26
	H	3	1.81–1.96	1.84	0.080	4.27
p4	L	2	0.98–1.22	1.10	0.172	15.71
	W	2	0.73–1.07	0.90	0.242	26.76
	H	2	1.26–1.61	1.44	0.242	16,81
m2	L	2	1.41–1.56	1.49	0.104	6.96
	TRW	2	0.83–0.83	0.83	0.000	0.00
	TAW	2	0.88–0.88	0.88	0.000	0.00
m3	L	2	1.32–1.32	1.32	0.000	0.00
	TRW	2	0.73–0.73	0.73	0.000	0.00
	TAW	2	0.73–0.73	0.73	0.000	0.00

Description. c inf. The crown base is subquadrate in occlusal view, its mesiolabial corner is round, and the posterior face is concave. The teeth have a well-developed cingulid, which forms a small cusplule disto-labially.

p4. The tooth is low and not pointed. It is subquadrate in occlusal view, and its cingulid is absent on the lingual side. The posterior face is concave, and the labial side is flat.

mm inf. The m2 is slightly longer and wider than the m3. The postcrisid is low and does not reach the hypoconulid, forming a wide postentoconid valley. The metaconid is located disto-lingually of the protoconid, forming a trigonid angle, wider on m2 and narrower on m3. The cingulid is continuous, but it is absent on the labial side.

P4. The tooth is almost oblong-shaped in occlusal view, and its lingual side is roundish. The postparacrista is short and slightly bent disto-labially; a mesio-lingual crest reaches the crown-base and forms a small cusplule on the mesial cingulum. The talon is linguallly extended. The distal face is concave, the mesial and labial faces are flat. The cingulum is continuous, and slightly narrower on the labial side.

MM sup. In M1 and M2, the ectoftexis shows a regular W form. The preprotocrista and paracingulum are continuous, as are the postprotocrista and metacingulum. The talon of M1 has a triangular projection directed posteriorly and

lingually. In the case of M2, the elongation of the talon is less pronounced; in M3, it does not appear. In M3, the postmetacrista is absent; therefore, no metastyle is present. The preprotocrista continues into the paracingulum, and the postprotocrista reaches its base below the metacone, but the metacingulum is absent. Metaloph, hypocone, paraconule and metaconule are absent on all teeth.

Comments. *Rhinolophus grivensis* is the smallest of the Csodabogyós *Rhinolophus* species (Text-fig. 10). The species, described from MN 7 La Grive, is reported primarily as “cf. *grivensis*” from at least 16 sites of MN 3 to MN 15 age. In short, the name widely used to denote the smallest Miocene *Rhinolophus* is also applied in our case, due to correspondence in dimensions, the morphology of p4, and the fact that the trigonid and talonid widths of m3 are the same.

Rhinolophus lissiensis MEIN, 1964

Text-figs 8a, b, 10b

Material. 1 maxillary fragment with P2–M2; isolated teeth: 2 p3, 3 p4, 2 m1, 3 m2, 3 C1, 1 P3, 2 P4, 1 M1, 2 M2, 3 M3.

Measurements. Raw measurement data are provided in the supplementary material, and summary data are presented in Table 9.

Description. p3. It is a single-rooted, tiny tooth, wider than long, with a broad cingulid. It has one central cusp, and slight mesial and distal crests.

p4. It is subtriangular in occlusal view, and the crown of the tooth forms a low pyramid. The posterior face is concave, and the labial side is flat. The thick cingulid is bent downwards on the labial side, and it is absent on the lingual side.

mm inf. The m1 is slightly longer than the m2, and the talon of m2 is somewhat wider. The postcrisid is low and does not reach the hypoconulid, forming a wide postentoconid valley. The metaconid is located disto-lingually of the protoconid, forming a trigonid angle, wider on m1, and narrower on m2. The cingulid is continuous, but it is absent on the labial side.

C sup. The tooth has a strong root and is oval-shaped in cross-section; the crown is curved distally. The labial face is convex, and the lingual face is flat; strong mesial and distal crests separate these. The cingulum is continuous; it is broad on the lingual side and curved on the labial one.

P2. It is ovoid in occlusal view, and it is wider than it is long. The teeth have one low cusp and a continuous cingulum.

P4. The tooth is almost oblong-shaped in occlusal view, and its lingual side is roundish. The postparacrista is short and slightly bent disto-labially. The talon is linguallly extended. The lingual face is concave, the mesial and labial faces are flat. The cingulum is continuous, it is slightly narrower on the labial side.

MM sup. The M1 is subquadrangular, and M2 is wider than long. In M1 and M2, the ectoftexis shows a regular W form. The preprotocrista and the paracingulum are continuous, and the postprotocrista and the metacingulum

Table 9. Measurements of *Rhinolophus lissiensis* material from the Csodabogyós Cave. Abbreviations: SD – standard deviation, CV – coefficient of variation.

Tooth	Data	n	min–max	mean	SD	CV
C1	L	3	1.27–1.37	1.33	0.056	4.22
	W	3	0.98–1.12	1.02	0.085	8.25
	H	3	2.15–2.68	2.51	0.400	12.37
P2	L	1	–	0.49	–	–
	W	1	–	0.58	–	–
P4	L	2	0.93–0.98	0.95	0.034	3.59
	W	2	1.22–1.42	1.32	0.138	10.48
	H	1	–	1.17	–	–
M1	L	1	–	1.46	–	–
	W1	1	–	1.22	–	–
	W2	1	–	1.80	–	–
M2	L	2	1.32–1.46	1.39	0.104	7.44
	W1	2	1.22–1.66	1.44	0.311	21.57
	W2	2	1.71–1.81	1.76	0.069	3.90
M3	L	3	1.02–1.17	1.12	0.085	7.53
	W1	3	1.46–1.56	1.50	0.056	3.77
	W2	3	1.12–1.31	1.25	0.110	8.75
p3	L	2	0.93–1.02	0.97	0.070	7.07
	W	2	0.63–0.68	0.65	0.036	5.51
p4	L	3	0.93–1.07	1.00	0.074	7.38
	W	3	0.78–0.97	0.84	0.113	13.32
	H	3	1.17–1.31	1.24	0.074	5.97
m1	L	2	1.61–1.66	1.63	0.035	2.11
	TRW	2	0.73–0.78	0.76	0.035	4.56
	TAW	2	0.83–0.88	0.85	0.035	4.04
m2	L	3	1.46–1.66	1.54	0.102	6.58
	TRW	3	0.78–0.83	0.80	0.028	3.49
	TAW	3	0.88–0.92	0.90	0.028	3.11

as well. The talon of M1 has a triangular projection directed posteriorly and lingually. The M2 has a less pronounced elongation of the talon; it looks like a broad cingulum. In M3, it does not appear. In M3, the postmetacrista is absent; therefore, a metastyle is not present. The preprotocrista continues into the paracingulum, and the postprotocrista reaches its base below the metacone; a metacingulum is absent. Metaloph, hypocone, paraconule and metaconule are missing on all teeth.

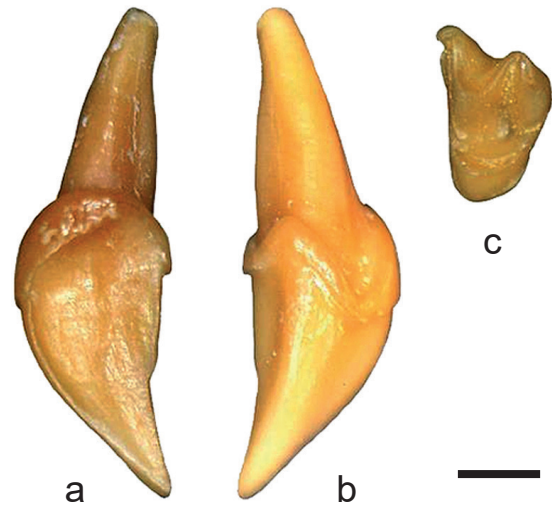
Comments. The teeth are slightly larger than *Rhinolophus grivensis* and much smaller than *R. delphinensis* (Text-fig. 10). Mein (1964) separated *lissiensis* as a subspecies within *R. grivensis*. Topál (1974) proposed an independent species status for *lissiensis*, based on the Osztramos material. However, Ziegler (2003) did not accept this suggestion, citing a “lack of sufficient morphological and size differences”. Although the current material is far from sufficient to discuss this topic, we are inclined to follow

Topál’s proposal, expecting, in analogy with our current fauna, a higher taxonomic diversity of Pliocene small- to medium-sized *Rhinolophus*. Since the p4 is morphologically the same as the figure of *R. grivensis lissiensis* published by Mein (1964), and differs from the teeth of *R. grivensis* as described above, we affiliate the respective form of these specimens to *R. lissiensis*.

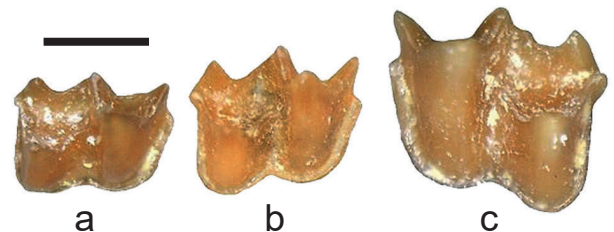
***Rhinolophus delphinensis* GAILLARD, 1899**

Text-figs 9a–c, 10c

Material. Isolated teeth: 1 m2, 3 C1, 1 M3.



Text-fig. 9. *Rhinolophus delphinensis*. a: right C1 in lingual view, b: right C1 in buccal view (VER 2024.401.4), c: left M3 (VER 2024.401.5) in occlusal view. Scale bar = 1 mm.



Text-fig. 10. Size comparison of *Rhinolophus* species. a: *Rhinolophus grivensis* right m2 (VER 2024.400.8), b: *Rhinolophus lissiensis* right m2 (VER 2024.402.7), c: *Rhinolophus delphinensis* left m2 (VER 2024.401.1). All in occlusal view. Scale bar = 1 mm.

Measurements. Raw measurement data are provided in the supplementary material, and summary data are presented in Table 10.

Description. m2. The tooth is robust, its talon is wide, metaconid is situated disto-lingually of the protoconid. The posteristid approaches behind the entoconid but does not reach it. The lingual cingulid is absent; on the other side of the tooth, the cingulid is broad and continuous.

C sup. The tooth has a strong root, and it is oval-shaped in cross-section; the crown is curved distally. The labial face is convex, and the lingual face is flat; these are separated by strong mesial and distal crests. The cingulum is continuous and curved.

Table 10. Measurements of *Rhinolophus delphinensis* material from the Csodabogyós Cave. Abbreviations: SD – standard deviation, CV – coefficient of variation.

Tooth	Data	n	min–max	mean	SD	CV
C1	L	3	1.80–2.19	1.98	0.197	9.95
	W	3	1.56–1.70	1.61	0.085	5.27
	H	3	3.26–3.66	3.41	0.213	6.24
M3	L	1	1.61	–	–	–
	W1	1	1.75	–	–	–
	W2	1	1.65	–	–	–
m2	L	1	2.14	–	–	–
	TRW	1	1.07	–	–	–
	TAW	1	1.22	–	–	–

M3. The preparacrista and postparacrista are almost the same length, the premetacrista is distinctly shorter, and the postmetacrista is completely absent. The preprotocrista is short, the postprotocrista is longer. Since there is no paraloph and metaloph, a relatively wide central valley is formed. The cingulum is continuous, but the metacingulum is thin.

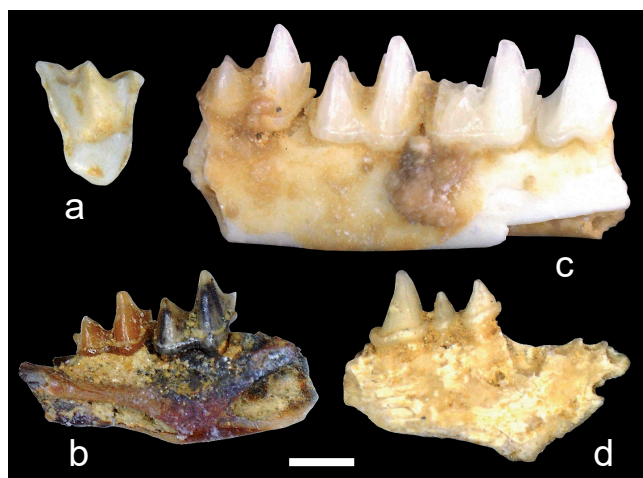
Comments. *Rhinolophus delphinensis* is the largest of the Csodabogyós *Rhinolophus* species (Text-fig. 10). The dimensions and morphology of the few teeth described here correspond to those of *Rhinolophus delphinensis* from Petersbuch, La Grive and Lisseu material (Tab. 2).

Family Vespertilionidae GRAY, 1821
Subfamily Vespertilioninae GRAY, 1821

Genus *Myotis* KAUP, 1829

***Myotis cf. bavaricus* ZIEGLER, 2003**
 Text-fig. 11a, b

Material. 1 maxillary fragment with P4; isolated teeth: 2 c1, 4 p4, 2 m1, 1 m2, 2 m3; 12 C1, 4 M1, 4 M2, 2 M3.



Text-fig. 11. *Myotis cf. bavaricus*. a: right M1 (VER 2024.405.25) in occlusal view, b: right mandible fragment with m2–m3 (VER 2024.405.7) in buccal view. *Myotis aff. gundersheimensis*. c: right mandible fragment with p4–m3 (VER 2024.403.7) in buccal view. *Myotis* sp. indet. 1. d: right mandible fragment with p2–p4 (VER 2024.404.3) in buccal view. Scale bar = 1 mm.

Table 11. Measurements of *Myotis cf. bavaricus* material from the Csodabogyós Cave. Abbreviations: SD – standard deviation, CV – coefficient of variation.

Tooth	Data	n	min–max	mean	SD	CV
C1	L	12	0.82–1.12	1.01	0.083	8.25
	W	12	0.68–0.92	0.79	0.072	9.14
	H	10	1.36–1.95	1.61	0.177	10.97
P4	L	1	1.12	–	–	–
	W	1	0.87	–	–	–
	H	1	0.97	–	–	–
M1	L	3	1.46–1.65	1.59	0.113	7.06
	W1	4	1.65–2.04	1.82	0.201	10.99
	W2	4	1.61–2.19	1.89	0.299	15.84
M2	L	3	1.36–1.41	1.39	0.028	2.02
	W1	4	1.51–1.75	1.59	0.108	6.77
	W2	4	1.46–1.80	1.58	0.152	9.56
M3	L	2	0.92–1.02	0.97	0.069	7.03
	W1	2	1.56–1.80	1.68	0.173	10.25
	W2	2	1.17–1.41	1.29	0.173	13.34
c1	L	2	0.87–0.92	0.90	0.035	3.84
	W	2	0.78–0.78	0.78	–	–
	H	2	1.12–1.46	1.29	0.242	18.7
p4	L	4	0.63–0.92	0.78	0.169	21.67
	W	4	0.48–0.63	0.60	0.084	13.84
	H	4	1.12–1.31	1.21	0.101	8.32
m1	L	2	1.31–1.36	1.34	0.035	2.58
	TRW	2	0.78–0.82	0.80	0.035	4.31
	TAW	2	0.87–0.87	0.87	–	–
m2	L	1	1.26	–	–	–
	TRW	1	0.78	–	–	–
	TAW	1	0.68	–	–	–
m3	L	2	1.12–1.41	1.26	0.207	16.33
	TRW	2	0.73–0.82	0.78	0.069	8.79
	TAW	2	0.58–0.68	0.63	0.069	10.93

Measurements. Raw measurement data are provided in the supplementary material, and summary data are presented in Table 11.

Description. **c inf.** Relatively low crowned tooth; the lingual side of the crown is slightly shorter than the root, but on the labial side, they are the same in length. The cusp is slightly curved backwards. In the occlusal view, the cusp is triangular, its lingual side is flat, the labial one is convex, and the distal one is concave. A well-developed cingulum surrounds the cusp. The mesial crest joins a mesio-lingual cingular cuspule. The disto-lingual and disto-labial crests connect the posterior cingulid. A bigger lingual and a smaller labial cusp are present on the posterior cingulid.

p4. It is a two-rooted tooth surrounded by a well-developed cingulum, wavy labial margin, and small antero-

and postero-lingual cuspids. The shape of the p4 is elongated in occlusal view. The cusp curves slightly backwards, the lingual side is flat, the distal side is concave, and the antero-labial surface is convex.

mm inf. All molars are myotodont. Relative molar size: $m1 \approx m2 > m3$. The protoconid is tall and robust, while para-, meta-, hypo- and entoconids are lower and nearly equal in height. The paralophid is angular. The trigonid is narrower than the talonid on $m1$ – $m2$ but is reversed on $m3$. The metaconid is situated slightly distally to the protoconid. The crista obliqua and the entocristid are short. The postcristid forms a V-shaped notch from the posterior view. Cingulid is continuous on three sides, but the lingual side is missing.

C sup. The sharp cusp curves slightly posteriorly and is surrounded by a well-developed cingulum. The labial face is convex, while the lingual one is slightly concave.

P4. The paracone is high; the postparacrista is slightly bent disto-labially. The cingulum is stronger on the mesial and lingual sides, weaker on the buccal side. A small mesio-lingual cingular tubercle is present in one of the specimens.

M1–M2. The metastyle is much longer than the parastyle, and the labial margin is oblique. This is less pronounced in M2 than in M1. Para- and metaloph are not present. The preprotocrista is continuous with the paracingulum, and extends to the parastyle.

M3. The protocone, preprotocrista, postprotocrista, paracone and preparacrista are well-developed, but the postparacrista and premetacrista are shorter. The metacone has a more lingual position than the paracone, and the postmetacrista is absent. A weak paracingulum is present.

Comments. *Myotis bavaricus* is a medium-sized *Myotis* form. The specimens from Csodabogyós are similar in measurements and morphology to the material described by Ziegler (2003) from Petersbuch.

***Myotis aff. gundersheimensis* HELLER, 1936**

Text-fig. 11c

Material. 1 mandible fragment with p4, 1 mandible fragment with p4–m3, 1 mandible fragment with p4–m1, 1 mandible fragment with m1–m2, 1 mandible fragment with m2, 1 mandible fragment with m3; isolated teeth: 4 p4, 8 m1, 1 m2, 5 m3, 6 C1, 5 P4, 2 M1, 4 M2, 5 M3.

Measurements. Raw measurement data are provided in the supplementary material, and summary data are presented in Table 12.

Description. **p4.** It is a two-rooted tooth, surrounded by a well-developed cingulum, with a wavy labial side, and with small postero-lingual cuspids. The shape of the p4 is oblong in occlusal view. The apex slightly curves backwards, the lingual side of the cusp is flat, the distal side is concave, and the antero-labial surface is convex.

mm inf. All molars are myotodont – relative molar size: $m1 \approx m2 > m3$. The protoconid is tall and robust, while para-, meta-, hypo- and entoconids are lower and nearly equal in height. The trigonid is narrower than the talonid on $m1$ – $m2$, but is reversed on $m3$. The $m1$ – $m2$ metaconid is situated slightly distal to the protoconid, but not on $m3$.

Table 12. Measurements of *Myotis aff. gundersheimensis* material from the Csodabogyós Cave. Abbreviations: SD – standard deviation, CV – coefficient of variation.

Tooth	Data	n	min–max	mean	SD	CV
C1	L	6	0.92–1.22	1.22	0.114	10.49
	W	6	0.87–0.97	0.91	0.048	5.24
	H	3	1.61–1.95	1.82	0.185	10.15
P4	L	5	1.07–1.36	1.22	0.111	9.05
	W	3	0.92–1.07	0.99	0.074	7.46
	H	5	1.07–1.75	1.28	0.279	21.70
M1	L	2	1.56–1.56	1.56	–	–
	W1	2	1.61–1.65	1.63	0.035	2.12
	W2	2	1.61–2.04	1.82	0.310	16.97
M2	L	4	1.61–1.70	1.64	0.047	2.85
	W1	4	1.95–2.04	1.97	0.049	2.45
	W2	4	1.85–2.04	1.91	0.092	4.82
M3	L	5	0.82–0.96	0.88	0.064	7.20
	W1	5	1.65–1.90	1.84	0.106	5.74
	W2	5	1.31–1.46	1.41	0.060	4.24
p4	L	7	0.87–1.12	1.03	0.082	7.96
	W	7	0.58–0.82	0.71	0.072	10.17
	H	7	1.17–1.46	1.29	0.105	8.09
m1	L	11	1.46–1.61	1.53	0.045	2.94
	TRW	11	0.68–0.92	0.84	0.079	9.37
	TAW	11	0.92–1.07	0.98	0.049	4.98
m2	L	5	1.51–1.70	1.58	0.082	5.19
	TRW	5	0.82–0.96	0.91	0.064	6.97
	TAW	5	0.97–1.02	1.00	0.026	2.62
m3	L	6	1.31–1.61	1.43	0.101	7.06
	TRW	6	0.82–0.97	0.86	0.066	7.59
	TAW	6	0.69–0.78	0.73	0.036	4.93

The talonid basin is open from three directions, because the crista obliqua, the postcristid, and the entocristid are short and steeply sloping. The labial, mesial and distal cingulid are present; the lingual one is missing.

C sup. The crown is shorter than the root. The cusp slightly bends posteriorly, and is surrounded by a well-developed, slightly wavy cingulum. The labial face of the cusp is convex, while the lingual one is slightly concave. A small disto-labial crest extends to the distal cingulum.

P4. The tooth is subtriangular in occlusal view. The paracone is obtuse, the postparacrista is slightly bent disto-labially. The cingulum continues around the tooth, but is stronger on the mesial and lingual sides than on the buccal and distal ones.

M1–M2. The metastyle is slightly longer than the parastyle. Paraloph and metaloph are not present. The preprotocrista is continuous with the paracingulum. The postprotocrista slopes steeply in the distal direction and does not reach the metacingulum, so the protofossa is open posteriorly. Metacone is not present.

M3. The preparacrista is long, the postparacrista is shorter. The premetacrista and metacone are present, but the postmetacrista and metastyle are absent. The preprotocrista is in contact with the paracingulum, the postprotocrista is short and steeply sloping. The paracingulum runs continuously along the front of the tooth, but the postcingulum is present only on the lingual half of the posterior margin.

Comments. Based on its dimensions, the form described here clearly belongs to the medium-sized category of *Myotis* species: it is closest to *M. kormosi* HELLER, 1936 (Gundersheim, MN 16; Horáček and Trávníčková 2019).

In the species-level definition, the morphology of p4 is the most essential character. This tooth of *Myotis kormosi* is square in occlusal view and taller than the protoconid of m1. In our specimens, it is longer and narrower (oblong-shaped) and not higher than m1. Our p4s are most similar in morphology and size to those of *M. gundersheimensis* (described from the same locality; Trávníčková 2016), but the m1 and m2 of that species are slightly shorter than those of our specimens. Based on the p4 morphology, we observe a closer relationship with *M. gundersheimensis*; therefore, the specimens from Csodabogyós are classified here as *Myotis* aff. *gundersheimensis*. This taxonomy is supported by the stratigraphic fact that *M. gundersheimensis* was also found in sites older than Gundersheim, e.g., Osztramos 1 (Tab. 2).

***Myotis* sp. indet. 1**

Text-fig. 11d

Material. 1 mandible fragment with p2–p4, 1 maxillary fragment with M1; isolated teeth: 1 c1, 3 p4, 3 m1, 2 m3, 1 M1, 1 M2.

Measurements. Raw measurement data are provided in the supplementary material, and summary data are presented in Table 13.

Description. **c1.** The shape of this low-crowned canine is round in occlusal view. The tip is barely curved backwards. The distal surface of the cusp is concave; the labial surface is convex. A small mesial edge extends to the well-developed, wavy cingulid.

p2. The shape of this unicuspid tooth is round in occlusal view. This cusp is higher than the p3 situated posterior to it.

p3. It is very similar to p2, but lower and shorter.

p4. In occlusal view, it is a rectangular tooth with rounded corners. The tip is curved very slightly backwards. The labial face of the conid is flat, the distal face is concave and the labial face is convex. The cingulid is well-developed around the tooth. There are distal and mesial cusps on the cingulid.

mm inf. All molars are myotodont. The protoconid is tall and robust. The paralophid is rounded. The metaconid is situated bucco-lingually in line with the protoconid, which is why the trigonid basin is tight. The postcristid forms a wide U-shaped notch in posterior view. The crista obliqua and entocristid are short and steep. TrW < TIW on m2 and TrW > TIW on m3.

MM sup. The postmetacrista is longer than the premetacrista and postparacrista, so the ectoloph is oblique. The preprotocrista joins the paracingulum. A paraloph is

Table 13. Measurements of *Myotis* sp. indet. 1 material from the Csodabogyós Cave. Abbreviations: SD – standard deviation, CV – coefficient of variation.

Tooth	Data	n	min–max	mean	SD	CV
M1	L	1	1.07	–	–	–
	W1	1	1.80	–	–	–
	W2	–	–	–	–	–
M2	L	–	–	–	–	–
	W1	1	1.90	–	–	–
	W2	1	1.85	–	–	–
c1	L	1	0.87	–	–	–
	W	1	0.78	–	–	–
	H	1	1.26	–	–	–
p2	L	1	0.58	–	–	–
	W	1	0.58	–	–	–
p3	L	1	0.43	–	–	–
	W	1	0.58	–	–	–
p4	L	3	0.87–0.96	0.92	0.049	5.29
	W	3	0.73–0.73	0.73	–	–
	H	3	1.26–1.17	1.22	0.049	3.98
m1	L	3	1.56–1.61	1.57	0.028	1.80
	TRW	3	0.78–0.97	0.87	0.098	11.16
	TAW	3	0.92–1.07	0.99	0.074	7.49
m3	L	2	1.36–1.46	1.41	0.069	4.90
	TRW	2	0.82–0.87	0.85	0.035	4.06
	TAW	2	0.68–0.73	0.70	0.035	4.90

present, the postparacrista slopes steeply backwards and does not reach the height of the cingulum. A paraloph is absent, which is why the protofossa is wide and open in the posterior direction. The paracingulum is wide.

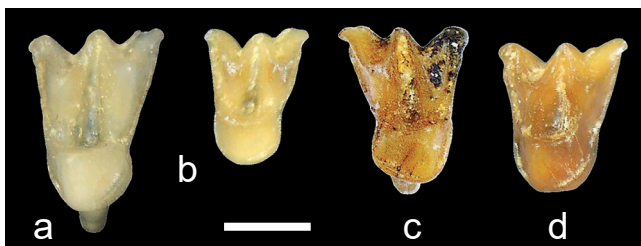
Comments. This form is distinguished from the other medium-sized *Myotis* species of the Csodabogyós locality by the combination of the following morphological characters: small c1, reduced p3, the shape of paralophid and postcristid on m1, the morphology of M1–M2. These characters resemble the morphological variation in the Early Pliocene clade *Myotis delicatus*-*M. subtilis*.

***Myotis* sp. indet. 2**

Text-fig. 12a

Material and measurements. Isolated teeth: 1 left M2 (L: 1.56, W1: 2.04, W2: 1.59), 1 right M2 (L: 1.36, W1: 1.85, W2: 1.75).

Description. **M2.** Because the postmetacrista is elongated, the ectoloph forms an irregular W-shape. The preprotocrista is continuous with the paracingulum. The postprotocrista extends to a weak metacingulum. Neither para- nor metaloph is present.



Text-fig. 12. *Myotis* sp. indet. 2. a: left M2 (VER 2024.406.1). *Myotis* sp. indet. 3. b: left M2 (VER 2024.407.5). *Myotis* sp. indet. 4. c: right M1 (VER 2024.408.1). *Plecotus* cf. *atavus*. d: left M1 (VER 2024.410.2). All in occlusal view. Scale bar = 1 mm.

Comments. A medium-sized *Myotis* species, but somewhat larger than the above-mentioned *Myotis* sp. indet. 1, considered to be an alternative a member of the *Myotis gundersheimensis* group.

Myotis sp. indet. 3

Text-fig. 12b

Material. Isolated teeth: 1 c1, 2 C1, 2 M2.

Measurements. Raw measurement data are given in the supplementary material, and summary data are presented in Tab. 14.

Table 14. Measurements of *Myotis* sp. indet. 3 material from the Csodabogyós Cave. Abbreviations: SD – standard deviation, CV – coefficient of variation.

Tooth	Data	n	min–max	mean	SD	CV
C1	L	2	0.82–0.97	0.90	0.104	11.52
	W	2	0.63–0.73	0.68	0.072	10.53
	H	2	1.61–1.65	1.63	0.035	2.12
M2	L	2	1.12–1.12	–	–	–
	W1	2	1.46–1.46	–	–	–
	W2	2	1.41–1.41	–	–	–
c1	L	1	0.78	–	–	–
	W	1	0.73	–	–	–
	H	1	1.17	–	–	–

Description. **c inf.** It is a low-crowned tooth. The well-developed cingulid has a smaller distal and a larger mesio-labial cusp.

C sup. It is an oval-shaped tooth in occlusal view, with a flat lingual and a convex buccal surface. The tip is slightly curved backwards. The cingulum continues around the tooth.

M2. The metastyle is slightly longer than the parastyle, causing the irregular W-shape of the ectoloph. The preprotocrista is continuous with the wide paracingulum. The postprotocrista joins the metaloph. The paraloph is present, therefore, the protofossa is closed and tight. The weak metacingulum is continuous.

Comments. This form is the smallest *Myotis* species in the sample. The small size of the tiny c1 and the short M2 distinguish this form from all others of the *Myotis* species in the sample.

Myotis sp. indet. 4

Text-fig. 12c

Material and measurements. Isolated teeth: 1 M1 (L: 1.41, W1: 1.65, W2: 1.70), 1 M2 (W1: 1.65, W2: 1.70).

Description. **M1–M2.** The ectoloph has a regular W-shape, with a mesostyle at the central position and all buccal styles in a straight single line. The preprotocrista is continuous with the paracingulum. A paraloph is present. The postprotocrista is short and steep along a distinct hypoconal undulation of the protocone wall. Metaloph is absent, so the protofossa opens widely backwards. A weak metacingulum is present.

Comments. This form is a medium-sized *Myotis* species.

Genus *Plecotus* GEOFFROY, 1818

Subgenus *Corynorhinus* ALLEN, 1865

Plecotus cf. *atavus* TOPÁL, 1989

Text-fig. 12d

Material and measurements. 1 maxillary fragment with M1 (L: 1.36, W1: 1.80, W2: 1.85); isolated tooth M1 (L: 1.41, W1: 1.69, W2: 1.51).

Description. **M1.** The preprotocrista is continuous with the paracingulum. The postprotocrista is directed towards the lingual base of the metacone. The para- and metaconule, and the para- and metaloph are absent, as typical of the genus, similarly as the high protocone complex lacks the hypoconal undulation. The tooth is surrounded by a well-developed cingulum, which is thicker on the lingual side.

Comments. The material from the Csodabogyós Cave is insufficient for an exact species identification. The measurements correspond to the data of *Plecotus atavus* type material from Polgárdi 4, *Plecotus* aff. *atavus* from Gritsev and *Plecotus* aff. *atavus* from Petersbuch 6, 18 specimens (Tab. 2).

Subfamily *Miniopterinae* DOBSON, 1875

Genus *Miniopterus* BONAPARTE, 1837

Miniopterus cf. *fossilis* ZAPFE, 1950

Material and measurements. Isolated teeth: 1 M1 (L: 1.36, W1: 1.76, W2: 1.95), 1 M3 (L: 0.92, W1: 1.65, W2: 1.26).

Description. **M1.** The shape of the tooth is sub-quadrangular. The anterior cingulum is wide, the labial cingulum is small, and the mesostyle is narrow. The tooth has a small hypocone, which is connected to the protocone. A wide cingulum covers the small talon.

M3. It is a subtriangular tooth with a wide anterior cingulum. The metacone is absent, as are the metastyle and the postmetacrista. The postprotocrista is short, and the talon is reduced.

Comments. The low number and poor preservation of the specimens do not allow for a more precise definition. However, the shape of the teeth leaves no doubt that they belong to the genus *Miniopterus* (Woloszyn 1987, Ziegler 2003, Mansino et al. 2016). The dimensions of both teeth are significantly smaller than in extant *Miniopterus schreibersii* (Kuhl, 1817), Early Pliocene *Miniopterus aproximatus* WOLOSZYN, 1988 (comp. also Popov 2004), and *Miniopterus rummeli* ZIEGLER, 2003 from MN 7 Petersbuch 6. In this respect, it seems roughly equivalent to *Miniopterus fossilis* ZAPFE, 1950, reported from Neudorf a. March (= Devínska Nová Ves), Goldberg and Petersbuch 7 (Tab. 2). This supports the persistence of more clades of the genus, as demonstrated in the MN 7 stage, in the European Late Miocene.

Order Rodentia BOWDICH, 1821

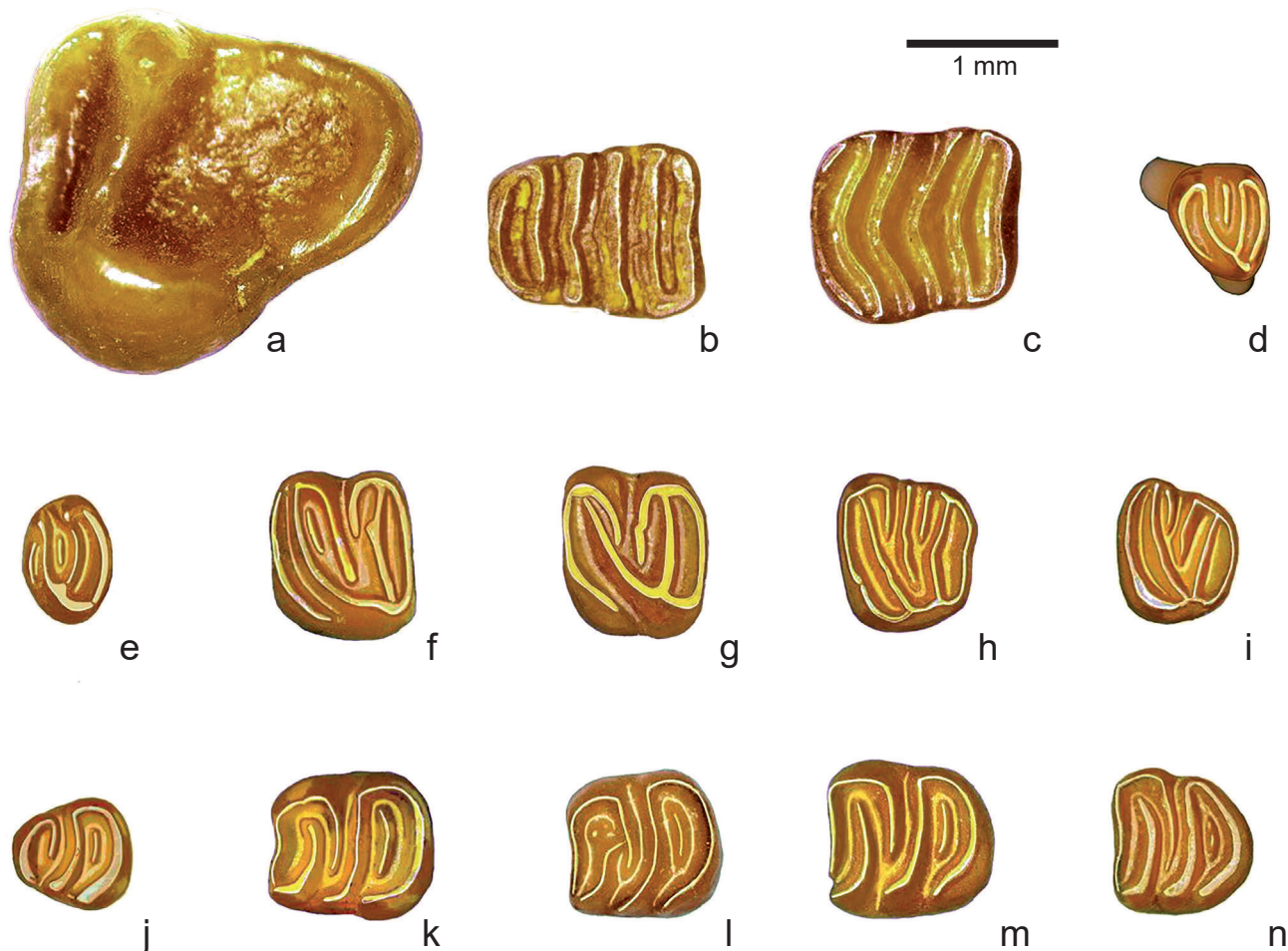
Comments. Many remains of various rodent mammals were found at the site. *Neocricetodon* cf. *skofleki* (KORDOS, 1987) and *Vasseuromys* n. sp., are not discussed in this paper. A detailed description of these two species is given in two separate papers in this volume (Hír 2025, Hír et al. 2025). The morphological terms in the taxonomical description of rodent taxa used are after Cuenca-Bescós (1988) (Sciuridae),

De Bruijn (1966) and Freudenthal (2004) (*Myomimus*, *Vasseuromys*), van den Hoek Ostende (2003) (*Muscardinus*) and Daxner-Höck and Höck (2015) (Eomyidae, Dipodidae, Cricetidae, Muridae and Anomalomyidae).

Family Sciuridae GRAY, 1821 Subfamily Sciurinae GRAY, 1821

Genus *Csakvaromys* KRETZOI, 1951

Nomenclature and history in short. Kretzoi (1951: 409) introduced the new genus and species “*Csákváromys sciurinus*” from the MN 11 *Hipparion* fauna of Csákvár, Eszterházy Cave (Fejér County). De Bruijn and Mein (1968) created a junior synonym, *Spermophilinus* (Kretzoi and Fejfar 2005), which has become more commonly used in the literature. De Bruijn and Bosma (2012) suggested the preference of the name *Spermophilinus* DE BRUIJN ET MEIN, 1968 because, referring to their opinion, the type material of *Csakvaromys* “is too poor to allow identification at the species level”. Sinitsa et al. (2022) and Sinitsa and Čermák (2024) questioned and refuted the argumentation of De Bruijn and Bosma (2012), providing a detailed history and nomenclatural deduction. As a result, they concluded that the name *Csakvaromys* has priority.



Text-fig. 13. Occlusal surfaces of sciurid and glirid teeth. *Csakvaromys sciurinus*. a: M3 reversed (VER 2024.453.2). *Muscardinus pliocaenicus austriacus*. b: m1 (VER 2024.452.3), c: m2 (VER 2024.452.4). *Myomimus dehmi*. d: D4, reversed (VER 2024.454.1), e: P4 (VER 2024.455.6), f: M1–2 (VER 2024.456.8), g: M1–2, reversed (VER 2024.456.16), h: M3 (VER 2024.457.3), i: M3 (VER 2024.457.6), j: p4 (VER 2024.459.4), k: m1 (VER 2024.460.2), l: m1 (VER 2024.460.35), m: m2 (VER 2024.461.14), n: m3 (VER 2024.462.3).

Csakvaromys sciurinus KRETZOI, 1951

Text-fig. 13a

Material. 1 P4 fr., 1 M3.

Measurements. Raw measurement data are provided in the supplementary material.

Description. **P4.** The outline is subtriangular. The mesial and the labial margins are worn. Four cusps: parastyle, protocone, paracone, metacone. Four transversal ridges: anteroloph, protoloph, metaloph, posteroloph. The parastyle is the smallest and lowest cusp on the antero-labial side. The protocone is the strongest and highest cusp; it occupies the lingual side of the occlusal surface. The lingual ends of the protoloph, metaloph and posteroloph are connected to the center of the protocone. The connection of the metaloph to the protocone is weak. The anteroloph is at a lower level; its lingual end connects to the anterior basis of the protocone. Three transversal sinuses: anterosinus, central sinus, posterosinus. The central sinus is the widest, and the posterosinus is the narrowest. Its lingual end is anteriorly curved.

M3. The outline is subtriangular. Two cusps: the large protocone and a smaller, higher paracone. Three lophs: anteroloph, protoloph, posteroloph. The transversal anteroloph connects the anterior bases of the two cusps. The transversal protoloph is present between the centers of these cusps. The anteroloph is at a low. A narrow, transversal anterosinus is surrounded by the two lophs. The semicircular posteroloph surrounds a large central sinus. Three roots.

Comments. The measurements of the M3 from the Csodabogyós Cave exceed the corresponding dimension ranges of *Csakvaromys bredai* (SCHLOSSER, 1884) from Felsőtárkány 3/2 (Hír 2003), Tauț (Hír et al. 2011), La Grive (Van de Weerd 1976) and Sansan (Ginsburg and Mein 2012). Still, they are referable to the ranges of *C. turolensis* from Maramena (De Bruijn 1995).

The *Csakvaromys* species are frequent elements of the microvertebrate faunas from the Early Miocene up to the Pliocene in Europe and Anatolia. During this long period, only minor changes were observed in dental morphology. The most significant evolutionary trend was the subsequent size increase, particularly in the case of M1–2s (De Bruijn 1995).

Family Gliridae THOMAS, 1897

Genus Muscardinus KAUP, 1829

Muscardinus pliocaenicus austriacus

BACHMAYER et WILSON, 1970

Text-fig. 13b, c

Material. 1 M3, 1 p4, 1 m1, 2 m2.

Measurements. Raw measurement data are provided in the supplementary material.

Description. **M3.** Subrectangular flat occlusal surface. The anterior margin is wider than the rounded posterior one.

7 complete ridges. The 2nd and the 6th ridges are vestigial and only present on the labial side.

p4. Oval occlusal surface. Four transversal ridges. The 1st and 3rd ones are short, and the 2nd and 4th ones are longer, reaching from the lingual margin to the labial margin. There are weak lingual connections between the 1st–2nd and the 3rd–4th ridges.

m1. Subrectangular flat occlusal surface. The anterior margin is narrower than the posterior one. 6 transversal ridges. The labial and lingual ends of the 1st and 2nd ridges are connected. 3rd and 4th ridges are free-ended on both sides. 5th and 6th ridges have a lingual connection.

m2. Rectangular flat occlusal surface, less elongated than the m1. The posterior margin is narrower than the anterior one. The anterior margin is slightly anteriorly arched. 6 transversal ridges. The central regions of the 2nd, 3rd, 4th, and 5th ridges are anteriorly arched. The lingual and labial ends of the 1st and 2nd ridges are connected. The 5th and 6th ridges have the same connection.

m3. Rectangular flat occlusal surface. The oblique posterior margin is narrower than the anterior one. Six complete ridges. The lingual and labial ends of the 1st and 2nd ridges are connected, like the lingual and labial ends of the 5th and 6th ridges. The ends of the other ridges are free.

Comments. The material is limited, but classification at the species or subspecies levels is possible.

- The *Muscardinus* material of the Csodabogyós Cave differs from *Muscardinus hispanicus* DE BRUIJN 1966 from Pedregueras, Spain (MN 9) in the larger dimensions of m2.
- The *Muscardinus* material of the Csodabogyós Cave differs from *M. pliocaenicus* KOWALSKI, 1963 from Węże, Poland (MN 15) in the more complex pattern of the occlusal surface of p4: having four transversal ridges. (*M. pliocaenicus* has only three transversal ridges). Bachmayer and Wilson (1970) modified the systematic status of the Polish species as subspecies: *M. pliocaenicus pliocaenicus* (KOWALSKI, 1963).
- The *Muscardinus* material of the Csodabogyós Cave is referable to *M. pliocaenicus austriacus* BACHMAYER et WILSON, 1970 from Kohfidisch, Austria (MN 11) because the similarity in morphology of p4 and in the dimensions of m2.

According to Daxner-Höck and Höck (2009), there is a close relationship between the taxa *Muscardinus hispanicus*, *M. pliocaenicus austriacus* and *M. pliocaenicus pliocaenicus*. Most probably, *M. pliocaenicus austriacus* is derived from *M. hispanicus*. In Austria, the latest occurrence of *M. hispanicus* is Richardhof-Wald. The earliest occurrence of *M. pliocaenicus austriacus* is in Schernham (Tab. 2). The biochronological range of this subspecies is MN 10–11.

The latest summary work on the evolution and systematics of the genus *Muscardinus* KAUP, 1829 is given by García-Alix et al. (2008). Three evolutionary lines are distinguished. Only one of them leads to the recent *Muscardinus avellanarius* (LINNAEUS, 1758). The species *M. hispanicus* and *M. pliocaenicus* are the Late Miocene – Pliocene members of this line. Referring to Daxner-Höck and Höck (2009), the *Muscardinus* specimens from Eichkogel and Kohfidisch are transitional forms between the Miocene (MN 9, MN 10) *M. hispanicus* and Pliocene (MN 14–16) *M.*

plioaenicus from Poland. The most significant evolutionary trends of this lineage are the reduction of accessory ridges and an increase in size (Nadachowski and Daoud 1995, Kowalski 1997).

Subfamily Myomiminae DAAMS, 1981

Genus *Myomimus* OGNEV, 1924

***Myomimus dehmi* DE BRUIJN, 1966**

Text-fig. 13d–n

Material. Isolated teeth: 1 D4, 26 P4, 56 M1–2, 30 M3, 1 d4, 15 p4, 35 m1, 32 m2, 31 m3.

Measurements. Raw measurement data are provided in the supplementary material, and summary data are presented in Table 15.

Description. **D4.** Text-fig. 13d. Triangular outline with rounded corners. 4 main transversal ridges: anteroloph, protoloph, metaloph, posteroloph. The protoloph, metaloph, and posteroloph are lingually connected in the protocone. Labial connections are anteroloph-protoloph to the paracone, and metaloph-posteroloph to the metacone. The lingual end of the anteroloph is free, and terminates at the anterior surface of the protocone. One centrally positioned, isolated ridge (anterior centroloph?) is present between the protoloph and the metaloph. Three diverging roots.

P4. Text-fig. 13e. 23 teeth are suitable for the morphological description. Oval outline. 4 main transversal ridges: anteroloph, protoloph, metaloph, posteroloph. The protoloph, metaloph, and posteroloph are always connected to the endoloph. The length of the anteroloph is variable. In 8 cases, only the labial part is present. One ridge (= anterior centroloph?) is found in all molars between the protoloph and the metaloph. In one case (no. 1196), an anterior centroloph and a short, posterior centroloph are present. Three roots.

M1–M2. Text-fig. 13f, g. 56 molars are suitable for the morphological description. We discuss the M1 and M2 positions together, because the distinction between the two molars is not always unambiguous. The outline is rectangular,

and the occlusal surface is concave. The lingual margin is rounded, and free of any ornamentation and of a cingulum. Six main transversal ridges: anteroloph, protoloph, anterior centroloph, posterior centroloph, metaloph and posteroloph. The connections of the anteroloph are variable: the labial end is mainly connected (or very close) to the paracone (53 specimens). The lingual end is mainly free; in four cases, it is fused to the endoloph. A completely isolated anteroloph is rare (3 specimens). A short, labially positioned prototrope is frequent (33 specimens). A short and labially positioned metatrope occurs in 18 cases. The protoloph is regularly connected to the endoloph and the paracone. The metaloph is regularly connected to the endoloph and the metacone. The labial end of the anterior centroloph is connected to the paracone. The labial end of the posterior centroloph is connected to the metacone. The lingual ends of the centrolophs can be either free or fused (22 specimens). The anterior centroloph is longer than the posterior one. The posterosinus is closed. Three roots.

M3. Text-fig. 13h, i. 30 molars are suitable for a morphological description. Rectangular outline. The posterior margin is shorter. The labial margin is concave. Four main transversal ridges: anteroloph, protoloph, metaloph and posteroloph. All of them are connected to the endoloph. Anterior and posterior centrolophs are developed. In 19 cases, the posterior centroloph is longer, and 11 cases, the anterior centroloph is longer. In one case, the two centrolophs are equal in length. In 9 molars, the centrolophs are fused. The additional ridges are short and labially positioned. A metatrope is found in 11 specimens. Prototrope is visible in 3 teeth. Prototrope and metatrope together are found in 1 molar. Posterotrope is developed in 1 case. The occurrence of a centrotrope is visible in 3 molars. Three roots.

d4. Triangular outline. In the anterior portion, the labial end of the metalophid is anteriorly curved and reaches the anteroconid. In the posterior portion, the labial end of the mesolophid is posteriorly curved and reaches the central part of the posterolophid. No additional ridges. One root.

p4. Text-fig. 13j. 17 teeth are suitable for a morphological description. Triangular outline, larger than d4. In the anterior portion, the curved anterolophid is regular. The metalophid is regular, but its connections are variable: in 8 cases, the

Table 15. Measurements of *Myomimus dehmi* material from the Csodabogyós Cave. Abbreviations: SD – standard deviation, CV – coefficient of variation.

Tooth	Length					Width				
	n	min–max	mean	SD	CV	n	min–max	mean	SD	CV
D4	1	–	0.64	–	–	1	–	0.80	–	–
P4	26	0.56–0.80	0.68	0.055	8.07	26	0.64–1.05	0.87	0.086	9.90
M1–2	57	0.91–1.06	0.98	0.042	4.26	56	0.90–1.26	1.12	0.069	6.14
M3	30	0.77–0.95	0.86	0.043	4.98	30	0.90–1.12	1.00	0.048	4.81
d4	1	–	0.70	–	–	1	–	0.60	–	–
p4	15	0.70–0.83	0.70	0.036	4.63	15	0.63–0.83	0.70	0.047	6.72
m1	35	0.94–1.15	1.06	0.042	3.94	34	0.85–1.08	0.97	0.046	4.76
m2	32	0.95–1.13	1.04	0.043	4.13	32	0.95–1.09	1.01	0.038	3.76
m3	31	0.83–1.06	0.95	0.059	6.19	31	0.83–1.05	0.91	0.062	6.79

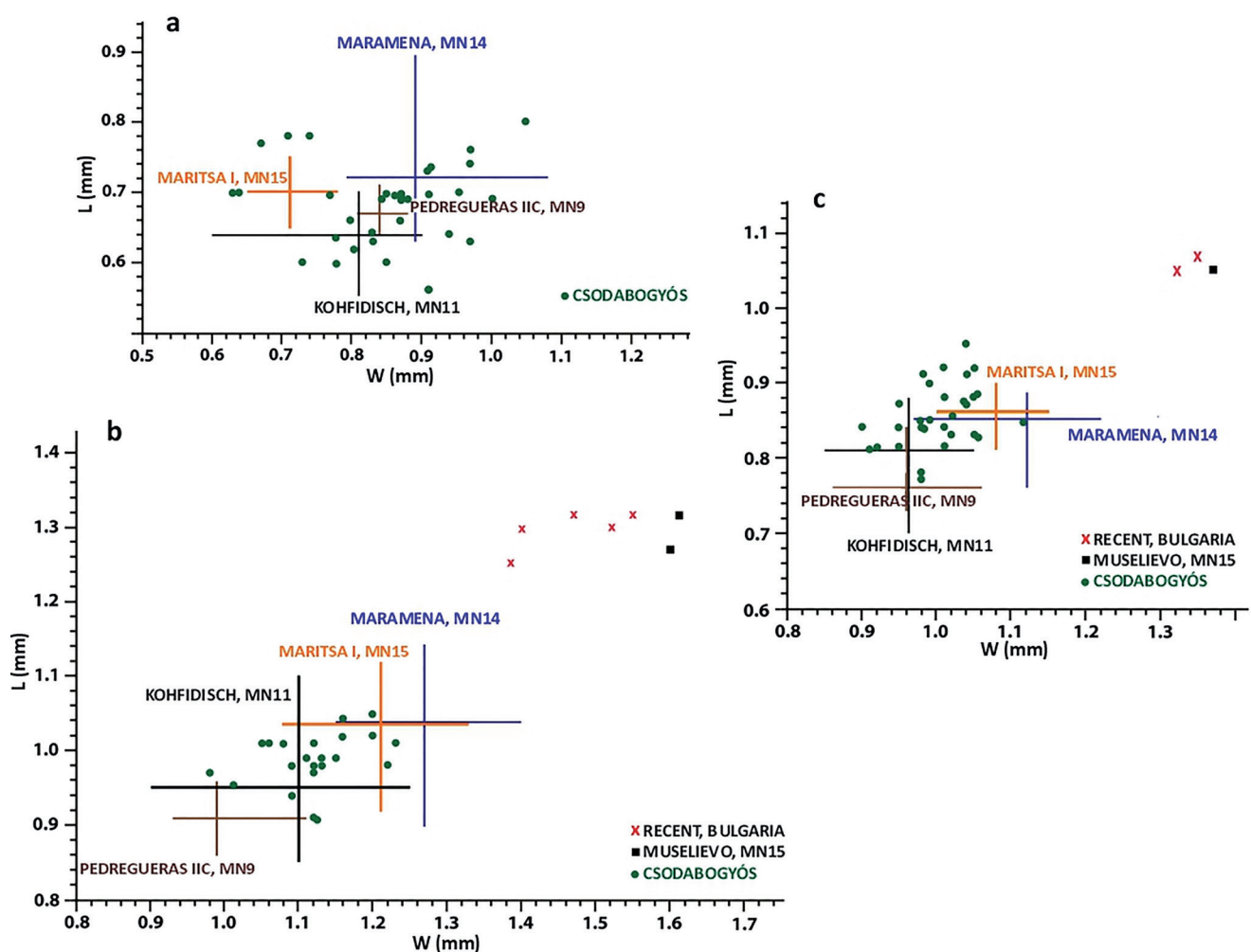
lingual and labial ends are fused with the corresponding ends of the anterolophid. In four cases, the labial ends are free. In three cases, the metalophids are isolated. In the posterior portion, the ridges mesolophid-posterolophid are regular with a rounded lingual connection. Posterotropid is frequent; it is absent only in one tooth. One root.

m1. Text-fig. 13k, l. 34 molars are suitable for a morphological description. Rectangular outline, the anterior margin is shorter than the posterior one. Five main transversal ridges: anterolophid, metalophid, centrolophid, mesolophid and posterolophid. Regular lingual connections: anterolophid-centrolophid in the metaconid, mesolophid-posterolophid in the entoconid. The lingual end of the metalophid is free. Labial connection: anterolophid-metalophid. The labial ends of the metalophid, centrolophid and posterolophid are anteriorly curved. Centrolophid is relatively long, extending beyond the longitudinal axis of the tooth crown. Among the additional ridges, the centrally positioned posterotropid is regular. A metatropid is rare and vestigial (2 specimens). Longitudinal connections between the main ridges, close to the longitudinal axis, occur between the anterolophid and metalophid (in 2 specimens), and between the metalophid and centrolophid (in 6 specimens). Three roots.

m2. Text-fig. 13m. 32 molars are suitable for a morphological description. Rectangular outline, anterior and posterior margins are equal in length, or the posterior one is a bit shorter. The structure of the main ridges and the posterotropid is referable to the m1. The labial end of the centrolophid reaches the middle of the occlusal surface, or longer. In one case, the posterotropid is double – a lingually positioned short ridge is found between the mesolophid and the posterotropid. In one molar, the lingual end of the metalophid reaches the middle part of the anterolophid. In another specimen, the labial end of the centrolophid reaches the middle part of the metalophid. A centrally positioned thin longitudinal ridge is found between the centrolophid and the metalophid in 2 molars. Three roots.

m3. Text-fig. 13n. 30 molars are suitable for a morphological description. The outline is triangular with rounded angles. The structure of the main ridges is similar to m1–m2. Posterolophid is curved. The labial end of the centrolophid reaches the middle of the occlusal surface, or longer. Posterotropid is absent in 6 molars. Vestigial anterotropid occurs in 9 cases.

Comments. The *Myomimus dehmi* population of the Csodabogyós Cave differs:

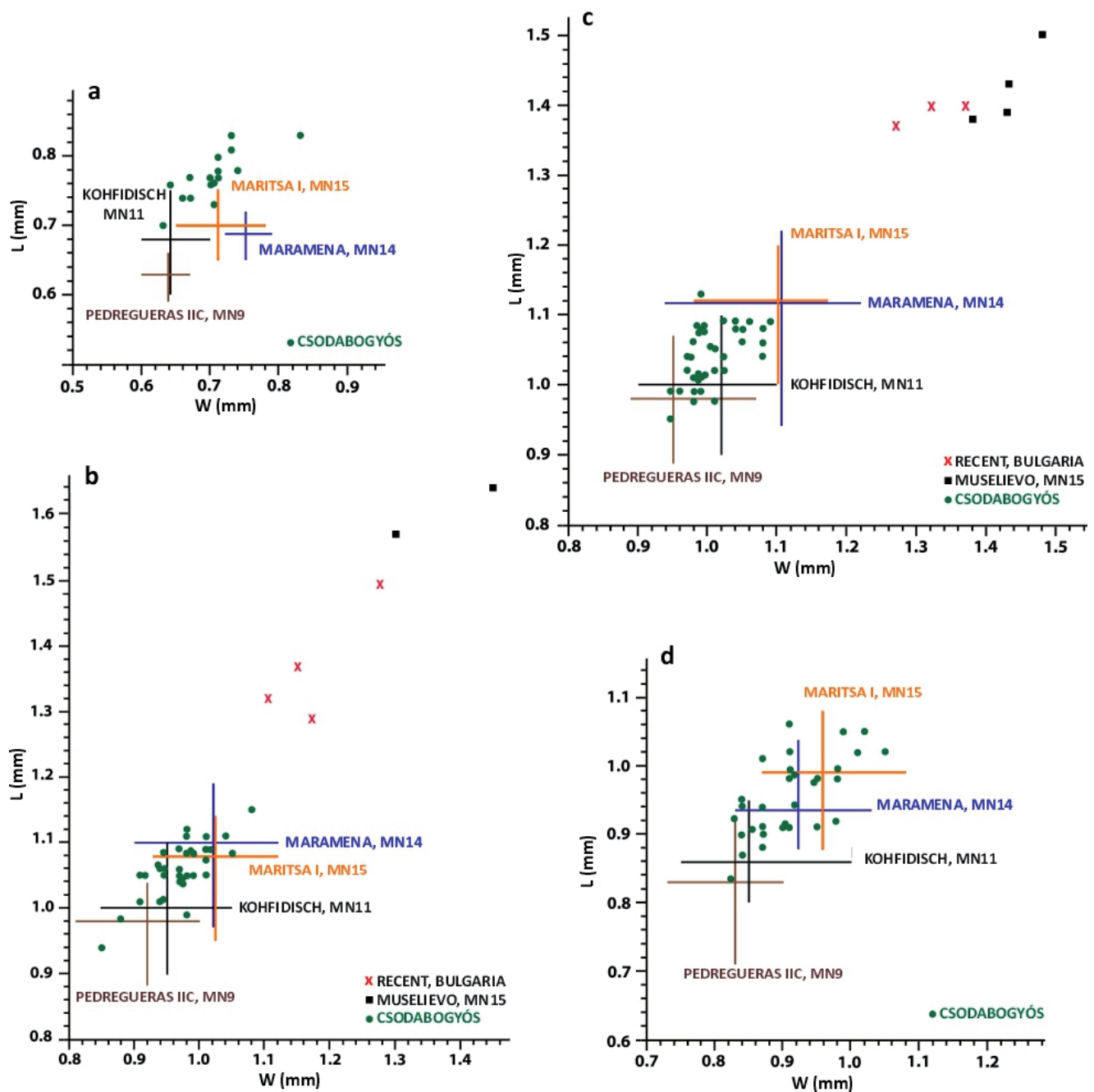


Text-fig. 14. Scatter plots of L/W values of *Myomimus dehmi* upper teeth from Csodabogyós Cave related to ranges and data of other *Myomimus* populations. a: P4 teeth, b: M1–M2 teeth, c: M3 teeth. Comparative data after De Bruijn (1966), De Bruijn et al. (1970), Daxner-Höck (1995), Popov (2004), and Daxner-Höck and Höck (2009).

- from *M. roachi* (BATE, 1937) and *M. qafzensis* HAAS, 1973 (Pleistocene) in the better-developed centrolophs in upper molars, and the smaller measurements;
- from *M. complicidentatus* POPOV, 2004 (MN 15b) in the smaller measurements, and the presence of the additional ridges prototrope and metatrope in M1–2;
- from *M. maritsensis* DE BRUIJN, DAWSON et MEIN, 1970 (Turolian-Ruscinian transition, MN 13–14) in the smaller mean measurements, and the longer centrolophids in the lower molars;
- from *M. sinensis* WU, 1985 (Ertente 2, Harr Obo 2; Tab. 2) in the absence of any ornamentation or cingulum in the lingual margin of the M1–2s, in the less frequent isolated

- anteroloph in M1s, and the less frequent occurrence of posterior centroloph in P4;
- from *Myomimus tanjuae* BILGIN, JONIAK, MAYDA, GÖKTAŞ, PELÁEZ-CAMPOMANES et VAN DEN HOEK OSTENDE, 2021 (Çapak; Tab. 2) in the presence of metatrope in M1–M2, and the more frequent occurrence of this ridge in M3, in the larger mean measurements (except the m3, which has the same measurements), and the three rooted m1–m2, and the occurrence of the posterotropid in p4,
- from *Myomimus sumbalenwalicus* MUNTHE, 1980 (Pakistan, Late Miocene) in the larger and more complicated P4 having four main ridges and one accessory ridge.

The first occurrence of *Myomimus dehmi* was reported



Text-fig. 15. Scatter plots of L/W values of *Myomimus dehmi* lower teeth from Csodabogyós Cave related to ranges and data of other *Myomimus* populations. a: p4 teeth, b: m1 teeth, c: m2 teeth, d: m3 teeth. Comparative data are after De Bruijn (1966), De Bruijn et al. (1970), Daxner-Höck (1995), Popov (2004), and Daxner-Höck and Höck (2009).

from the late Aragonian of Spain (Daams and Freudenthal 1988, Daams and De Bruijn 1995). At the Turolian-Ruscinian transition, *M. dehmi* was replaced by *M. maritsensis* (Daxner-Höck 1995). From the Turolian up to the present, a gradual reduction is observable in the geographical range of *Myomimus*. During the MN 11–12, the genus was found in central, eastern, and southeastern Europe, as well as Anatolia. Their Pliocene and Pleistocene areas are reduced to Bulgaria, Greece, Anatolia and Palestine. The present European distribution is a relict area in the southeastern part of Bulgaria and Turkish Thrace. Some localities are described from the western Anatolian region (Kryštufek and Vohralík 2005).

According to Daams (1981) and Popov (2004), the most significant evolutionary trends among Late Miocene-Pliocene-recent populations are size increase and morphological simplification (Text-figs 14, 15).

Family Eomyidae WINGE, 1887

Genus *Eomyops* ENGESSER, 1979

Eomyops sp.

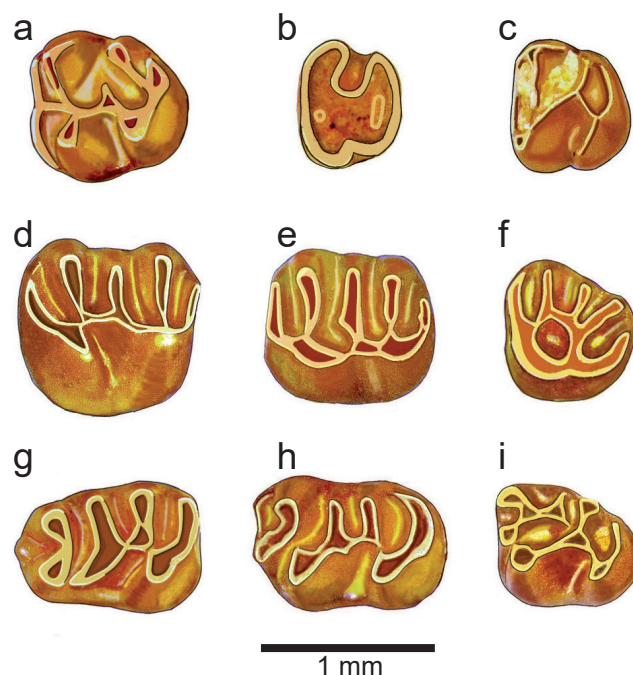
Text-fig. 16a

Material. One left m3.

Measurements. L: 0.94 mm, W: 0.90 mm (see supplementary material).

Description. **m3**. The tooth is rectangular in occlusal outline, but narrow in its posterior part; the corners are rounded; protoconid, metaconid, entoconid and hypoconid are approximately equal in size; labial and lingual anterolophid almost equal; metalophid transverse and attached to the anterior arm of protoconid; longitudinal crest labial; sinusid transverse; short mesolophid transverse; hypolophid connecting to the posterolophid and the posterior arm of the hypoconid.

Comments. *Eomyops* is one of the smallest European eomyid genera. Its range in Europe extends from the Early Miocene (MN 2) to the Pleistocene (MN 17). Frequently, the genus occurs in Middle and Late Miocene faunas all over Europe. The tooth morphology of the genus *Eomyops* has remained relatively conservative, and species definitions are primarily based on size. There are four European species. Of the species occurring in central Europe during the Middle Miocene, *E. oppligeri* ENGESSER, 1990 is the smallest, followed by *E. catalaunicus* (HARTENBERGER, 1966), and *E. hebeiseni* KÄLIN, 1997 is the largest. The stratigraphic range of *E. cf./aff. catalaunicus* is Late Miocene to the beginning of the Pliocene (MN 9–14). The morphological differences between *E. catalaunicus* and *E. oppligeri* were defined by Engesser (1990) and later reassessed by Kälin (1997). Nevertheless, there is much uncertainty in the separation of the two species. In several cases, the robustness of the determination is questionable due to the small number of finds. For this reason, the single tooth from the Csodabogyós Cave was not assigned to a species level.



Text-fig. 16. Occlusal surfaces of eomyid and zapodid teeth. *Eomyops* sp. a: left m3 (VER 2024.472.1). *Keramidomys* sp. b: left P4 (VER 2024.473.1), c: right m3 (VER 2024.473.2, reversed). *Eozapus intermedius*. d: right M1 (VER 2024.475.1, reversed), e: left M2 (VER 2024.476.7), f: left M3 (VER 2024.477.7), g: right m1 (VER 2024.478.4, reversed), h: right m2 (VER 2024.479.5, reversed), i: right m3 (VER 2024.480.2, reversed).

Genus *Keramidomys* HARTENBERGER, 1966

Keramidomys sp.

Text-fig. 16b, c

Material. 1 left P4, 1 right m3.

Measurements. See supplementary material.

Description. **P4**. A heavily worn specimen, not suitable for detailed morphological description.

m3. 4 distinct lophids; mesolophid not visible (due to sediment); anterolophid, metalophid lingually connected; longitudinal crest oblique; 2nd and 3rd synclinids merged and lingually open; 4th synclinids lingually open.

Comments. *Keramidomys* is the smallest known eomyid genus. *Keramidomys* shows an extremely lophodont tooth pattern, with the cusps almost completely incorporated into the crests. The genus spans the period from the Early Miocene (MN 4) to the Pliocene (MN 14). Seven species are known from Europe, but only *Keramidomys thaleri* HUGUENEY et MEIN, 1968, *K. mohleri* ENGESSER, 1972 and *Keramidomys* sp. have been found in Hungary. A conservative line, which starts with *Keramidomys thaleri* (MN 5), can be followed via *K. mohleri* (MN 8–14), and undergoes only minor morphological changes. The latter species is not well-suited for biostratigraphy, due to its long species range. The only morphologically descriptive m3 recovered from the Csodabogyós Cave is not classified at the species level.

Table 16. Measurements of *Eozapus intermedius* material from the Csodabogyós Cave. Abbreviations: SD – standard deviation, CV – coefficient of variation.

Tooth	Length					Width				
	n	min–max	mean	SD	CV	n	min–max	mean	SD	CV
M1	13	0.96–1.10	1.03	0.040	3.89	14	0.76–1.02	0.86	0.069	8.01
M2	10	0.84–1.04	0.98	0.061	6.21	10	0.77–0.91	0.85	0.044	5.20
M3	7	0.67–0.78	0.73	0.037	5.01	7	0.70–0.84	0.77	0.056	7.24
m1	9	0.94–1.15	1.07	0.060	5.57	9	0.66–0.86	0.78	0.058	7.38
m2	6	0.99–1.09	1.06	0.039	3.68	6	0.74–0.85	0.80	0.037	4.66
m3	6	0.81–0.99	0.91	0.063	6.95	6	0.64–0.77	0.70	0.046	6.61

Family Dipodidae FISCHER, 1817
Subfamily Zapodinae COUES, 1875

Genus *Eozapus* PREBLE, 1899

***Eozapus intermedius* (BACHMAYER et WILSON, 1970)**

Text-fig. 16d–i

Material. Isolated teeth: 14 M1, 10 M2, 7 M3, 9 m1, 6 m2, 6 m3.

Measurements. Raw measurement data are provided in the supplementary material, and summary data are presented in Table 16.

Description. **M1.** The paracone is continuous with the protolophule, and the metacone is continuous with the metalophule. The protolophule attaches to the posterior part of the protocone. The metalophule attaches to the central or rarely posterior part of the hypocone. The entoloph- protocone connection is usually constricted, seldom interrupted, and the sinus is directed forward.

M2. The protocone and hypocone are elongate and continuous with the entoloph, but this connection is restricted between the two lingual cusps in 40 % of the specimens. The anteroloph labial, in some specimens, is directed forward. The mesoloph is either straight or anterolingually widened and joins the entoloph at the anterior part of the hypocone in the case of 50 % of the teeth. The sinus is flat or absent, rarely directed forward.

M3. The tooth is short and rounded, with an occlusal pattern similar to that of M2. The mesoloph in the mesial part of the tooth is often fused with both the protolophule and the metalophule, and an enamel ring forms in the posterior part of the protocone. The sinus is flat or absent.

m1. Elongated tooth, wider posteriorly. The protoconid and metaconid are arranged in a chevron. The anteroconid is in an antero-central position (66 %) or absent (33 %). There is a shallow transverse valley that separates the protoconid and mesoconid, whereas the mesolophid and mesoconid are fused, forming a field of triangular shape. The entoconid continues with the hypolophulid, and the hypolophulid-hypoconid connection is frequently constricted, whereas the hypolophulid-ectolophid connection may be interrupted. The sinusid is directed backwards.

m2. The anterolophid is frequently double, the lingual one longer than the labial one. The metalophulid is continuous

with the metaconid and anterolophid. The metalophulid- anterolophid part is separated from the protoconid (50 %) and protosinusid continuous with lingual synclinid II. The hypolophulid-hypoconid connection is constricted or interrupted.

m3. Subtriangular tooth, its anterior part wider than the rounded posterior part. There is no labial branch of the anterolophid. The metalophulid-protoconid-mesolophid connection is strong. The hypoconid is not visible in the posterolophid. The hypolophulid-hypoconid connection is frequently constricted or interrupted (83 %), but the rest of its morphology is similar to that of m2.

Comments. *Eozapus* has a very conservative molar pattern. The species differ only in size and minor morphological characters. *E. intermedius*, from the Late Miocene (MN 9–11), is the oldest and smallest species, characterized by a relatively short m1 (Daxner-Höck and Höck 2015). *E. intermedius* was recovered from the early Turolian (MN 11) in Spain (Van de Weerd 1976). In central Europe, the species is also a dominant fossil of MN 11 assemblages. However, sporadic Vallesian occurrences from Austria (Richardhof-Golfplatz, Götzensdorf), the Czech Republic (Suchomasty) and Russia (Vallesian part of Saray 1) indicate a pre-Turolian immigration from eastern regions. The teeth of *Eozapus intermedius* from the Csodabogyós Cave match in size and morphology the type material of *E. intermedius* described by Bachmayer and Wilson (1970) from Kohfidisch (Tab. 2).

Family Cricetidae FISCHER, 1817
Subfamily Microscoptinae KRETZOI, 1955
Tribe Microscoptini KRETZOI, 1955

Genus *Microscoptes* SCHAUB, 1934

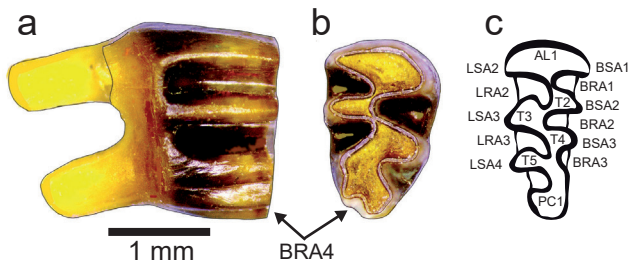
***Microscoptes* sp.**

Text-fig. 17a, b

Material. One right upper M3.

Measurements. L: 1.89 mm, W: 1.04 mm (see supplementary material).

Description. **M3.** The tooth has four prominent triangles (= buccal salient angles BSA 1 – BSA 4) and three lingual ones (LSA 1 – LSA 3) (Text-fig. 17c). BSA 2 is slightly



Text-fig. 17. *Microscoptes* sp. right M3 (VER 2024.474.1, reversed). a: labial view, b: occlusal surface. c: Nomenclature of left upper M3 of Arvicolinae, without BSA 4 characteristic of *Microscoptes* (from Piñero et al. 2015).

smaller than BSA 1, LSA 1 and LSA 2. The re-entrant angles BRA 1, BRA 2 and LRA 1 are incised to approximately the same depth, but LRA 2 is a bit shallower, and BRA 3 is much shallower. There is also a distinct postero-buccal fourth re-entrant angle (BRA 4, or bucco-distal indentation).

Comments. The present find from the Csodabogyós Cave is an upper right M3 of the genus *Microscoptes*, since it shows the closest resemblance to depicted specimens of this genus from the Chinese site Ertemte 2 (Fahlbusch 1987, Fejfar et al. 2011).

The tribe Microscoptini, comprising the genera *Microscoptes*, *Paramicroscoptes* MARTIN, 1975, and *Goniodontomys* WILSON, 1937, belongs to the so-called microtoid Cricetidae (Fejfar et al. 2011). Although the molars of members of this group exhibit characteristics typical of the Arvicolinae (high tooth crowns, prismatic tooth structure, etc.), most authors have long agreed that they are not their ancestors (Kretzoi 1969, Gromov and Polyakov 1977, Fejfar et al. 2011). Representatives of the Microscoptini (Maul et al. 2017) are known from over 30 sites in North America (*Paramicroscoptes* and

Goniodontomys) and Eurasia (*Microscoptes*). To date, there are a total of over 20 localities from Eurasia, ranging from Ukraine in the west, via Kazakhstan, Mongolia, and Russia, to China in the east, as well as a further 13 from North America. The oldest finds of Microscoptini to date come from MN 10, and the youngest from MN 13.

The finds from Ertemte 2, whose age corresponds to MN 13, belong to *Microscoptes praetermissus* SCHAUB, 1934 (Fahlbusch 1987). M3s from comparable relative crown heights (ratio between crown height and tooth length – H/L; the value in the Csodabogyós Cave ca. 70 %) from this locality do not show the BRA 4. Only one juvenile, characterized by a higher-crowned tooth (H/L approx. 100 %) (Fahlbusch 1987: fig. 28), exhibits this structure in a weaker and more lingual position. Fahlbusch (1987) mentions “in the center of the posterior dentine area there is recognisable a small, flat, but distinct enamel pit (pl. 4 fig. 12)”. In more worn M3s from Ertemte 2, which has approximately the same height as the tooth from Hungary, the indentation is missing and BSA3 and LSA2 (dentin fields T2 and T3, respectively) merge into a common wide lobe (Fahlbusch 1987: text-figs 28–30).

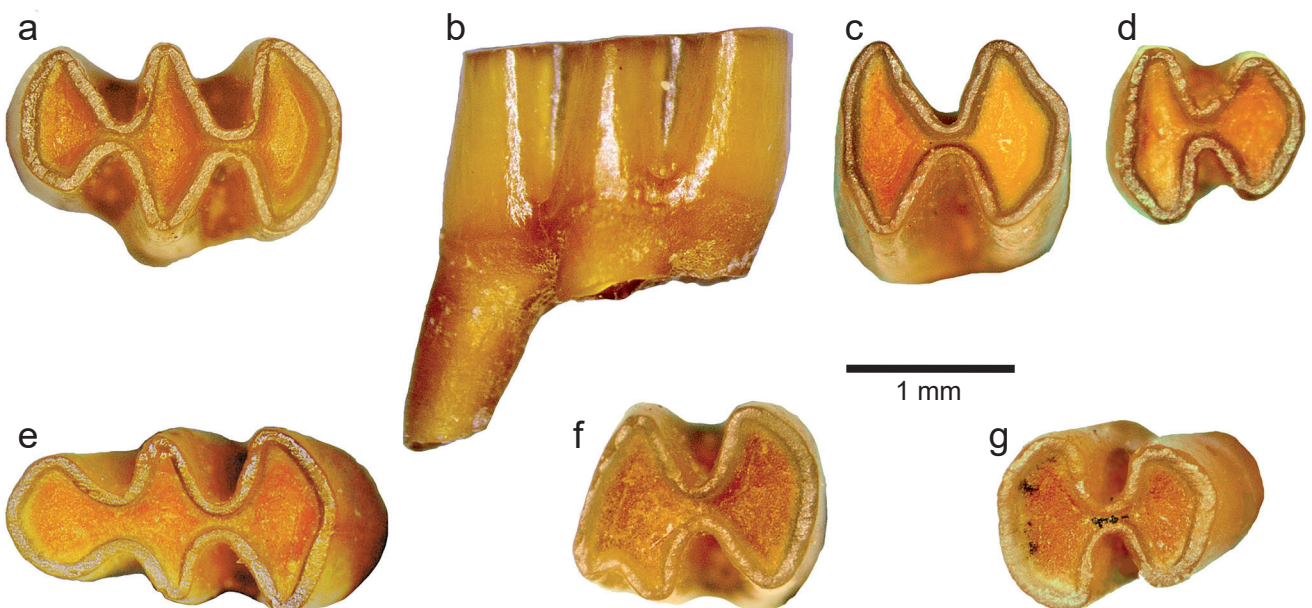
Thus, the morphology of the M3 from the Csodabogyós Cave is more ancestral, as is also the case for older respective finds from Ukraine (Rekovets, Maul and collaborators, in preparation). The find from the Hungarian locality Csodabogyós Cave is thus the westernmost and one of the oldest finds of the genus *Microscoptes*.

Family Muridae ILLEGER, 1811
Subfamily incertae sedis

Genus *Epimeriones* DAXNER-HÖCK, 1972

***Epimeriones austriacus* DAXNER-HÖCK, 1972**

Text-fig. 18a–g



Text-fig. 18. Molars of *Epimeriones austriacus*. a: left M1 occlusal view (VER 2024.487.8), b: left M1 lingual view (VER 2024.487.8), c: left M2 occlusal view (VER 2024.488.7), d: left M3 occlusal view (VER 2024.489.9), e: right m1 occlusal view (VER 2024.490.8, reversed), f: left m2 occlusal view (VER 2024.491.4), g: right m3 occlusal view (VER 2024.492.6, reversed).

Table 17. Measurements of *Epimeriones austriacus* material from the Csodabogyós Cave. Abbreviations: SD – standard deviation, CV – coefficient of variation.

Tooth	Length					Width				
	n	min–max	mean	SD	CV	n	min–max	mean	SD	CV
M1	13	1.74–2.12	1.95	0.102	5.25	14	0.97–1.23	1.14	0.070	6.19
M2	18	1.19–1.48	1.33	0.076	5.69	18	0.90–1.30	1.13	0.104	9.18
M3	11	0.96–1.30	1.13	0.099	8.74	11	0.99–1.14	1.05	0.051	4.84
m1	12	1.72–2.16	1.95	0.126	6.44	12	0.97–1.17	1.08	0.065	6.01
m2	7	1.29–1.47	1.37	0.062	4.52	8	1.00–1.25	1.13	0.094	8.31
m3	10	0.96–1.29	1.13	0.115	10.19	10	0.81–1.16	0.96	0.110	11.47

Material. Isolated teeth: 14 M1, 18 M2, 11 M3, 12 m1, 8 m2, 10 m3.

Measurements. Raw measurement data are given in the supplementary material, and summary data are presented in Table 17.

Description. **M1**. There are three labial and lingual anticlines and two labial and lingual synclines, in opposite positions on the tooth. The tooth is wider towards the posterior and tilted backwards. The first labial anticline is shorter and more pointed than the lingual one. The tooth has three roots; the median root is located on the lingual side of the tooth.

M2. The tooth has two labial and lingual anticlines, and one labial and lingual syncline in the opposite position. It is wider towards the anterior and tilted backwards. It has three roots; the median root is located on the lingual side of the tooth.

M3. There are two labial and lingual anticlines, and one labial and lingual syncline in the opposite position on the tooth. The tooth is wider towards the anterior and tilted backwards. It has two or three (18 %) roots.

m1. The tooth has three labial and lingual anticlinids, and two labial and lingual synclinids in opposite positions. The tooth is wider towards the posterior and tilted forward. The less worn specimens have additional anterior-lingual (42 %) and posterior-lingual (17 %) synclinids, whereas enamel islands are present on the juvenile specimens. It has two roots.

m2. There are two labial and lingual anticlinids, and one labial and lingual synclinid, in the opposite position on the tooth; the two lobes are approximately the same width. The tooth is tilted forward. There is a weak labial anterolophid on the unworn specimens, but enamel islands on the juvenile specimens. The tooth has two roots.

m3. The tooth has two labial and lingual anticlinids, and one labial and lingual synclinid in the opposite position. It is narrower towards the posterior and tilted forward. It has two roots.

Comments. Originally, *Epimeriones* was classified as a gerbil, because of its strong affinities with the *Meriones-Rhombomys* molar morphology and the shape of the grooved upper incisors (Daxner-Höck 1972). Several researchers later questioned the taxonomic classification of *Epimeriones* in the subfamily Gerbillinae, and the genus was reclassified as Cricetinae incertae sedis (Tong 1989, Kälin 1999, Wessels

1999). The debate remains unresolved, with some believing that the genus *Epimeriones* belongs in the subfamily Gerbillinae (Agusti and Casanovas-Vilar 2003), while others place it in Muridae incertae sedis (McKenna and Bell 1997, Daxner-Höck and Höck 2015). However, comparisons with recent species of Gerbillinae revealed substantial differences, especially in root morphology (Pavlinov 2008), which support the classification of Muridae incertae sedis; this is followed in our paper.

The genus *Epimeriones* was first mentioned from the Late Miocene, Eichkogel (Daxner-Höck 1972), but was also recovered from another Austrian site of similar age Kohfidisch (8.6–8.5 Ma; Tab. 2). However, the range of the genus extends as far as the Pliocene (*Epimeriones progressus* KOWALSKI, 1974) from Kroczyce in Poland and the Early Pleistocene from Romania (*Epimeriones dacicus*, Betfia-XIII; Terzea 1978). The geographic distribution of the genus is almost entirely restricted to eastern and central Europe (Austria, Poland and Romania), with only two late Turolian sites in western Europe, Lissieu and Can Vilella (Agusti and Casanovas-Vilar 2003). The *Epimeriones* material of the Csodabogyós Cave is very similar in size and morphology to the *Epimeriones austriacus* material of the age MN 11 of Kohfidisch and Eichkogel, which are closest to it in both age and geographic location.

Subfamily Murinae ILLIGER, 1811

Genus *Progonomys* SCHAUB, 1938

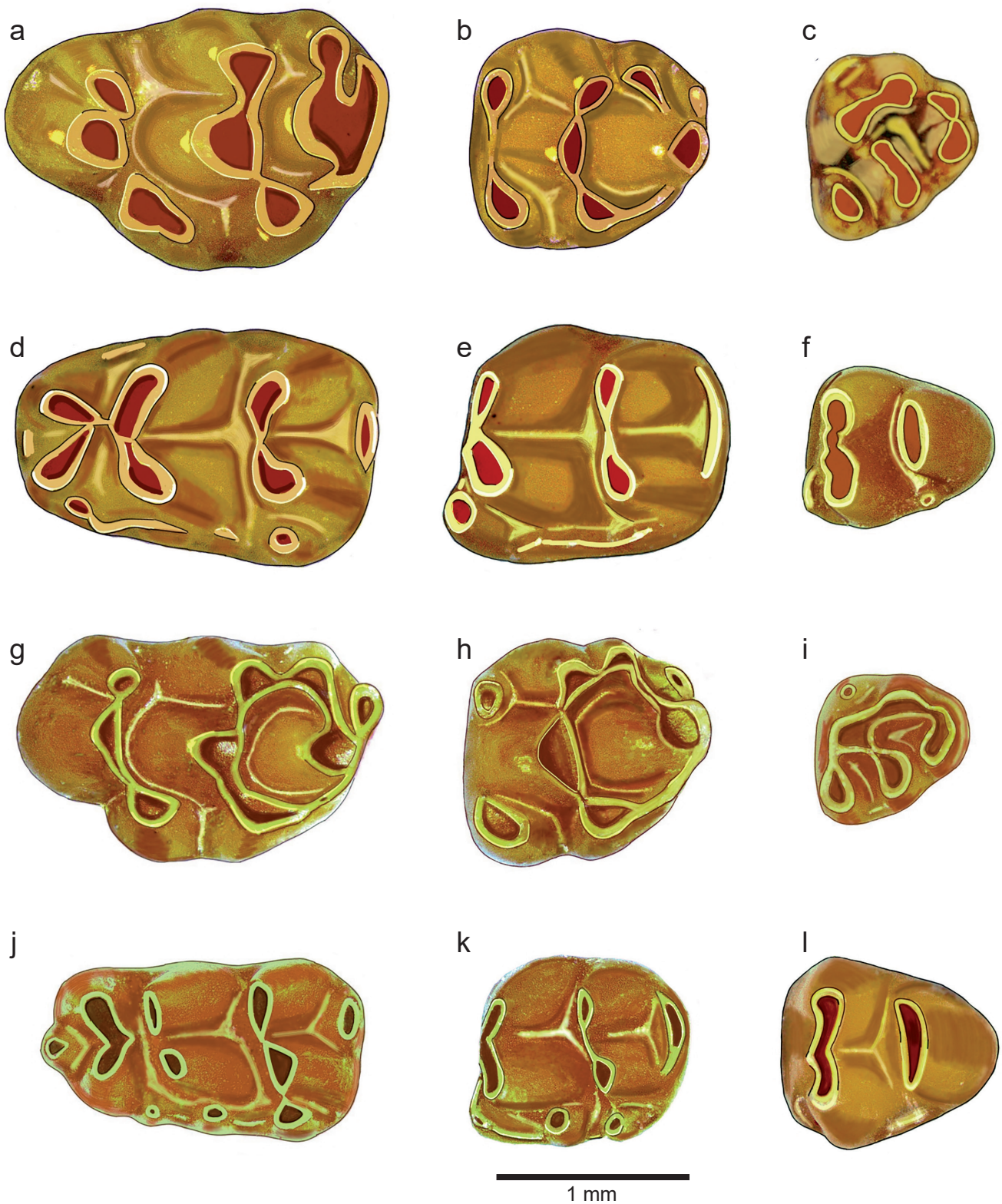
Progonomys hispanicus MICHAUX, 1971

Text-fig. 19a–f

Material. Isolated teeth: 6 M1, 23 M2, 13 M3, 9 m1, 8 m2, 9 m3.

Measurements. Raw measurement data are provided in the supplementary material, and summary data are presented in Table 18.

Description. **M1**. The t6-t9 connection and the t1bis are absent. The connection of t4-t8 is absent (2 specimens) or visible as a low crest (4 specimens), and the t4-t5 connection is also lacking in one specimen. The t1 and t4 are elongate, and posterior to t3 and t6. The t7 is absent. The orientation of the t8-t9-pair is at a right angle to the longitudinal axis (van Dam 1997: fig. 3.8); the t12 is weak. The tooth has three roots.



Text-fig. 19. Occlusal surfaces of Murinae molars. *Progonomys hispanicus*. a: left M1 (VER 2024.493.6), b: left M2 (VER 2024.494.7), c: right M3 (VER 2024.495.1, reversed), d: left m1 (VER 2024.496.4), e: left m2 (VER 2024.497.1), f: left m3 (VER 2024.498.3). *Apodemus lugdunensis*. g: right M1 (VER 2024.499.29, reversed), h: right M2 (VER 2024.500.131, reversed), i: left M3 (VER 2024.501.41), j: rights m1 (VER 2024.502.30, reversed), k: left m2 (VER 2024.503.24), l: left m3 (VER 2024.504.60).

M2. The t6-t9 connection and the t1bis are absent. The connection of t4-t8 is usually a low crest (91 %) or absent (9 %), and the t4-t5 connection is also missing in two specimens. The t1 and t4 are elongated. The t1 is much larger than t3, whereas t2 is absent. The tooth has three roots.

M3. The t1 is large, the t2 is absent, and the t3 is usually small (85 %) or absent (15 %). The t4, t5 and t6 are connected and arranged in a chevron, but the t4-t5 connection is missing on one specimen. The chevron is asymmetric in some specimens (38 %), because of the reduction of t6. The

Table 18. Measurements of *Progonomys hispanicus* material from the Csodabogyós Cave. Abbreviations: SD – standard deviation; CV – coefficient of variation.

Tooth	Length					Width				
	n	min–max	mean	SD	CV	n	min–max	mean	SD	CV
M1	6	1.72–1.97	1.86	0.109	5.86	6	1.08–1.33	1.18	0.101	8.54
M2	23	1.14–1.40	1.27	0.074	5.81	23	1.03–1.24	1.15	0.051	4.43
M3	13	0.80–1.01	0.88	0.065	7.32	13	0.78–0.91	0.85	0.038	4.41
m1	9	1.55–1.82	1.63	0.103	6.29	9	0.93–1.17	1.01	0.087	8.59
m2	8	1.15–1.38	1.29	0.068	5.27	8	0.99–1.20	1.09	0.071	6.52
m3	9	0.86–1.06	0.99	0.059	5.98	9	0.86–0.99	0.91	0.049	5.42

t8 and t9 are fused (69 %) or t9 is reduced (31 %). The tooth has three roots.

m1. The antero-central cusp is very weak and low (78 %) or absent (22 %). The longitudinal spur is absent. The c1 and the other accessory cusps are weak (56 %), or the cusps cannot be separated; only a cingulum extends along the labial side of the tooth (44 %). The elliptical terminal heel and the anteroconid-metaconid connection are positioned lingually concerning the longitudinal axis. This connection is weak or may be absent. The tooth has two roots.

m2. The longitudinal spur is absent, and the labial accessory cusps are weak. The elliptical terminal heel is positioned lingually with respect to the longitudinal axis. The labial and lingual conids form transverse lobes. The tooth has two roots.

m3. The protoconid and metaconid are fused to a transverse lobe, whereas the hypoconid and entoconid are fused to an elliptical lobe positioned lingually with respect to the longitudinal axis. The antero-labial cusp and c1 are small. The tooth has two roots.

Comments. The majority of the Murinae material from the Csodabogyós Cave consists of teeth belonging to the species *Apodemus lugdunensis* (see below). However, based on morphology, we also clearly identified some specimens of *Progonomys hispanicus*. The two species are compared in size and morphology.

Using the R software environment (v. 4.3.1; R Core Team 2023), the distribution of tooth length and width was analyzed separately for each tooth, plotted on a boxplot, and the means of the sizes of the two species were compared using Welch's t-test. The results indicate that the two species cannot be separated by size, with the only statistical difference in the length of M1 ($p = 0.04$); however, this may be due to the small sample size of *P. hispanicus* M1 ($n = 6$). Morphologically, the main difference between the two species is the lack of longitudinal connections in *Progonomys*. On the M1, the t3 has no spur, the t6-t9 connection is absent, while on the m1, the antero-central cusp is either poorly developed or entirely missing.

Although the material of *Progonomys hispanicus* from the Csodabogyós Cave is relatively poor, we attempted to compare the teeth morphologically and in size with material from the type locality, the Teruel-Alfambra region, and to place them within the evolutionary sequence suggested by van Dam (1997). M1 is morphologically similar to the more evolutionarily advanced *Progonomys hispanicus*, with

all specimens lacking the t6-t9 connection and t1bis, still, with t4-t8 connection common (van Dam 1997: fig. 3.6). The antero-central cusp, which is abundant on m1, is also characteristic of the more advanced *P. hispanicus* specimens, but none of the specimens has a longitudinal spur. Based on the size and W/L ratio of the teeth (M1, M2, m1, m2), the material from the Csodabogyós Cave is similar to that of *P. hispanicus* from Peralejos C (8.8 Ma) and Peralejos D (8.7 Ma) in Spain (van Dam 1997), suggesting that the accumulation of the fossiliferous sediment occurred around the MN 10/11 zonal boundary, in the latest Vallesian or earliest Turolian (Tab. 2).

Genus *Apodemus* KAUP, 1829

Apodemus lugdunensis (SCHAUB, 1938)

Text-fig. 19g–l

Material. Maxilla fragment with M1–M2, 1 mandible fragment with m1–m3, 1 mandible fragment with m2–m3; isolated teeth: 205 M1, 205 M2, 116 M3, 158 m1, 187 m2, 112 m3.

Measurements. Raw measurement data are provided in the supplementary material, and summary data are presented in Table 19.

Description. **M1.** The t6-t9 connection is always present (100 %), although in some cases only a low ridge connects the two cusps. The t4-t8 connection is also present (98 %). There is a small t7 on a few specimens (3 %). The t12 is well developed, often comma-shaped (76 %). There is a small t1bis on a few specimens (2 %). The tooth usually has three roots, but a minute central fourth root can be present on few specimens (3 %).

M2. The t6-t9 connection (99 %) and the t4-t8 connection are present (100 %). There is a small t7 (1 %), and a small t1bis on a few specimens (1 %). The t12 is well developed. The tooth usually has three roots, but a minute central fourth root can be present in a few specimens (4 %).

M3. The t1 is well developed, whereas t3 is present but very small. The t4-t5 and t5-t6 connections are always present and strong, but the t6-t8 connection is weaker. Thirty per cent of the specimens had a central enamel ring connected by t4-t5-t6-t8. The t8 and t9 are fused in most cases. The tooth has three roots.

m1. The antero-central cusp is weak (22 %) to pronounced (78 %). The anteroconid-metaconid connection is close to

Table 19. Measurements of *Apodemus lugdunensis* material from the Csodabogyós Cave. Abbreviations: SD – standard deviation, CV – coefficient of variation.

Tooth	Length					Width				
	n	min–max	mean	SD	CV	n	min–max	mean	SD	CV
M1	203	1.50–1.95	1.73	0.089	5.15	206	0.96–1.28	1.13	0.051	4.53
M2	202	1.11–1.44	1.25	0.065	5.21	206	0.99–1.31	1.15	0.054	4.73
M3	116	0.71–1.06	0.86	0.062	7.25	115	0.76–1.06	0.86	0.056	6.45
m1	154	1.51–1.83	1.64	0.073	4.43	159	0.88–1.13	0.99	0.047	4.71
m2	184	1.08–1.41	1.24	0.061	4.91	188	0.92–1.23	1.08	0.056	5.18
m3	113	0.84–1.14	0.98	0.055	5.64	114	0.78–1.04	0.89	0.055	6.11

the longitudinal axis (68 %), or weak and slightly lingual position (32 %). The longitudinal spur is absent or very weak in a few specimens (5%). The terminal heel is elliptical or round (3 %). The accessory cusps on the labial cingulum are well developed (60 %), the posterior accessory cusps pronounced, others weak or variable (40 %). The tooth has two roots.

m2. The antero-labial cusp is pronounced, whereas the other accessory cusps on the cingulum are variable. The terminal heel is elliptical to more rounded.

m3. The protoconid and metaconid are connected, whereas the hypoconid and entoconid are fused to form an elliptical conid. The antero-labial cusp is present, but weak in some specimens (31 %).

Comments. The rich *Apodemus* material in the Csodabogyós Cave also provides the opportunity to carry out statistical analyses. In all cases, the length and width of the molars are normally distributed, indicating that only one species of *Apodemus*, *Apodemus lugdunensis*, was present at the site. The *Apodemus lugdunensis* population from the Csodabogyós Cave was compared with material from two nearby sites, Kohfidisch (Pannonian Basin) and Eichkogel (Vienna Basin), by statistical methods, as well as compared with other Late Miocene Muridae material (*Progonomys* SCHAUB, 1938, *Parapodemus* SCHAUB, 1938, *Apodemus*) described from the Teruel-Alfambra region (Van de Weerd 1976), Triblavina and Northern Caucasus (Tesakov et al. 2017) by morphology and size. A pairwise Welch's t-test in the R software environment (v. 4.3.1; R Core Team 2023) was used to determine whether the populations from different sites were identical or distinct in terms of mean size.

The results show no significant difference in the width of molars between the *A. lugdunensis* material from the three sites. The test showed a p-value above 0.05 when comparing the material from the Csodabogyós Cave with Kohfidisch for four molars (M2, M3, m1, m3). Similarly, when comparing the same material with Eichkogel for all molars, the p-value was also above 0.05. However, the analysis of the molars' length showed that the population of *A. lugdunensis* from the Csodabogyós Cave is closer to the material from Kohfidisch. For four molars (M2, M3, m1, m3), the test showed a p-value above 0.05 when comparing the material from the Csodabogyós Cave with Kohfidisch,

but only for one molar (M3) when comparing the material with Eichkogel.

The material is very similar in both size and morphology to the material from the Kohfidisch and Eichkogel sites (Wöger 2011, Daxner-Höck and Höck 2015), although there are morphological features such as the enamel ring observed in the third of the teeth of M3, which is more typical of the older *A. lugdunensis* populations (Schernham) (Daxner-Höck and Höck 2015). Morphological features suggestive of older age are also observed on m1. In the material from the Csodabogyós Cave, the antero-central cusp is poorly developed in 22 % of m1s, compared to 12 % (Kohfidisch) and 5 % (Eichkogel) for the two MN 11 sites. A similar difference is observed for the anteroconid-metaconid connection, which is weak in 32 % of specimens and slightly lingual to the longitudinal axis, a characteristic typical of the *A. lugdunensis* population from the older (Schernham) site.

Based on comparisons with material from other sites (Teruel-Alfambra region, Triblavina, Gaverdovsky, Volchaya Balka), the *Apodemus* material from the Csodabogyós Cave is morphologically identical to *Apodemus lugdunensis*. Based on size, *Apodemus lugdunensis* cannot be distinguished from *Progonomys hispanicus*. Still, morphological features such as the presence of t6-t9 and t6-t8 connections on M1, which are absent in *Progonomys hispanicus*, allow for morphological separation. The other Miocene Muridae species (*Parapodemus gaudryi* (DAMES, 1883), *Progonomys woelferi* BACHMAYER et WILSON, 1970) are larger.

Although both Austrian sites are of early Turolian age, Kohfidisch is slightly older (8.5 Ma) than Eichkogel (8.5–8.0 Ma) (Daxner-Höck and Höck 2015). Based on the size and morphology of the *A. lugdunensis* molars, Csodabogyós Cave may be closer to the Kohfidisch site (8.5 Ma) or slightly older than that.

Subfamily Anomalomyinae SCHAUB, 1925

Genus *Prospalax* MÉHELY, 1908

Dental nomenclature. Anomalomyid dental nomenclature was published by Kordos (2005) and Daxner-Höck and Höck (2015). Nevertheless, the morphology of *Prospalax* molars is simple, and the application of the terminology proposed by Daxner-Höck and Höck (2015) is more apt.

Table 20. Measurements of *Prospalax petteri* material from the Csodabogyós Cave. Abbreviations: SD – standard deviation, CV – coefficient of variation.

Tooth	Length					Width				
	n	min–max	mean	SD	CV	n	min–max	mean	SD	CV
M1	76	1.58–2.39	2.09	0.112	5.33	76	1.18–2.04	1.58	0.215	13.62
M2	85	1.64–2.18	1.86	0.094	5.02	85	1.01–2.10	1.57	0.207	13.21
M3	69	1.02–1.48	1.24	0.121	9.72	69	0.98–1.47	1.24	0.106	8.56
m1	67	1.96–2.59	2.13	0.102	4.77	67	1.09–1.82	1.43	0.150	10.46
m2	84	1.79–2.38	2.12	0.108	5.07	84	1.19–2.07	1.59	0.168	10.60
m3	59	1.23–2.10	1.60	0.175	10.93	59	0.98–1.82	1.40	0.145	10.35

***Prospalax petteri* BACHMAYER et WILSON, 1970**

Text-figs 20, 21

Material. Isolated teeth: 76 M1, 85 M2, 69 M3, 67 m1, 84 m2, 59 m3.

Measurements. Raw measurement data are provided in the supplementary material, and summary data are presented in Table 20.

Description. The molars are hypsodont (or hypselodont). All of them have flat occlusal surfaces, with three large, obliquely aligned dentin folds, surrounded by an enamel layer: the anterior lobe, intermediate lobe, and posterior lobe. The upper molars have three roots, and the lower molars have two roots.

M1. 43 juvenile and adult molars are suitable for morphological description. The occlusal outline is subrectangular-elliptical. The anterior lobe is isolated in 20 specimens (Text-fig. 20a). There is a narrow labial connection between the anterior and the intermediate lobes in 23 specimens (Text-fig. 20d). The intermediate and the posterior lobes have a postero-lingual, or postero-central connection. Enamel rings in the anterior lobe are rare (in 3 specimens; Text-fig. 20b). In one case, there are two rings. A large enamel ring in the labial part of the intermediate lobe is frequent (in 35 specimens; Text-fig. 20c). In two cases, there are two rings. An enamel ring in the posterior lobe is found in 11 cases. Enamel rings are entirely absent in 6 specimens.

M2. 48 juvenile and adult molars are suitable for morphological study. The occlusal outline of M2 is squarer than M1, and the lingual part of the anterior lobe is posteriorly curved. The morphotypes are as follows:

- there is a labial connection between the anterior and the intermediate lobe; posterior, or posterolingual connection between the intermediate and the posterior lobe; a big enamel ring in the labial part of the intermediate lobe: in 26 (Text-fig. 20h);
- the same pattern, but there is also an enamel ring in the posterior lobe: in 12 (Text-fig. 20g);
- anterior lobe isolated, but there is an enamel ring in the intermediate lobe: in 6 (Text-fig. 20e, f);
- posterior lobe isolated: in 1 (Text-fig. 20f);
- the pattern of the main lobes is the same as the above mentioned type, however, enamel rings are absent: in 7;
- the three lobes are isolated: in 1.

M3. The smallest molar. A coherent morphological description of the occlusal surface is difficult. In the juvenile molars, there are two lobes because the intermediate lobe is fused with the anterior one. The posterior lobe is mainly isolated. Enamel rings are frequent in the labial part of the anterior lobe (Text-fig. 20i–l).

m1. 37 juvenile and adult molars are suitable for morphological study. The occlusal outline is antero-posteriorly elongated elliptically. In the juvenile molars, the three lobes are isolated (in 12; Text-fig. 21a). In the subadult-adult phase, connections appeared between the lobes:

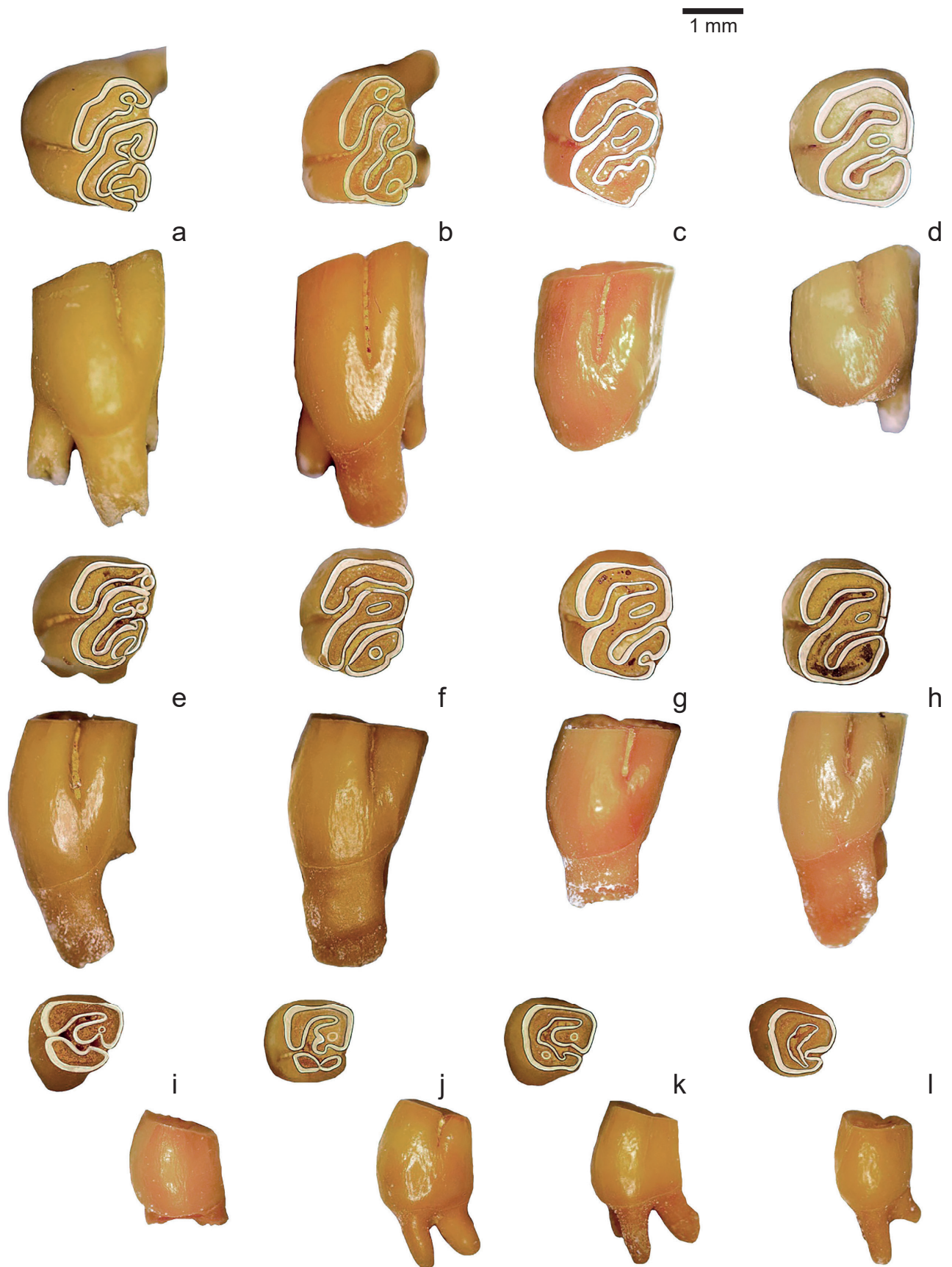
- the lingual connection between the anterior and the intermediate lobes: in 24 (Text-fig. 21d);
- the central connection between the intermediate and the posterior lobes: in 21 (Text-fig. 21b);
- the lingual connection between the intermediate and posterior lobes: in 1.

Enamel rings in the anterior and intermediate lobes occurred. In the anterior lobe, the presence of one ring (in 13), two rings (in 13), and three rings (in 1) is visible (Text-fig. 21c). In the intermediate lobe, there is one closed ring (in 6), or “*Anomalomys* marker” (large anteriorly open enamel ring) in 7 (Text-fig. 21c). No enamel ring in the posterior lobe.

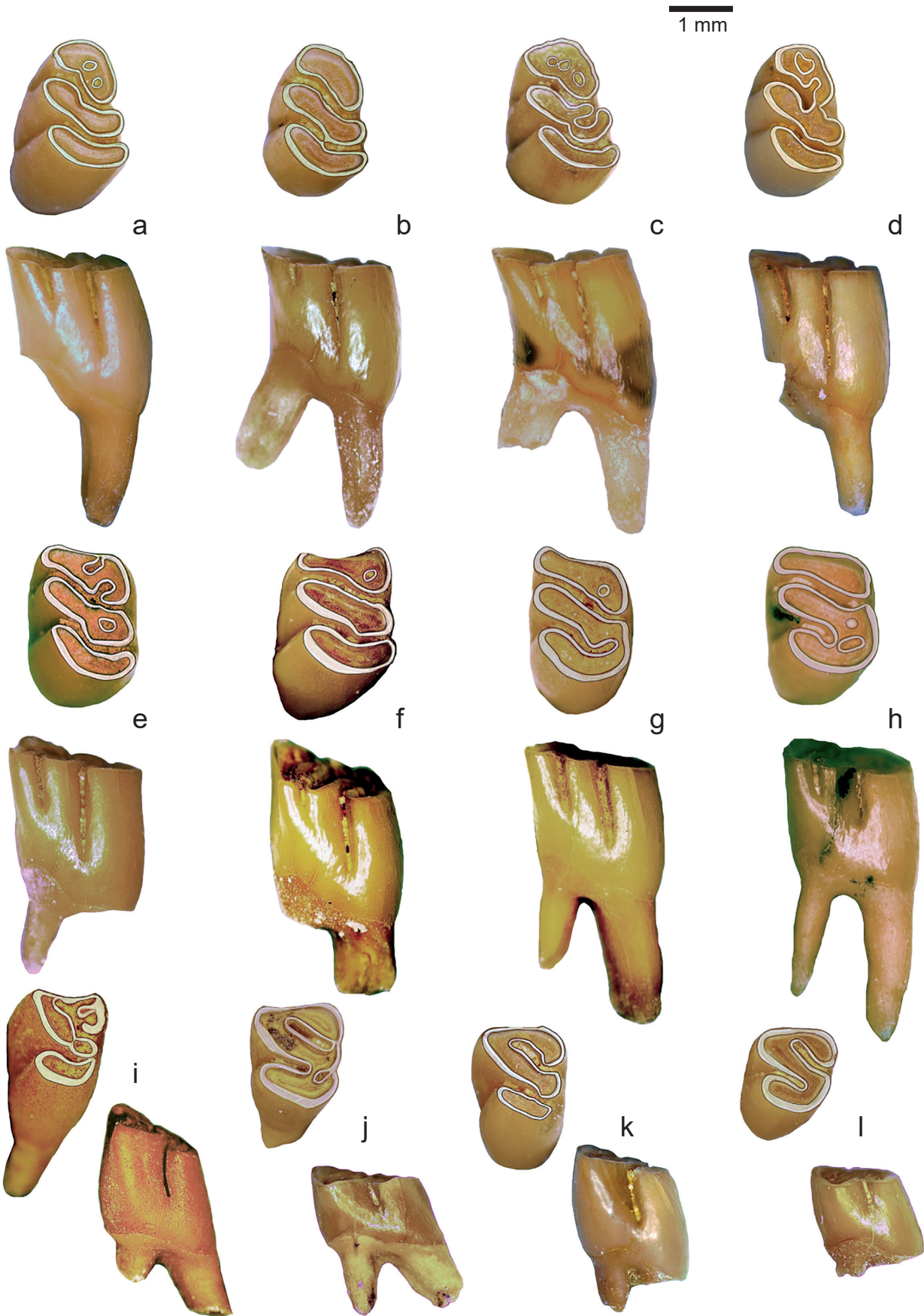
m2. 61 juvenile and adult molars are suitable for morphological study. The occlusal outline is rectangular with rounded angles. In the juvenile molars, the three lobes are isolated (in 41; Text-fig. 21e, f). Connections in subadult-adult stages:

- anterior lobe isolated, intermediate and posterior lobes are lingually connected: in 3 (Text-fig. 21g);
- anterior lobe isolated, intermediate and posterior lobes are centrally connected: in 4;
- anterior lobe isolated, intermediate and posterior lobes have a lingual and central connection: in 2 (Text-fig. 21h);
- lingual connections between the anterior and the intermediate lobes and between the intermediate and posterior lobes: in 5;
- the lingual connection between the anterior and the intermediate lobes, lingual and central connections between the intermediate and the posterior lobes: in 4;
- lingual and labial connection between the anterior and the intermediate lobes, lingual and central connections between the intermediate and the posterior lobes: in 1.

There are enamel rings in the anterior and the intermediate lobes:



Text-fig. 20. *Prospalax petteri* upper molars, occlusal and lingual views. a: left M1 (VER 2024.505.36), b: left M1 (VER 2024.505.39), c: left M1 (VER 2024.505.55), d: left M1 (VER 2024.505.75), e: left M2 (VER 2024.506.41), f: right M2 (VER 2024.506.42, reversed), g: right M2 (VER 2024.506.16, reversed), h: right M2 (VER 2024.506.44, reversed), i: right M3 (VER 2024.507.42, reversed), j: right M3 (VER 2024.507.40, reversed), k: left M3 (VER 2024.507.43), l: left M3 (VER 2024.507.30).



Text-fig. 21. *Prospalax petteri* lower molars, occlusal and labial views. a: left m1 (VER 2024.508.12), b: left m1 (VER 2024.508.18), c: left m1 (VER 2024.508.27), d: left m1 (VER 2024.508.49), e: left m2 (VER 2024.509.77), f: left m2 (VER 2024.509.58), g: right m2 (VER 2024.509.75, reversed), h: left m2 (VER 2024.509.56), i: right m3 (VER 2024.510.38, reversed), j: right m3 (VER 2024.510.50, reversed), k: left m3 (VER 2024.510.42), l: left m3 (VER 2024.510.49).

- no enamel ring in the anterior lobe: in 13;
- 1 enamel ring in the anterior lobe: in 20;
- 2 enamel rings in the anterior lobe: in 28 (Text-fig. 21e);
- no enamel ring in the intermediate lobe: in 35;
- 1 enamel ring in the intermediate lobe: in 18 (Text-fig. 21e);
- 2 enamel rings in the intermediate lobe: in 1;
- “*Anomalomys* marker” in the intermediate lobe: in 7.

There is no enamel ring in the posterior lobe.

m3. 31 juvenile and adult molars are suitable for morphological study. The occlusal outline is subtriangular with a rounded posterior angle. Among the juvenile molars, isolated anterior lobes (in 2) and isolated posterior lobes (in 5) are found. The connection of the anterior and the intermediate lobes:

- close to the labial part of the mesial surface: in 7;
- close to the central part of the mesial surface: in 22.

The connection of the intermediate and the posterior lobes can be lingual (in 17; Text-fig. 21i) or central (in 5; Text-fig. 21j). Enamel rings are rare. Those are found in the anterior unit of the juvenile molars (in 4; Text-fig. 21i).

Comparison. *Anomalomys gaudryi* GAILLARD, 1900 and *A. rudabanyensis* KORDOS, 1989 differ from the Csodabogyós population because of the following morphological characteristics of these taxa: smaller size, more frequent occurrence of enamel rings in the anterior lobes of M1/m1, the central connection of the anterior and intermediate lobes in M1/M2, the occurrence of distinct mesoloph in M1/M2, the labial connection of anterior and intermediate lobes in m1/m2, frequent occurrence of “*Anomalomys* marker” in m1/m2.

Anomalomys grytsivensis NESIN et KOVALCHUK, 2021 differs from the Csodabogyós population in several respects: it has a smaller size, a central connection of the anterior and intermediate lobes in M1/M2, the occurrence of a distinct mesoloph in M1/M2, and a labial connection of the anterior and intermediate lobes in m1/m2. However, this species exhibits some morphological markers similar to those of *Prospalax*, including the frequent isolation of the three lobes in juvenile m1/m2 and a rare occurrence of the “*Anomalomys* marker” in m1/m2.

Anomalospalax tardosi KORDOS, 1985 and *Anomalospalax viretschaubi* (KRETZOI, 1971) differ from the Csodabogyós population, because these taxa have a central connection of the anterior and the intermediate lobes in M1/M2, the enamel ring is absent in the intermediate lobe of M2, the anterior and intermediate lobes have labial connections in m1/m2, and the “*Anomalomys* marker” is frequent in m1.

The relation to *Anomalomys gaillardi* VIRET et SCHAUB, 1946 is difficult to define, because this species is represented by populations having only a few molars (e.g., Nebelbergweg, Montredon, Bujor, Pezinok; Tab. 2).

Prospalax priscus MÉHELY, 1908 differs from the Csodabogyós population in its more simplified morphology. The enamel rings have entirely disappeared from the dentine lobes, except from M3 (Luckett 2024).

The best similarity was found between the Csodabogyós population and the *Prospalax petteri* BACHMAYER et WILSON, 1970 specimens from Eichkogel and Kohfidisch, due to the same degree of hypsodonty, the same connections and isolations of the three lobes, and similar occurrences of enamel rings.

Comments. To date, the origin of *Prospalax* remains unresolved. Kordos (1989, 1992) questioned the origin of *Prospalax* (“*Allospalax* KRETZOI, 1971” in the original text) from *A. rudabanyensis*, and he presumed a theoretical ancestor to be in a transitional evolutionary phase between *A. gaudryi* and *A. gaillardi*. Later, he changed his idea, and Kordos (2005) described the *Anomalomys gaudryi*-*A. rudabanyensis*-*A. petteri* lineage. Referring to his observation, the characteristic dental morphological changes in the lineage include: increasing hypsodonty, a simpler dental fold system, the disappearance of the mesoloph, and the partial or total separation of the folds of m1 and m2.

Bolliger (1996) presumed that *Prospalax petteri* probably evolved from a form like *Anomalomys gaudryi*. Later, Bolliger (1999: fig. 40.3.) concluded *Prospalax* to be a new immigrant in Europe, but he does not exclude possible evolutionary connection between *Prospalax* and *A. rudabanyensis* or *A. gaillardi*. According to Daxner-Höck and Höck (2015), the unworn teeth of *Prospalax petteri* exhibit more archaic structures, similar to those of *Anomalomys rudabanyensis*. They regard *P. aff. petteri* from Schernham as a transitional population between advanced species of *Anomalomys* GAILLARD, 1900 (e.g., *A. rudabanyensis*, *A. gaillardi*) and *Prospalax petteri*. Nesin and Kovalchuk (2021) described *Anomalomys grytsivensis* from Grytsiv, and postulated that the new species can be a transitional form between *Anomalomys* and *Prospalax petteri*. Luckett (2024) gave a cladistic phylogenetic analysis of selected species of *Anomalomys*, *Prospalax* and *Anomalospalax* KORDOS, 1985. She concluded that the *Prospalax*-*Anomalospalax* lineage evolved from *Anomalomys*, and she found no indication of immigration.

Paleoecology and paleobiogeography

The fauna of the Csodabogyós Cave comprises species that prefer a wide range of environments, from woodland species to opportunists and those that thrive in open, dry environments. The same is true for both herpetofauna and mammals.

None of the Soricidae genera indicate a dry climate or open vegetation. Recent relatives of *Crusafontina* live in moist, closed forests (Ziegler 2006). We therefore think that shrews were inhabitants of forested or bushy areas near the coast. This is supported by the probably forest-preferring Erinaceomorpha and the aquatic Desmaninae among the insectivorous mammals.

All bat species except *Plecotus* are cave dwellers (Rosina and Sinita 2014). Therefore, there may have been some open caves near the site. *Rhinolophus* and *Miniopterus* prefer Mediterranean, warm, open grassy or scrubby areas. In contrast, *Plecotus* mostly lives in the hollows of old trees, which supports the mosaic nature of the environment (Crespo et al. 2020).

In the case of rodents, there is a roughly 50/50 split between species that prefer open areas (*Csakvaromys sciurinus*, *Myomimus dehmi*, *Vasseuromys* n. sp., *Eozapus intermedius*, *Neocricetodon* cf. *skofleki*, *Epimeriones austriacus*, *Prospalax petteri*) and those that prefer forest environments (*Muscardinus pliocaenicus*, *Eomyops* sp., *Keramidomys* sp., *Progonomys hispanicus*, *Apodemus lugdunensis*), which also indicates mosaic vegetation (van Dam 1997).

as that locality yielded only 5 Soricidae specimens. Based on the new findings, the present study extends the FAD to the beginning of MN 11. This record can be supported in the future by re-examining the dubiously determined species, described from Kohfidisch by Bachmayer and Wilson (1977). On the other hand, the occurrence of *A. gibberodon* and “*Petenya*” *dubia* in this assemblage indicates that this site is younger than the Sümeg locality nearby Csodabogyós Cave from the MN 10, where the two species certainly do not yet occur (Mészáros 1996).

The presence of *Crusafontina kormosi* suggests that the geological age of the material may not be earlier than the early Turolian, as seen at the Kohfidisch locality in Austria (the beginning of the MN 11), where the species first occurs. The direct descendant of this species is *Amblycoptus oligodon*, whose presence we cannot detect in the Csodabogyós and Kohfidisch samples; however, Tesakov et al. (2017) reported it from a later part of MN 11. As shown in the taxonomic chapter, many of the *Crusafontina* specimens in our sample are transitional between the two forms, meaning that this population may represent the time immediately before the species change. Based on this, we assume that the Csodabogyós Soricidae assemblage represents the early part of MN 11. Compared to the Csodabogyós *Paenelimoecus* specimens of the same age, the dimensions show a close relationship with those of the Csákvár and Kohfidisch specimens. In contrast, they differ somewhat from the smaller Eichkogel ones (Mészáros 1996: tab. 8, Ziegler 2006: tab. 23).

Among the rodents, both Austrian sites (Kohfidisch and Eichkogel) show species that are also important in the fauna of the Csodabogyós Cave: *Muscardinus pliocaenicus*, *Myomimus dehmi*, *Neocricetodon skofleki*, *Epimeriones austriacus*, *Prospalax petteri*, *Apodemus lugdunensis*, *Eozapus intermedius*. The significant differences between the two Austrian sites and the rodent fauna of the Csodabogyós Cave, e.g., the complete absence of flying squirrels in the Csodabogyós Cave, can be attributed to ecological differences.

Based on the size of the *A. lugdunensis* and *P. hispanicus* molars, Csodabogyós Cave may be closer in age to Kohfidisch (8.5 Ma), Peralejos C (8.8 Ma), and Peralejos D (8.7 Ma) sites in Spain. In addition, the morphology of the *Neocricetodon* cf. *skofleki* population from the Csodabogyós Cave (less divided anterocones and anteroconids on M1/m1) suggests an early form of *N. skofleki*, less developed than the material from the Eichkogel and Tardosbánya sites (Hír et al. 2025, this volume). These observations indicate that the accumulation of the Csodabogyós Cave material occurred in the earliest Turolian (8.7–8.5 Ma).

Conclusion

During the taxonomic process of the Csodabogyós Cave fossils, we described a new species of dormice (*Vasseuromys* n. sp.; see Hír 2025, this volume), found one of the oldest and westernmost occurrences of the genus *Microscoptes*, and reported the presence of a *Progonomys hispanicus*, a species significantly smaller than *P. woelferi*, common in nearby sites of similar age (Kohfidisch, Eichkogel). We raised for a

new genus “*Petenya*” *dubia* in the shrew material, extended the stratigraphic range of *Asoriculus gibberodon* to the MN 11, and described the morphological transition between *Crusafontina kormosi* and its descendant *Amblycoptus oligodon*. In addition, for some species (*Progonomys hispanicus*, *Apodemus lugdunensis*, *Neocricetodon* cf. *skofleki* (see Hír et al. 2025, this volume)), we have used statistical methods to compare the fauna of the Csodabogyós Cave with other faunas and species.

Thus, by providing a detailed taxonomic description of this extremely rich vertebrate fauna, primarily consisting of small mammals, and by giving raw size data (see supplementary material), we have created a database that can serve as a reference for future descriptions of sites of similar age.

Paleoecological analysis indicates that the vegetation surrounding the site was diverse. The climate may have been drier than that of the Middle Miocene, characterized by hot/dry summers and cool/wet winters.

Based on the biostratigraphically relevant small mammals, the age of the Csodabogyós Cave fauna is approximately 8.7–8.5 million years (early Turolian, MN 11).

Acknowledgements

We would like to thank Máté Gregorits and József Haász for discovering the initial finds, and Dr. Krisztina Sebe, who brought the material to the Hungarian Natural History Museum and subsequently actively participated in the collection and excavation. To the cavers and colleagues who helped with the excavation (Julianna Ba, József Haász, Károly Foki, Fédra Bükösi-Garai, Dorina Szalai, and Bálint Jagasics), and especially to the leader of the caving team, Zsolt Polacsek. Thanks to Márton Szabó for the pictures of the large mammal remains. We want to thank Dr. Wilma Wessels for her thorough review. The NKFI K 147412 project supported the research. This is HUN-REN-MTM-ELTE Paleo contribution No. 424.

References

- Aguilar, J. (1982): Contribution à l'étude des micro-mammifères du gisement miocène supérieur de Montredon (Hérault). – *Palaeovertebrata*, 12(3): 81–117.
- Agusti, J., Casanovas-Vilar, I. (2003): Neogene gerbils from Europe. – In: Reumer, J. W. F., Wessels, W. (eds): *Distribution and migration of Tertiary mammals in Europe*. *Deinsea*, 10: 13–22.
- Bachmayer, F., Wilson, R. W. (1970): Die Fauna der altpliozänen Höhlen- und Spaltenfüllungen bei Kohfidisch, Burgenland (Österreich). – *Annalen des Naturhistorischen Museums in Wien, A*, 74: 533–587.
- Bachmayer, F., Wilson, R. W. (1977): A second contribution to the small mammal fauna of Kohfidisch, Austria. – *Annalen des Naturhistorischen Museums in Wien*, 81: 129–161.
- Bernor, R. L., Kordos, L., Rook, L., Agustí, J., Andrews, P., Armour-Chelu, M., Begun, D. R., Cameron, D. W., Damuth, J., Daxner-Höck, G., de Bonis, L., Fejfar, O., Fessaha, N., Fortelius, M., Franzen, J., Gasparik, M.,

- Gentry, A., Heissig, K., Hernyak, G., Kaiser, T., Koufos, G. D., Krolopp, E., Jánossy, D., Llenas, M., Meszáros, L., Müller, P., Renne, P., Roček, Z., Sen, S., Scott, R., Szyndlar, Z., Topál, G., Ungar, P. S., Utescher, T., van Dam J. A., Werdelin, L., Ziegler, R. (2004): Recent advances on multidisciplinary research at Rudabánya, Late Miocene (MN9), Hungary: A compendium. – *Palaeontographia Italica*, 89: 3–36.
- Bilgin, M., Joniak, P., Mayda, S., Göktaş, F., Peláez-Campomanes, P., van den Hoek Ostende, L. W. (2021): Micromammals from the late early Miocene of Çapak (western Anatolia) herald a time of change. – *Journal of Paleontology*, 95(5): 1079–1096.
<https://doi.org/10.1017/jpa.2021.27>
- Bolliger, T. (1996): A current understanding about the Anomalomyinae (Rodentia). Reflections on stratigraphy, paleobiogeography, and evolution. – In: Bernor, R., Fahlbusch, V., Mittmann, H. (eds), *The evolution of Western Eurasian Neogene mammal faunas*. Columbia University Press, New York, pp. 235–245.
- Bolliger, T. (1999): Family Anomalomyidae. – In: Rössner, G. E., Heissig, K. (eds), *The Miocene Land Mammals of Europe*. Verlag Dr. Friedrich Pfeil, München, pp. 411–421.
- Botka, D., Mészáros, L. (2017): *Asoriculus* and *Neomys* (Mammalia, Soricidae) remains from the late Early Pleistocene Somssich Hill 2 locality (Villány Hills, Southern Hungary). – *Fragmenta Palaeontologica Hungarica*, 34: 105–125.
<https://doi.org/10.17111/FragmPalHung.2017.34.105>
- Crespo, V. D., Sevilla, P., Montoya, P., Ruiz-Sánchez, F. J. (2020): A relict tropical forest bat assemblage from the early Miocene of the Ribesalbes-Alcora Basin (Castelló, Spain). – *Earth and Environmental Science Transactions of the Royal Society of Edinburgh*, 111(4): 247–258.
<https://doi.org/10.1017/S1755691020000122>
- Cuenca-Bescós, G. (1988): Revision de los Sciuridae del Aragoniense y del Ramblense en la fossa de Calatayud-Montalban [Revision of Aragonian and Ramblian Sciuridae from Calatayud-Montalbán Basin]. – *Scripta Geologica*, 87: 1–115. (in Spanish)
- Daams, R. (1981): The dental pattern of the dormice *Dryomys*, *Myomimus*, *Microdryomys* and *Peridyromys*. – *Utrecht Micropaleontological Bulletins, Special Publication 3*: 1–115. (in Spanish)
- Daams, R., De Bruijn, H. (1995): A classification of the Gliridae (Rodentia) on the basis of dental morphology. – *Hystrix*, N. S., 6(1-2): 3–50.
- Daams, R., Freudenthal, M. (1988): Synopsis of the Dutch-Spanish collaboration program in the Neogene of the Calatayud-Teruel Basin 1976–1986. – In: Freudenthal, M. (ed), *Biostratigraphy and Paleocology of the Neogene micromammalian Faunas from the Calatayud-Teruel Basin (Spain)*. *Scripta Geologica, Special issue 1*: 3–18.
- van Dam, J. (1997): The small mammals from the Upper Miocene of the Teruel-Alfambra Region (Spain): Paleobiology and paleoclimatic reconstructions. – *Geologica Ultraiectina*, 156: 1–204.
- Daxner-Höck, G. (1972): Die Wirbeltierfauna aus dem Alt-Pliozän (Pont) vom Eichkogel bei Mödling (Niederösterreich). IV. Gerbillinae (Rodentia, Mammalia). – *Annalen des Naturhistorischen Museum in Wien*, 76: 143–150.
<https://doi.org/10.1007/BF02990149>
- Daxner-Höck, G. (1995): 9. Some Glirids and Cricetids from Maramena and other late Miocene localities in Northern Greece. – In: Schmidt-Kittler, N. (ed.), *The vertebrate locality Maramena (Macedonia, Greece) at the Turolian-Ruscinian boundary (Neogene)*. *Münchner Geowissenschaftliche Abhandlungen, A*, 28: 103–120.
- Daxner-Höck, G. (2009): New data on Eomyidae and Gliridae (Rodentia, Mammalia) from the late Miocene of Austria. – *Annalen des Naturhistorischen Museum in Wien, A*, 111: 375–444.
- Daxner-Höck, G., Böhme, M., Kossler, A. (2013): New data of Miocene biostratigraphy and paleoclimatology of Olkhon Island (Lake Baikal, Siberia). – In: Wang, X., Flynn, L. J., Fortelius, M. (eds), *Fossil mammals of Asia. Neogene biostratigraphy and chronology*. Columbia University Press, New York, pp. 508–517.
<https://doi.org/10.7312/columbia/9780231150125.003.0022>
- Daxner-Höck, G., Harzhauser, M., Göhlich, U. B. (2016): Fossil record and dynamics of Late Miocene small mammal faunas of the Vienna Basin and adjacent basins, Austria. – *Comptes Rendus Palevol*, 15(7): 855–862.
<https://doi.org/10.1016/j.crpv.2015.06.008>
- Daxner-Höck, G., Höck, E. (2009): New data on Eomyidae and Gliridae (Rodentia, Mammalia) from the Late Miocene of Austria. – *Annalen des Naturhistorischen Museums in Wien, A*, 11: 375–444.
- Daxner-Höck, G., Höck, E. (2015): *Rodentia neogenica (Catalogus Fossilium Austriae, Bd. 4)*. – Verlag der Österreichischen Akademie der Wissenschaften, Wien, 158 pp.
<https://doi.org/10.2307/j.ctt1vw0qvk>
- Daxner-Höck, G., Winkler, V., Kalthoff, D. C. (2025): The porcupine *Hystrix parvae* (Kretzoi, 1951) from the Late Miocene (Turolian, MN11) of Kohfidisch in Austria. – *Palaeobiodiversity and Palaeoenvironments*, 105: 313–334.
<https://doi.org/10.1007/s12549-024-00616-3>
- De Bruijn, H. (1966): Some new Miocene Gliridae (Rodentia, Mammalia) from the Calatayud Area (prov. Zaragoza, Spain). – *Proceedings of the Koninklijke Nederlandse Akademie van Wetenschappen, Ser. B*, 69(1): 1–21.
- De Bruijn, H. (1995): The Vertebrate locality Maramena (Macedonia, Greece) at the Turolian-Ruscinian Boundary (Neogene). 8. Sciuridae, Petauristidae and Eomyidae (Rodentia, Mammalia). – *Münchner Geowissenschaftliche Abhandlungen, A*, 28: 87–102.
- De Bruijn, H., Bosma, A. A. (2012): *Spermophilinus* and *Csakvaromys*, two names for the same genus of ground squirrel (Tamiini, Sciuridae, Rodentia, Mammalia) from the Neogene of Europe. – *Annalen des Naturhistorischen Museums in Wien, A*, 114: 317–320.
- De Bruijn, H., Dawson, M., Mein, P. (1970): Upper Pliocene Rodentia, Lagomorpha and Insectivora (Mammalia) from the Isle of Rhodes (Greece). Parts I, II, III. – *Proceedings of the Koninklijke Nederlandse Akademie van Wetenschappen, Ser. B*, 73(5): 535–584.
- De Bruijn, H., Mein, P. (1968): On the mammalian fauna of the *Hipparion*-beds in the Calatayud-Teruel Basin (Prov. Zaragoza, Spain). Part V. The Sciuridae. – *Koninklijke Nederlandse Akademie van Wetenschappen, Ser. B*, 71: 73–90.

- Engesser, B. (1990): Die Eomyidae (Rodentia, Mammalia) der Molasse der Schweiz und Savoyens. – Schweizerische Paläontologische Abhandlungen, 112: 1–144.
- Fahlbusch, V. (1987): The Neogene Mammalian faunas of Ertemte and Harr Obo in Inner Mongolia (Nei Mongol), China. 5. The genus *Microscoptes* (Rodentia, Cricetidae). – Senckenbergiana Lethaea, 67: 345–373.
- Fejfar, O. (1989): The Neogene VP sites of Czechoslovakia: A contribution to the Neogene terrestrial biostratigraphy of Europe based on Rodents. – In: Lindsay, E. H., Fahlbusch, V., Mein, P. (eds), European Neogene mammal chronology. Plenum Press, New York, pp. 211–236. https://doi.org/10.1007/978-1-4899-2513-8_15
- Fejfar, O., Heinrich, W.-D., Kordos, L., Maul, L. C. (2011): Microtoid cricetids and the early history of arvicolids (Mammalia: Rodentia). – Palaeontologia Electronica, 14(3): 27A (38 pp.).
- Freudenthal, M. (2004): Gliridae (Rodentia, Mammalia) from the Eocene and Oligocene of the Sierra Palomera (Teruel, Spain). – Treballs del Museu de Geologia de Barcelona, 12: 97–173.
- Furió, M., van Dam, J., Kaya, F. (2014): New insectivores (Lipotyphla, Mammalia) from the Late Miocene of the Sivas Basin, Central Anatolia. – Bulletin of Geosciences, 89: 163–181. <https://doi.org/10.3140/bull.geosci.1472>
- Fuss, J., Prieto, J., Böhme, M. (2015): Revision of the bose-laphin bovid *Miotragocerus monacensis* Stromer, 1928 (Mammalia, Bovidae) at the Middle to Late Miocene transition in Central Europe. – Neues Jahrbuch für Geologie und Paläontologie, Abhandlungen, 276(3): 229–265. <https://doi.org/10.1127/njgpa/2015/0481>
- García-Alix, A., Minwer-Barakat, A., Martín-Suárez, E., Freudenthal, M. (2008): *Muscardinus meridionalis* sp. nov., a new species of Gliridae (Rodentia, Mammalia) and its implications for the phylogeny of *Muscardinus*. – Journal of Vertebrate Paleontology, 28(2): 568–573. [https://doi.org/10.1671/0272-4634\(2008\)28\[568:MMS NAN\]2.0.CO;2](https://doi.org/10.1671/0272-4634(2008)28[568:MMS NAN]2.0.CO;2)
- Ginsburg, L., Mein, P. (2012): Les Sciuridae (Rodentia) de Sansan. – In: Peigné, S., Sen, S. (eds), Mammifères de Sansan. Muséum national d’Histoire naturelle, Paris, pp. 81–94.
- Gradstein, F. M., Ogg, J. G., Schmitz, M. D., Ogg, G. M. (eds) (2020): Geologic Time Scale 2020. Volume 2. – Elsevier, Amsterdam, pp. 565–1357 pp. <https://doi.org/10.1016/C2020-1-02369-3>
- Gromov, I. M., Polyakov, I. Y. (1977): Fauna SSSR. Mleko-pitayushchie, III, 8: polevki (Microtinae) [Fauna of the USSR. Mammals, III, 8: voles (Microtinae)]. – Nauka, Leningrad, 504 pp.
- Harzhauser, M., Daxner-Höck, G., Piller, W. E. (2004): An integrated stratigraphy of the Pannonian (Late Miocene) in the Vienna Basin. – Austrian Journal of Earth Sciences, 95(96): 6–19.
- Hír, J. (2003): The Middle Miocene (Late Astaracian, MN7/8) Rodent Fauna of Felsőtárkány 3/2 (Hungary). – Acta Palaeontologica Romaniaae, 5(4): 125–136.
- Hír, J. (2025): *Vasseuromys balatonicus* n. sp., a new Late Miocene, Turolian (MN 11) glirid from the Csodabogyós Cave (Keszthely Hills, western Hungary). – Fossil Imprint, 81(1-2): 166–176. <https://doi.org/10.37520/fi.2025.011>
- Hír, J., Pazonyi, P., Virág, A. (2025): The Late Miocene, Turolian (MN 11) *Neocricetodon* population from the Csodabogyós Cave (Keszthely Hills, western Hungary). – Fossil Imprint, 81(1-2): 154–165. <https://doi.org/10.37520/fi.2025.010>
- Hír, J., Prieto, J., Ştiucă, E. (2011): A new interpretation of the Miocene rodent faunas from Comăneşti 1 and Tauţ. – Geobios, 44: 215–223. <https://doi.org/10.1016/j.geobios.2011.01.003>
- van den Hoek Ostende, L. (2003): Gliridae (Rodentia, Mammalia) from the Upper Pliocene of Tegelen (province of Limburg, The Netherlands). – Scripta Geologica, 126: 203–215.
- Horáček, I., Špoutil, F. (2012): Why tribosphenic? On variation and constraint in developmental dynamics of chiropteran molars. – In: Gunnell, G., Simmons, N. (eds), Evolutionary History of Bats: Fossils, Molecules and Morphology. Cambridge University Press, Cambridge, pp. 410–455. <https://doi.org/10.1017/CBO9781139045599.013>
- Horáček, I., Trávníčková, E. (2019): *Myotis gerhardstorchi* sp. n. and comments on the European fossil record of *Myotis frater* group (Mammalia, Chiroptera). – Fossil Imprint, 75(3-4): 315–342. <https://doi.org/10.2478/if-2019-0021>
- Joniak, P. (2016): Upper Miocene rodents from Pezinok in the Danube Basin, Slovakia. – Acta Geologica Slovaca, 8(1): 1–14.
- Kälin, D. (1997): *Eomyops hebeiseni* n. sp., a new large Eomyidae (Rodentia, Mammalia) of the Upper Freshwater Molasse of Switzerland. – Eclogae Geologicae Helvetiae, 90(3): 629–637.
- Kälin, D. (1999): Tribe Cricetini. – In: Rössner, G. H., Heissig, K. (eds), The Miocene Land Mammals of Europe. Verlag Dr. Friedrich Pfeil, München, pp. 373–387.
- Kälin, D., Engesser, B. (2001): Die jungmiozäne Säugetierfauna vom Nebelbergweg bei Nunningen (Kt. Solothurn, Schweiz). – Schweizerische Paläontologische Abhandlungen, 121: 63–99.
- Kordos, L. (1989): Anomalomyidae (Mammalia, Rodentia) remains from the Neogene of Hungary. – A Magyar Állami Földtani Intézet Jelentése az 1987. évről [Annual Report of the Hungarian Geological Institute on 1987], pp. 293–311.
- Kordos, L. (1991): Mezőföld, Polgárdi, késő-miocén őserinces lelőhelyek [Late Miocene paleovertebrate localities, Polgárdi, Mezőföld] (Magyarország Geológiai Alapszelvényei [Geological Key Sections of Hungary]). – Magyar Állami Földtani Intézet, Budapest, 6 pp. (in Hungarian)
- Kordos, L. (1992): Magyarország harmad- és negyedidőszaki emlősfajának fejlődése és biokronológiája [The evolution and biochronology of the Tertiary and Quaternary Mammalian Fauna of Hungary]; D.Sc. Thesis. – MS, Hungarian Geological Institute, Budapest, Hungary, 103 pp. (in Hungarian) (copy in library of SZTFH [earlier Hungarian Geological Institute])
- Kordos, L. (2005): *Anomalomys* (Rodentia, Mammalia) from Rudabánya, Hungary (Miocene, MN9): Terminology of

- molars, age categories and phylogenetic interpretation. – *Fragmenta Palaeontologica Hungarica*, 23: 19–28.
- Kowalski, K. (1974): Remains of Gerbillinae (Rodentia, Mammalia) from the Pliocene of Poland. – *Bulletin of the Polish Academy of Sciences*, 22(9): 591–595.
- Kowalski, K. (1997): Gliridae (Mammalia, Rodentia) from the Miocene of Belchatow in Poland. – *Acta Zoologica Cracoviensia*, 36(2): 251–258.
- Kretzoi, M. (1951): A Csákvári *Hipparion*-fauna / The *Hipparion*-fauna from Csákvár. – *Földtani Közlöny*, 81: 384–417. (in Hungarian and English)
- Kretzoi, M. (1969): Skizze einer Arvicoliden-Phylogenie – Stand 1969. – *Vertebrata Hungarica*, 11: 155–193.
- Kretzoi, M., Fejfar, O. (2005): Sciurids and Cricetids (Mammalia, Rodentia) from Rudabánya. – *Palaeontographia Italica*, 90: 113–148.
- Kryštufek, B., Vohralík, V. (2005): Mammals of Turkey and Cyprus. Rodentia I: Sciuridae, Dipodidae, Gliridae, Arvicolinae. – *Zgodovinsko društvo za južno Primorsko*, Koper, 292 pp.
- Luckett, N. (2024): *Prospalax priscus* from the upper Pliocene (MN16) of Ridjake, Serbia and its phylogenetic position within Anomalomyinae (Rodentia, Muridae); MSc Thesis. – MS, Earth, Life and Climate, Utrecht University, Utrecht, The Netherlands, 38 pp. (copy in library of János Hír)
- Lungu, A. (1981): Fauna *Hipparion* srednego sarmatskogo perioda Moldovy: nasekomoyadnye, zaiceobraznye i gryzuny [*Hipparion* fauna of middle Sarmatian of Moldova: Insectivores, lagomorphs and rodents]. – *Shtintsa*, Kishinev, 118 pp. (in Russian)
- Mansino, S., Crespo, V. D., Lázaro, M., Ruiz-Sánchez, F. J., Abella, J., Montoya, P. (2016): Fossil micromammals of the early Pliocene locality of Almenara MB: biostratigraphical and palaeoecological implications. – *Spanish Journal of Palaeontology*, 31(2): 253–270. <https://doi.org/10.7203/sjp.31.2.17153>
- Martínez-Navarro, B., Rook, L., Segid, A., Yosief, D., Ferretti, M. P., Shoshani, J., Teclé, T. M., Libsekal, Y. (2004): The large fossil mammals from Buia (Eritrea): systematics, biochronology and paleoenvironments. – *Rivista Italiana di Paleontologia e Stratigrafia*, 110: 61–88.
- Maul, L. C., Rekovets, L. I., Heinrich, W.-D., Bruch, A. A. (2017): Comments on the age and dispersal of *Microscaptini* (Rodentia: Cricetidae). – *Fossil Imprint*, 73(3-4): 495–514. <https://doi.org/10.2478/if-2017-0026>
- McKenna, M. C., Bell, S. K. (1997): Classification of mammals above the species level. – Columbia University Press, New York, 631 pp.
- Mein, P. (1964): Chiroptera (Miocene) de Lissieu (Rhône). – In: *Comptes Rendus du 89e Congrès national des Sociétés Savantes, Section Sciences*, Lyon, pp. 237–253.
- Menu, H. (1985): Morphotypes dentaires actuels et fossiles des chiroptères vespertilioninés. I^e partie: Étude des morphologies dentaires. – *Palaeovertebrata*, 15: 71–128.
- Mészáros, L. (1996): Soricidae (Mammalia, Insectivora) remains from three Late Miocene localities in western Hungary. – *Annales Universitatis Scientiarum Budapestinensis de Rolando Eötvös Nominatae, Sectio Geologica*, 31: 5–25.
- Mészáros, L. (1998): Late Miocene Soricidae (Mammalia) fauna from Tardosbánya (Western Hungary). – *Hantkeniana*, 2(2): 103–125.
- Mészáros, L. (1999): An exceptionally rich Soricidae (Mammalia) fauna from the upper Miocene localities of Polgárdi (Hungary). – *Annales Universitatis Scientiarum Budapestinensis de Rolando Eötvös Nominatae, Sectio Geologica*, 32: 5–34.
- Mészáros, L. (2000): New results for the Late Miocene Soricidae stratigraphy of the Pannonian Basin. – *Newsletters on Stratigraphy*, 38(1): 1–11. <https://doi.org/10.1127/nos/38/2000/1>
- Nadachowski, K., Daoud, A. (1995): Patterns of myoxid evolution in the Pliocene and Pleistocene of Europe. – *Hystrix*, 6(1-2): 141–149.
- Nesin, V., Kovalchuk, O. (2021): A new late Miocene *Anomalomys* species from western Ukraine with implications for the diversity and evolution of anomalomyid rodents in Eastern Europe. – *Historical Biology*, 33(9): 1809–1816. <https://doi.org/10.1080/08912963.2020.1742711>
- Papp, A. (1951): Das Pannon des Wiener Beckens. – *Mitteilungen der Geologischen Gesellschaft in Wien*, 39-41(1946-1948): 99–193.
- Pavlinov, I. Ya. (2008): A review of phylogeny and classification of Gerbillinae (Mammalia: Rodentia). – Moscow University Publishing, Moscow, 68 pp.
- Piller, W. E., Harzhauser, M., Mandic, O. (2007): Miocene Central Paratethys stratigraphy – current status and future directions. – *Stratigraphy*, 4(2): 151–168. <https://doi.org/10.29041/strat.04.2.09>
- Piñero, P., Agustí, J., Blain, H., Furió, M., Laplana, C. (2015): Biochronological data for the Early Pleistocene site of Quibas (SE Spain) inferred from rodent assemblage. – *Geologica Acta*, 13(3): 229–241.
- Polacsek, Z., Szittner, Z. (2006): Csodabogyós-barlang, Balatonedrics, Alaprajz [Csodabogyós Cave, Balatonedrics, Map]; research report. – MS, Alpin Generál Kft., Balaton-felvidéki National Park, Csopak, Hungary. (in Hungarian) (copy in library of Piroaska Pazonyi)
- Popov, V. (2004): Pliocene small mammals (Mammalia, Lipotyphla, Chiroptera, Lagomorpha, Rodentia) from Muselievo (North Bulgaria). – *Geodiversitas*, 16(3): 403–491.
- R Core Team (2023): R: A Language and Environment for Statistical Computing. – R Foundation for Statistical Computing, Vienna, Austria. <https://www.R-project.org/>
- Rabeder, G. (1985): Die Säugetiere des Pannonien. – In: Papp, A., Jámbo, Á., Steininger, F. F. (eds), *Chronostratigraphie und Neostatotypen Miozän der Zentralen Paratethys*. M6. Akadémiai Kiadó, Budapest, pp. 440–463.
- Rachl, R. (1983): Die Chiroptera (Mammalia) aus den mittelmiozänen Kalken des Nördlingers Rieses (Süddeutschland); Ph.D. Thesis. – MS, Ludwig-Maximilians-Universität München, München, Germany, 284 pp.
- Reumer, J. W. F. (1984): Ruscinian and early Pleistocene Soricidae (Insectivora, Mammalia) from Tegelen (The Netherlands) and Hungary. – *Scripta Geologica*, 73: 1–173.
- Rose, J., Moore, A., Russell, A., Butcher, M. (2014): Functional osteology of the forelimb digging apparatus of badgers. – *Journal of Mammalogy*, 95(3): 543–558. <https://doi.org/10.1644/13-MAMM-A-174>

- Rosina, V. V., Kruskop, S., Semenov, Y. (2019): New Late Miocene plecotine bats (Chiroptera, Vespertilionidae: Plecotini) from Gritsev, Ukraine. – *Palaeovertebrata*, 42(1): e2 (13 pp).
<https://doi.org/10.18563/pv.42.1.e2>
- Rosina, V. V., Sinitsa, M. V. (2014): Bats (Chiroptera, Mammalia) from the Turolian of the Ukraine: phylogenetic and biostratigraphic considerations. – *Neues Jahrbuch für Geologie und Paläontologie, Abhandlungen*, 272(2): 147–166.
<https://doi.org/10.1127/0077-7749/2014/0403>
- Rzebik-Kowalska, B. (1989): Pliocene and Pleistocene Insectivora (Mammalia) of Poland V. Soricidae: *Petenya* KORMOS, 1934 and *Blarinella* THOMAS, 1911. – *Acta zoologica cracoviensia*, 32(11): 521–546.
- Rzebik-Kowalska, B. (2013): *Sorex bifidus* n. sp. and the rich insectivore mammal fauna (Erinaceomorpha, Soricomorpha, Mammalia) from the Early Pleistocene of Żabia Cave in Poland. – *Palaeontologia Electronica*, 16(2): 12A (35 pp.).
<https://doi.org/10.26879/376>
- Salesa, M. J., Siliceo, G., Antón, M., Fabre, A.-C., Pastor, J. F. (2020): Functional inferences on the long bones of *Ischyriactis zibethoides* (Blainville, 1841) (Carnivora, Mustelidae) from the middle Miocene locality of Sansan (Gers, France). – In: Bonis, L. de, Werdelin, L. (eds), Memorial to Stéphane Peigné. Carnivores (Hyaenodonta and Carnivora) of the Cenozoic. *Geodiversitas*, 42(1): 1–16.
<https://doi.org/10.5252/geodiversitas2020v42a1>
- Shapiro, S. C., Wilk, M. B. (1965): An analysis of variance test for normality (complete samples). – *Biometrika*, 53(3-4): 591–611.
<https://doi.org/10.1093/biomet/52.3-4.591>
- Sinitsa, M. V., Čermák, S. (2024): Redescription of the type specimen of *Csakvaromys sciurinus* (Rodentia, Sciuridae, Xerinae) from the Late Miocene of Hungary and its bearing on the systematics of early ground squirrels. – *Fossil Imprint*, 80(2): 258–268.
<https://doi.org/10.37520/fi.2024.020>
- Sinitsa, M. V., Čermák, S., Kryuchkova, L. Y. (2022): Cranial anatomy of *Csakvaromys bredai* (Rodentia, Sciuridae, Xerinae) and implications for ground squirrel evolution and Systematics. – *Journal of Mammalian Evolution*, 29: 149–189.
<https://doi.org/10.1007/s10914-021-09561-w>
- Steininger, F. F. (1999): The Continental European Miocene. Chronostratigraphy, Geochronology and Biochronology of the Miocene “European Land Mammal Mega-Zones (ELMMZ)” and the Miocene “Mammal-Zones (MN-Zones)”. – In: Rössner, G. E., Heissig, K. (eds), *The Miocene Land Mammals of Europe*. Verlag Dr. Friedrich Pfeil, München, pp. 9–24.
- Storch, G. (1995): The Neogene mammalian faunas of Ertemte and Harr Obo in Inner Mongolia (Nei Mongol), China. 11. Soricidae (Insectivora). – *Senckenbergiana Lethaea*, 75(1-2): 221–251.
- Terzea, E. (1978): *Epimeriones dacicus* n. sp. (Rodentia, Mammalia) du Villafranchien supérieur de Roumanie. – *Travaux de l'Institut de Spéologie “Èmile Racovitza”*, 17: 135–138.
- Tesakov, A., Titov, V., Simakova, A., Frolov, P., Syromyatnikova, E., Kurshakov, S., Volkova, N., Trikhunkov, Y., Sotnikova, M., Kruskop, S., Zelenkov, N., Tesakova, E., Palatov, D. (2017): Late Miocene (early Turolian) vertebrate faunas and associated biotic record of the northern Caucasus: geology, taxonomy, palaeoenvironment, biochronology. – *Fossil Imprint*, 73(3-4): 383–444.
<https://doi.org/10.2478/if-2017-0021>
- Tong, H. (1989): Origine et évolution des Gerbillidae (Mammalia, Rodentia) en Afrique du Nord. – *Mémoires de la Société Géologique de France*, 155: 1–120.
- Topál, G. (1974): The first record of *Megaderma* in Hungary (Pliocene sediments of Osztramos, Locality 10). – *Vertebrata Hungarica*, 15: 95–104.
- Topál, G. (1979): Fossil bats of the *Rhinolophus ferrumequinum* group in Hungary (Mammalia: Chiroptera). – *Fragmenta Mineralogica et Palaeontologica*, 9: 61–101.
- Topál, G. (1989): Tertiary and Early Quaternary remains of *Corynorhinus* and *Plecotus* from Hungary (Mammalia, Chiroptera). – *Vertebrata Hungarica*, 23: 33–55.
- Trávníčková, E. (2016): Změny středoevropské netopýří fauny na hranici pliocén/pleistocén: rod *Myotis* [Changes in mid-European bat fauna along the Plio/Pleistocene boundary: genus *Myotis*]; MSc Thesis. – MS, Charles University, Faculty of Sciences, Department of Zoology, Prague, the Czech Republic, 141 pp. (in Czech) (available online)
<http://hdl.handle.net/20.500.11956/73784>
- Van Valen, L. M. (1966): Deltatheridia, a new order of mammals. – *Bulletin of the American Museum of Natural History*, 132(1): 1–126.
- Van de Weerd, A. (1976): Rodent faunas of the Mio-Pliocene continental sediments of the Teruel-Alfambra region, Spain. – *Utrecht Micropaleontological Bulletin, Special Publication 2*: 1–216.
- Welch, B. L. (1947): The generalization of ‘Student’s’ problem when several different population variances are involved. – *Biometrika*, 34(1-2): 28–35.
<https://doi.org/10.2307/2332510>
- Wessels, W. (1999): Family Gerbillidae. – In: Rössner, G. E., Heissig, K. (eds), *The Miocene Land Mammals of Europe*. Verlag Dr. Friedrich Pfeil, München, pp. 395–400.
- Woloszyn, B. W. (1987): Pliocene and Pleistocene bats of Poland. – *Acta Palaeontologica Polonica*, 32(3-4): 207–325.
- Wöger, J. (2011): The Murines (Rodentia, Mammalia) of Kohfidisch (Burgenland, Austria) at second glance. A comparative morphological study. – *Beiträge zur Paläontologie*, 32: 1–42.
- Wu, W. Y. (1985): Neogene mammalian faunas of Ertemte and Harr Obo in Nei Mongol, China – 6. Gliridae (Rodentia, Mammalia). – *Senckenbergiana Lethaea*, 66(3-4): 69–88.
- Ziegler, R. (2003): Bats (Chiroptera, Mammalia) from Middle Miocene karstic fissure fillings of Petersbuch near Eichstätt, Southern Franconian Alb (Bavaria). – *Geobios*, 36(4): 447–490.
[https://doi.org/10.1016/S0016-6995\(03\)00043-3](https://doi.org/10.1016/S0016-6995(03)00043-3)
- Ziegler, R. (2006): Insectivores (Lipotyphla) and bats (Chiroptera) from the late Miocene of Austria – *Annalen des Naturhistorischen Museums in Wien, A*, 107: 93–106.